ECOLOGICAL ANALYSIS AND SIMULATION MODELS OF LANDSCAPE PATTERNS IN MANGROVE FOREST DEVELOPMENT AND SOIL CHARACTERISTICS ALONG THE SHARK RIVER ESTUARY, FLORIDA

A dissertation
Presented to the
Graduate Faculty of the
University of Southwestern Louisiana
In Partial Fulfillment of the
Requirements for the Degree
Doctor of Philosophy

Ronghua Chen

Summer 1996

EDITH GARLAND DUPRE LIBRARY
UNIVERSITY OF SOUTHWESTERN LOUISIANA
LAFAYETTE, LA. 70504

ECOLOGICAL ANALYSIS AND SIMULATION MODELS OF LANDSCAPE PATTERNS IN MANGROVE FOREST DEVELOPMENT AND SOIL CHARACTERISTICS ALONG THE SHARK RIVER ESTUARY, FLORIDA

Ronghua Chen

APPROVED:

Robert R. Twilley, Chair
Professor of Biology

Charles L. Burras
Assistant Professor of Agronomy
Iowa State University

Paul L. Klerks
Assistant Professor of Biology

Joseph E. Neigel
Associate Professor of Biology

Samuel C. Snedaker
Professor of Biology
RSMAS, University of Miami

Lewis Pyenson
Dean, Graduate School

ACKNOWLEDGEMENTS

I first would like to express my sincere thanks to my major advisor, Dr. Robert R. Twilley, for his insightful guidance, encouragement and support. I also want to thank my committee Drs. Charles L. Burras, Paul L. Klerks, Joseph E. Neigel and Samuel C. Snedaker for their valuable advice and suggestions on my dissertation.

Special thanks must go to my past advisor, Professor Lin Peng, at Xiamen University who introduced me into the world of mangroves and has continued to support me.

Field work in the Everglades National Park would have been nearly impossible without the assistance of fellow students: John Foret, Patricia Rafferty, Laura Lawton, John Bourgeois, Stephanie Cogburn and C. Coronado-Molina who had to endure the relentless pursuit of mosquitoes. Many thanks also go to the following for analytical support: Patricia Rafferty, John Foret, Mike Radford, Robert Bourgeois, Stephanie Cogburn, Russell Garrett and Claudia Muñoz.

This research was supported by U.S. Department of Interior, National Park Service, Cooperative Agreement No. CA 5280-4-9019 with the Everglades National Park and by U.S. Environmental Protection Agency, CR 820667, to Dr. Twilley. I am grateful to Drs. Tom Armentano, Tom Smith and Dewitt Smith for assistance in providing access to the Everglades National Park.

I deeply appreciate the love and support of my wife, Jie, and my daughter, Grace, during this long journey.

Finally, I dedicate this dissertation to my farther and my mother for their love, sacrifice and encouragement in all my endeavors over the years.

LD
3091
.L666
1996
Chen2

TABLE OF CONTENTS

ACKNOWLEDGEMENTS iv

TABLE OF CONTENTS v

LIST OF TABLES vii

LIST OF FIGURES viii

CHAPTER 1 INTRODUCTION 1
Background 2
Research goal 5

CHAPTER 2 SOIL NITROGEN AND PHOSPHORUS AVAILABILITIES IN A MANGROVE LAND-MARGIN ECOSYSTEM 8
Abstract 9
Introduction 10
Materials and methods 13
Study area 13
Field sampling and vegetation measurement 14
Soil property determination 15
N and P mineralization 16
P fractionation 17
Statistical analysis 18
Results 19
Tree height, salinity and soil nutrient content 19
Soil N and P availabilities along the estuary 20
Soil N and P availabilities in canopy gaps and forests 22
Discussion 23
The effect of vegetation on N and P availability 23
Landscape trends and control of N availability 24
Landscape trends and control of P availability 28

CHAPTER 3 LANDSCAPE PATTERNS OF MANGROVE FOREST STRUCTURE AND SOIL CHARACTERISTICS ALONG THE SHARK RIVER ESTUARY, FLORIDA 45
Abstract 46
Introduction 47
Materials and methods 50
Study area 50
Forest structure and growth 51
Pore water analyses 52
Soil nutrients 53
Statistical analysis 53
Results 54
Forest structure and growth 54
Pore water characteristics 56
Soil nutrients 57

Discussion 59
Soil sulfide and salinity stress along the estuarine gradient 59
Soil N and P resources along the estuarine gradient 61
Forest structure 64
Forest biomass accumulation in relation to nutrient limitation 66

CHAPTER 4 MODELING THE VERTICAL DISTRIBUTIONS OF ORGANIC MATTER, NITROGEN AND PHOSPHORUS IN MANGROVE SOILS 81
Abstract 82
Introduction 83
Materials and methods 84
Model description 85
Soil organic matter dynamics 85
Soil nitrogen and phosphorus 90
Model parameterization 91
Results and model validation 93
Discussion 97

CHAPTER 5 MODELING THE DEVELOPMENT OF MANGROVE FORESTS ALONG SPATIAL GRADIENTS OF SOIL RESOURCE AVAILABILITY AND TOXIC STRESS 113
Abstract 114
Introduction 115
Methods 118
Model description 118
The study forest 125
Model simulations 126
Results 128
Regeneration following disturbance 128
Projection of mangrove succession 130
Salinity and nutrient response surfaces 131
Discussion 132

LITERATURE CITED 151

ABSTRACT 166

BIOGRAPHICAL SKETCH 168

LIST OF TABLES

CHAPTER 2

Table 2.1. Soil C, N and P concentrations and bulk density along the Shark River estuary 32

Table 2.2. Summary of F statistics from repeated measures ANOVA of site and season effects on nutrient availability 33

Table 2.3 Phosphorus fractionation at 0-20 cm depth in sediments from intact mangrove forests and canopy gaps 34

Table 2.4. Summary of F statistics from repeated measures ANOVA of vegetation (intact forest vs canopy gap) and season effects on nutrient availability 35

Table 2.5 Linear correlations among N mineralization, P mineralization and other soil properties within the 0-20 cm depth in mangrove forests and gaps 36

CHAPTER 3

Table 3.1 Average basal area increment and biomass increment per tree, and total annual basal area increment and woody growth per unit area of mangroves along the Shark River estuary 70

Table 3.2. Summary of F statistics from repeated measures ANOVA of site and season effects on pore water chemistry 71

Table 3.3 Summary of F statistics from repeated measures ANOVA of site, depth and season effects on soil C, N and P 72

Table 3.4 Structural characteristics of mangrove forests of southern Florida, Puerto Rico, Mexico and Costa Rica 73

CHAPTER 4

Table 4.1. Definition and values of parameters used in the NUMAN model 103

Table 4.2. Site specific parameters for simulations of the NUMAN model 104

Table 4.3. Comparisons of mangrove forest structure and sediment characteristics . . . 105

CHAPTER 5

Table 5.1. Species-specific parameters used in the MANGAL model 137

LIST OF FIGURES

CHAPTER 1

Figure 1.1. Spatial pattern of mangrove forests in relation to hierarchical environmental factors 7

CHAPTER 2

Figure 2.1. Study site locations along the Shark River estuary in the Everglades National Park 37

Figure 2.2. Changes of mean tree height of mangrove forests and salinity along the Shark River estuary 38

Figure 2.3. Changes of soil C, N and P in mangrove forests along the Shark River estuary 39

Figure 2.4. Extractable nitrate+nitrite, ammonium and phosphorus at four mangrove sites along the Shark River estuary 40

Figure 2.5. Relationship between mean extractable ammonium, extractable phosphorus, net ammonification, and the distance from the mouth of the Shark River estuary 41

Figure 2.6. Net ammonification and phosphorus mineralization within the 0-20 cm soil at four mangrove sites along the Shark River estuary 42

Figure 2.7. Changes in P fractionations in percent of total P at four mangrove sites along the Shark River estuary 43

Figure 2.8. The relative ammonification rate of mangrove sediments in relation to the spatial gradient of the Shark River estuary 44

CHAPTER 3

Figure 3.1 Mangrove forest structure by species at sites along the Shark River estuary . . 74

Figure 3.2 Size class distribution of mangroves by species along the Shark River estuary 75

Figure 3.3 Spatial and temporal variation in pore water stressors including salinity and sulfide measured along the Shark River estuary 76

Figure 3.4 Spatial and temporal variation in pore water nutrients including nitrite, nitrate, ammonium and phosphate measured along the Shark River estuary 77

Figure 3.5 Vertical profiles of available phosphorus and extractable ammonium in mangrove soils along the Shark River estuary 78

Figure 3.6 Vertical profiles of C, N and P in mangrove soils along the Shark River estuary 79

Figure 3.7 Basal area of mangrove forests relative to total phosphorus in mangrove soils 80

CHAPTER 4

Figure 4.1. Conceptual diagram of the NUMAN model that simulates the biogeochemistry of sediment cohorts changing with depth in a mangrove ecosystem 106

Figure 4.2. Comparison of observed concentrations of organic matter and simulated concentrations in mangrove soils along the Shark River estuary 107

Figure 4.3. Comparison of observed and simulated bulk density in mangrove soils along the Shark River estuary 108

Figure 4.4. Comparison of observed concentrations of total nitrogen and simulated concentrations in mangrove soils along the Shark River estuary 109

Figure 4.5. Comparison of observed and simulated nitrogen mineralization in mangrove soils along the Shark River estuary 110

Figure 4.6. Comparison of observed concentrations of total phosphorus and simulated concentrations in mangrove soils along the Shark River estuary 111

Figure 4.7. Comparison of observed and simulated N:P ratios in mangrove sediments along the Shark River estuary 112

CHAPTER 5

Figure 5.1. Conceptual model of mangrove forest development including edaphic constraints 138

Figure 5.2. Growth multiplier curves for three mangrove species 139

Figure 5.3. Comparison of simulated and measured total basal area of three mangrove forests along the Shark River estuary 140

Figure 5.4. Comparison of relative dominance for three mangrove species using basal area between field surveys and simulations of the MANGAL model 141

Figure 5.5. Comparison of size-class distribution of *Rhizophora mangle* for three mangrove sites between field surveys and simulations using the MANGAL model 142

Figure 5.6. Comparison of size-class distribution of *Laguncularia racemosa* for three mangrove sites between field surveys and simulations using the MANGAL model 143

Figure 5.7. Comparison of size-class distribution of *Avicennia germinans* for three mangrove sites between field surveys and simulations using the MANGAL model 144

Figure 5. 8. Projected basal area of three mangrove species at the marine site of the Shark River estuary by the MANGAL model 145

Figure 5.9. Simulated total basal area of mangrove forests along gradients of soil nutrient availability and salinity by the FORMAN model 146

Figure 5.10. Simulated succession of mangrove forest gaps after 35 years of development along gradients of soil nutrient availability and salinity by the FORMAN model 147

Figure 5.11. Simulated succession of mangrove forest gaps after 100 years of development along gradients of soil nutrient availability and salinity by the FORMAN model 148

Figure 5.12. Simulated succession of mangrove forest gaps after 200 years of development along gradients of soil nutrient availability and salinity by the FORMAN model 149

Figure 5.13. Simulated succession of mangrove forest gaps after 300 years of development along gradients of soil nutrient availability and salinity by the FORMAN model 150

CHAPTER 1

INTRODUCTION

BACKGROUND

Mangrove ecology has a long tradition of interest in the spatial patterns of plant communities and the factors that control these patterns. Climatic factors including temperature, precipitation and solar radiation are major variables governing the geographical distribution of mangrove species and biomass (Pool et al. 1977, Blasco 1984, Woodroffe and Grindrod 1991, Twilley et al. 1992, Saenger and Snedaker 1993). Since regional scale climate is much less variable, geomorphological processes of the coastal zone may explain the regional pattern of mangrove forest (Thom 1982). The agents which control spatial variations of mangrove forest structure within a region can be classified into three explanatory models.

Environmental gradient constraints: Heterogeneity of environmental variables is responsible for the species-specific dispersal, survival, growth and reproduction of mangrove tree species. The resource ratio hypothesis predicts that resources varying widely in space create a gradient or mosaic that may favor different plant species in different places (Tilman 1982). Lugo and Snedaker (1974) identified ecological types as fringe, riverine, basin, dwarf, hammock and overwash mangroves, which related mangrove forest physiognomy with gradients of hydrology and topography. Fine-scale soil conditions as a function of past and present geomorphological and hydrological processes have a direct control on growth of mangroves (Thom 1982, Boto and Wellington 1984). Effects of climatic, geomorphological, hydrological and edaphic variables on mangrove forest development depend on spatial scale and their hierarchical relationships in space are summarized in Figure 1.1.

Biomass and structure of mangroves have been correlated with soil nutrient resources, especially phosphorus (Boto and Wellington 1984). However, numerous studies

have revealed that the gradients of toxic substances in soil can also determine the zonation, structure and function of mangroves. These stressors include hypersalinity (Lugo and Snedaker 1974, Cintrón et al. 1978), sulfide concentrations (Nickerson and Thibodeau 1985, McKee et al. 1988, McKee 1993), and redox potential (Thibodeau and Nickerson 1986, McKee et al. 1988). Greenhouse studies reveal that three Caribbean mangrove species differ in resource use and in tolerance to toxic stressors (McKee 1993, Mckee 1995b). While considerable attention has been given to the zonation of mangrove species parallel to shoreline as a response to the gradients of intertidal environmental conditions, few studies have focused on the landscape pattern of mangrove forest structure across the longitudinal axis of an estuary.

Biotic processes: In the biotic control model, competition and predation are considered to be two primary factors structuring mangrove communities. The species-specific tolerance to light has been suggested as a competitive mechanism to explain the succession of Florida and Malaysian mangroves (Ball 1980, Putz and Chan 1986). Ball (1980) found that seedlings of *Rhizophora mangle* tend to persist for a longer period than those of *Laguncularia racemosa* under the forest canopy and suggested that *L. racemosa* was being replaced by *R. mangle* because of their difference in shade-tolerance. Putz and Chan (1986) observed that shade-tolerant species, such as *Bruguiera gymnorrhiza*, steadily increased in abundance in the mangrove forest dominated by *Rhizophora apiculata*. Predation has been demonstrated using manipulated experiments where the consumption of propagules by grapsid crabs greatly influences the mangrove forest regeneration and distribution of certain species, especially *Avicennia* spp. (Smith 1987a, Smith et al. 1989). Insects may also selectively attack and kill propagules and seeds of some mangrove species (Robertson et al. 1990).

Disturbance events: Patterns of plant community distribution can be viewed as a

result of numerous patches in various stages of development, which can be caused by the death of an individual plant (Watt 1947, see Pickette and White 1985b). Disturbance is defined as "any relative discrete event in time that disrupts ecosystem, community, or population structure and changes resources, substrate availability, or the physical environment" (Pickett and White 1985a). These disturbance events can also be viewed as part of the natural dynamics of a forest. Although the importance of disturbance events is a contemporary concept in ecological theory (Pickett and White 1985b), few empirical studies document their effect on spatial patterns of mangrove wetlands. Mangroves are exposed to many types of disturbance, from the death of a single tree caused by insects (Putz and Chan 1986) to large-scale effects of hurricanes (Smith et al. 1994). Hurricanes regularly occur throughout the Caribbean, and their impact on the structure and function of tropical systems is often significant (Loope et al. 1994, Roman et al. 1994, Smith et al. 1994, Tilmant et al. 1994). The ecological effects of hurricanes on landscape patterns of mangrove forest development have been reported (Egler 1952, Craighead and Gilbert 1962, Lugo and Snedaker 1974, Lugo 1980), but only recently have quantitative data been collected (Roth 1992, Smith et al. 1994, Doyle et al. 1995). These observed results indicated that there are species-specific tolerances to the intensity of wind speeds during a hurricane. Catastrophic disturbances caused by hurricanes are viewed as recurrent events in the natural disturbance regime of Caribbean mangrove landscape (Lugo and Snedaker 1974). In south Florida, landscape patterns of mangroves reflect whole-scale disturbance such as hurricanes, as well as zonation across intertidal gradients. However, it is unknown how gradients of soil nutrient resources and toxic stresses affect patterns of mangrove forest development following disturbance.

All three models may operate and interact with each other in the specific formation of mangrove development along an estuary. Field observations show that predation on mangrove propagules varies with size of gaps, with higher predation occurring in smaller

gaps (Osborne and Smith 1990). The outcome of competition between two mangrove species (*Ceriops tagal* and *Ceriops australis*) depends on soil salinity (Smith 1988). A primary effect of disturbance is the opening of space associated with a change in the availability of light and soil nutrient resources. Thus disturbances can cause multiple levels of change in environmental heterogeneity (Denslow 1985). Further study is necessary to understand the relative contribution and interactions of environmental gradients, biotic processes, and disturbance events to landscape patterns of mangrove forest development.

RESEARCH GOAL

The goal of this research is to determine the landscape and temporal patterns of mangrove forest development following large-scale disturbance and the environmental variables controlling these patterns along an estuary in south Florida. To do this, both ecological surveys and model simulations of forest structure and soil characteristics are integrated in a study of mangrove wetlands in the Shark River estuary. More than 60,000 ha of mangroves in southwest Florida form one of the most extensive mangrove wetlands in the Gulf of Mexico (Davis 1940, Smith et al. 1994). The continuous distribution of mangrove forests in this broad coastal region represents a land-margin landscape gradient from marine to freshwater environments. However, few if any comprehensive system-level studies across this estuarine gradient have been performed on these coastal forested wetlands.

The landscape pattern of mangrove forest development along the Shark River estuary offers opportunities to study several facets of mangrove ecology. In 1960, Hurricane Donna swept through the Shark River region (Craighead and Gilbert 1962), which provides a unique natural experiment to investigate the landscape development of mangrove wetlands following whole-scale disturbance along the estuarine gradient. There is increasing concern over the sensitivity of mangroves to climate change associated with sea level rise and

hurricane frequency (Snedaker et al. 1994, Smith et al. 1994, Wanless et al. 1994). Increased loading of nutrients from agriculture in the upper watershed of the Shark River Slough, which has changed species composition of freshwater marshes in Everglades (Davis 1991, Davis 1994), may also influence mangrove community structure. Therefore, this research not only identifies some of the key environmental factors controlling landscape patterns and development of mangrove wetlands in this region, but also provides essential information to develop ecological models to project the responses of mangroves to natural and human disturbances.

Field measurements were conducted along the gradients of an estuary across complex landscapes from the marine to oligohaline environments. I examined the landscape and seasonal variations in soil nutrient resources and stressors along the Shark River estuary (Chapters 2 and 3). Assessments of nutrient resources include concentrations of total soil nitrogen (N) and phosphorus (P), extractable N and P, P fractions, and pore water nutrients, along with measures of N and P mineralization rates. Stressors include pore water salinity and sulfide concentrations. I quantified the landscape patterns of forest structure after 34 years of regeneration following hurricane disturbance in 1960 as a function of soil resources and stressors along the estuary (Chapter 3). In order to investigate the landscape pattern and development of mangrove forest, I first developed a soil organic matter model to simulate the landscape gradient and vertical distribution of soil nutrients (Chapter 4). I then linked this soil model to a gap dynamic model to simulate mangrove forest development (Chapter 5). The multiple simulations were used to explore the relative importance of gradients in nutrient resources and stressors as controls in the landscape patterns of mangrove forest development.

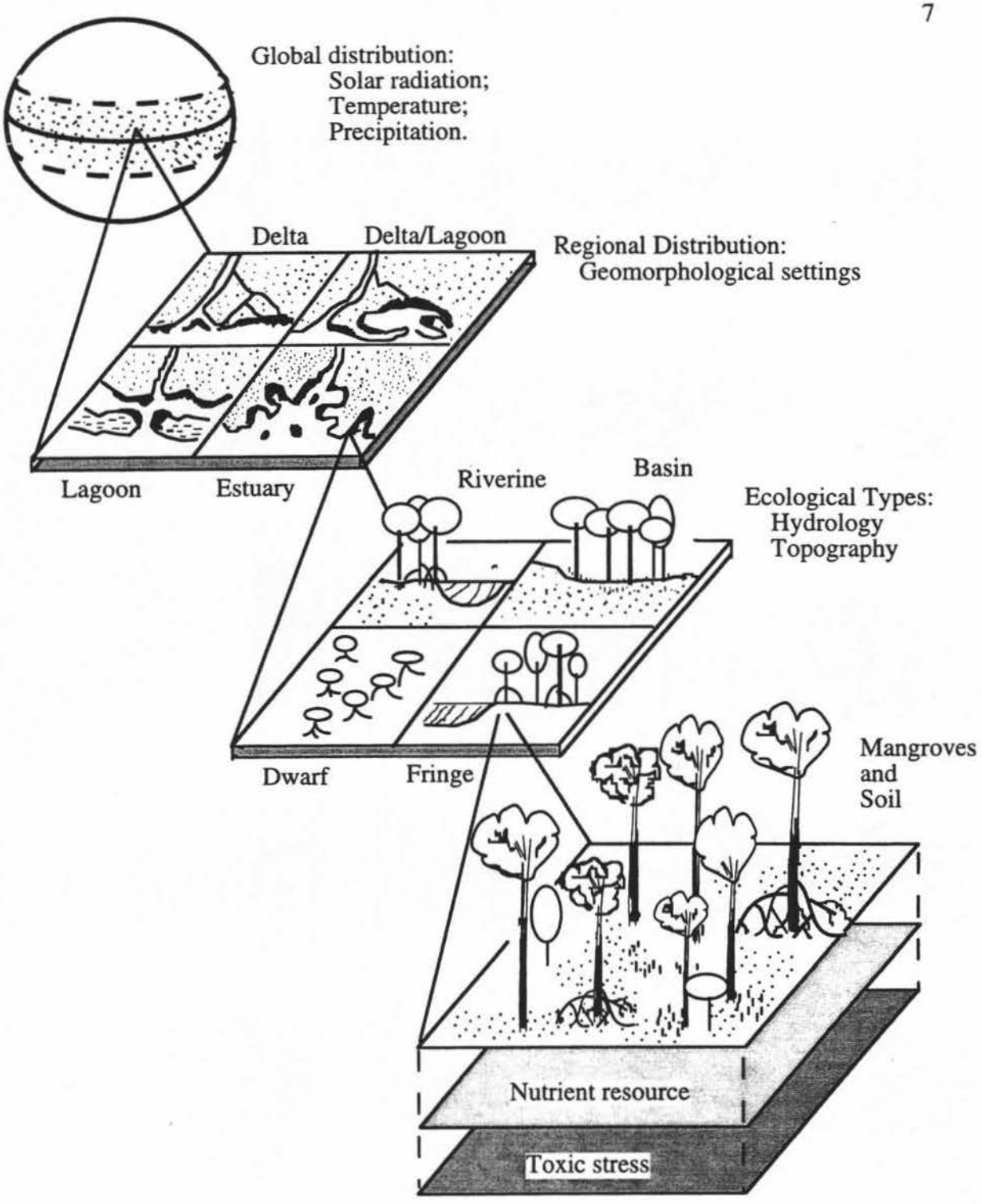


Figure 1.1 Spatial pattern of mangrove forests in relation to hierarchical environmental factors including global climate, regional geomorphological setting, local hydrology and topography, and soil nutrient resource and toxic stress.

CHAPTER 2

SOIL NITROGEN AND PHOSPHORUS AVAILABILITIES IN A MANGROVE LAND-MARGIN ECOSYSTEM

ABSTRACT

The spatial gradients of soil nitrogen (N) and phosphorus (P) mineralization rates, extractable N and P pools, and P fractionation were examined in a mangrove land-margin ecosystem along the Shark River estuary in the Everglades National Park. The mean tree height of mangrove forests linearly declined with distance from the mouth near the Gulf of Mexico to the oligohaline regions of the estuary. Mangrove forests along the estuary represented a landscape gradient of soil N and P availabilities. Higher amounts of extractable ammonium were found in the marine site of the estuary near the Gulf of Mexico. Mean rates of net ammonification and relative ammonification per unit of total N based on 45 d incubation periods decreased exponentially with distance from the estuary mouth to inland sites. N mineralization was positively correlated with total P and available P, but negatively with N:P ratio. Total P and available P increased from the oligohaline to marine sites. There was no net P mineralization in the marine sites based on 45 d incubation periods. Residual P was the largest P fraction in all soils and decreased from 70% in the oligohaline site to 45% in the marine site along the estuary. The percentage of Ca-bound-P increased from 3.3% at the oligohaline site to 32.3% at marine sites. Ca-bound-P pool was larger than Fe-Al-bound P pool in the marine sites, while the reverse was found in the mesohaline and oligohaline sites. The landscape gradient of P in the study area indicates that the Gulf of Mexico is the major source of P in this mangrove land-margin ecosystem rather than direct terrigenous input from inland watershed.

INTRODUCTION

Inputs from terrestrial runoff are generally considered the major nutrient source to support mangrove forest development (Lugo and Snedaker 1974, Day et al. 1987, Twilley 1995). This hypothesis predicts that nutrient availability in mangrove soils will decrease from the landward to seaward zones along the longitudinal axis of a tropical estuary (Carter et al. 1973, Odum et al. 1982, McIvor et al. 1994). The spatial gradient of nutrient availability is suggested as a critical determinant of plant community structure and development based on the inequality of resource utilization by plants along the gradient (Tilman 1982). Greenhouse experiments have demonstrated that seedlings of three Neotropical mangrove species differ significantly in their growth responses to the levels of nutrient availability (McKee 1995*a*). McKee (1995*b*) further showed that seedling recruitment patterns in mangrove forests were related to nutrient gradients. Nutrient enrichment experiments have revealed that the productivity and growth of mangrove forests in Florida (Onuf et al. 1977), Australia (Boto and Wellington 1983) and Belize (Feller 1995, Twilley 1995) can be limited by nutrient availability. These results suggest that studies of nutrient gradients along estuaries can provide valuable information on the effect of landscape patterns of soil nutrient availability on development of mangrove wetlands. However, little research has been performed on the spatial gradient of nutrient availability in a mangrove land-margin ecosystem along a tropical estuary.

Nitrogen (N) and phosphorus (P) availabilities are often implicated as the principal factors controlling forest stature and productivity of mangrove ecosystems (Lugo and Snedaker 1974, Boto and Wellington 1984, Lugo et al. 1988, Clough 1992, Twilley 1995). Soil N mineralization, the microbial transformation of organically combined N into inorganic forms, is an important determinant of N availability in mangrove wetlands. Soil remineralization can

supply a major portion of the N required by plants for growth and reduce the requirement for new nutrients to maintain high levels of productivity. N mineralization is generally used as an index of N availability in terrestrial ecosystems, which is strongly controlled by environmental factors (temperature and moisture), microbes, and substrate quality (Burke 1989, Binkley and Vitousek 1989, Nadelhoffer et al. 1991). Organic N content (Frank et al. 1994), C:N ratio (Wedin and Pastor 1993, Frank et al. 1994), P content (Pastor et al. 1984) and labile pool of mineralizable N (Wedin and Pastor 1993) in soils are recognized as potential factors controlling mineralization rates. In wetland ecosystems, these indices of substrate quality are a function of past and present hydrological processes and plant production (Lugo et al. 1988). Therefore, soil N mineralization in mangrove forests may change with the gradient of substrate quality along a tropical estuary.

Phosphorus availability depends on mineralization of organic matter and is constrained by inorganic chemical reactions (Binkley and Vitousek 1989). Although P has been found to be the primary nutrient limiting the development of mangrove forests (Boto and Wellington 1984, Feller 1995), P mineralization rates have not been measured in mangrove soils (Ellison and Farnsworth 1993). Mangrove soils contain a high proportion of organic P, but most of the organic P tends to be recalcitrant (Alongi et al. 1992). Moreover, most inorganic P is adsorbed and fixed by calcium, iron and aluminum minerals as different chemical forms in mangrove soils (Hesse 1962, 1963). Studies on P fractionation have indicated that the amount and proportion of P forms were related to the degree of weathering and soil development in a desert (Lajtha and Schlesinger 1988) and in Hawaiian islands (Crews et al. 1995). Hydrology is considered the single most important determinant of wetland processes such as soil deposition and erosion, and may determine the spatial gradients of P availability and P forms in mangrove soils along an estuary.

Vegetation can influence spatial patterns of soil nutrient availability by uptake of inorganic nutrients and return of organic materials to soil by litter fall (Pastor et al. 1984). The loss of biomass in canopy gaps may disrupt the spatial pattern of soil nutrient availability by reducing rates of uptake and increasing rates of decomposition and nutrient mineralization stored in living biomass (Canham and Marks 1985). Leaf fall and dead roots associated with canopy gaps caused by lightning strikes, storms and insect herbivory in mangrove forests (Jiménez et al. 1985, Smith 1992) result in a significant pulse of organic matter and associated nutrients to the forest floor and soil (Smith et al. 1994). These changes in nutrient pools and potential shifts in availability of nutrient resources can be important determinant of patterns and rates of mangrove forest regrowth (Clarke and Allaway 1993). Although considerable research has been conducted to measure the effect of enhanced light availability on the growth of mangrove seedlings in canopy gaps, relatively little information is available concerning soil nutrient availability in these disturbed patches of mangrove forest.

More than 60,000 ha of mangroves in southwest Florida including part of the Everglades National Park form one of the greatest land-margin mangroves in the Gulf of Mexico (Smith et al. 1994). The continuous distribution of mangrove forests in this broad coastal region represents an exceptional estuarine gradient, formed by the low energy mixing of fresh and salt water, to evaluate spatial gradients of soil N and P availabilities. I tested the hypotheses that the major N and P source is the direct input of terrestrial runoff in this estuary. I used this estuarine landscape gradient of mangrove forests to describe N and P availabilities by addressing the following questions: (1) Do N and P availabilities in mangrove soils decrease from the landward to seaward zones along the estuary? (2) Are there changes in the fractionation of P in mangrove soils along the estuarine gradient? (3) What is the relative effect of vegetation process in N and P availabilities along this estuarine landscape gradient?

MATERIALS AND METHODS

Study area

The study area was located in the Shark River estuary on the west coastal plain of the Everglades National Park (Fig. 2.1). Mangrove peats deposited over Miami Oolite formed in this region about 3000 yrs ago, coinciding with the most recent rise in sea level at the mid to late Holocene epoch (Scholl 1964*a*, *b*). The Everglades area is topographically flat with an average gradient of 2.8 cm/km from the inland region to the coast (SFWMD 1992). Mangrove forests consisting of three mangrove species, *Rhizophora mangle* L., *Avicennia germinans* (L.) Stearn and *Laguncularia racemosa* (L.) Gaertn., form a continuous band and extend from the Gulf of Mexico to the upland limit of periodic salt water influence, a distance of about 10-20 km. *Conocarpus erecta* L. is also found in coastal forests where the salinity does not exceed 10 g/kg.

The Shark River is one of the largest coastal streams to carry freshwater from the upland Everglades region through the Shark River Slough to the Gulf of Mexico. Mangrove wetlands in this region receive most of the surface fresh water from the Everglades through this Slough. Depending on timing, duration, and magnitude of regional meteorological conditions, the velocity of sheet flow in the Shark River Slough may vary from zero to 480 m/d (SFWMD 1992). The present quantity and quality of water input to the Shark River Slough is modified by human land-use in northern part of the Everglades. Water delivery has been determined to be a function of rainfall, evaporation, and water level in the water conservation areas and the previous week's discharge (Light and Dineen 1994). Tides within the Everglades National Park are predominantly diurnal with a mean amplitude of 1.1 m (Provost 1973, Wang et al. 1994). Monthly sea levels are above the mean annual height from May to November in the

Gulf Coast of Florida (Provost 1973). This results in highly seasonal tidal inundations of mangrove wetlands in southwestern Florida, with peak number of tides occurring in the forest from August to October (Twilley 1985).

Mean annual air temperature in the Everglades National Park is 24°C with little seasonal change (Thomas 1974, Duever el al. 1994). Mean monthly air temperatures range from a January low of 19°C, to a high in August of 28°C (Thomas 1974). Average annual precipitation in the Everglades National Park is 1320 mm with distinct wet and dry seasons (Thomas 1974). Precipitation in the wet season (June to September) is approximately 60% of annual precipitation, and is produced primarily by thunderstorms. About 25% of the annual precipitation falls during the dry season (November to April), which results from the passage of warm and cold air masses. Rainfall in May and October tends to be transitional.

Field sampling and vegetation measurement

Vegetation and soil properties were examined at four mangrove forests along a natural gradient of the Shark River estuary from the Gulf of Mexico to the inland mangrove-marsh ecotone (Fig. 2.1). The four sites ranged from 25°19'N, 81°08'W to 25°25'N, 80°58'W and are located about 1.4, 4.1, 9.9 and 18.2 km inland from the estuary mouth, respectively. These mangrove sites represent a salinity gradient from tide-dominated inundation near the estuary mouth to fresh water runoff from the Shark River Slough in the upstream region. According to Duke's (1992) classification of mangrove habitats and the terminology of Odum et al. (1984) for salinity zones of an estuary, S1 and S3 sites are downstream locations in marine zone of the Shark River estuary, while S4 is in an intermediate location in the mesohaline zone and S6 is an upstream location in the oligohaline zone (Fig. 2.2). Since mangrove forests in this region are recovering from destruction by Hurricane Donna in 1960

(Craighead and Gilbert 1962), mangrove forests at each site along the Shark River region are assumed approximately even aged.

A 20 x 20 m plot about 10 to 20 m inland from the estuary was established at sites S1, S3 and S4. A smaller plot (10 x 15 m) about five m from the estuary was set at S6, due to the restricted band of mangroves along the river in this upstream region. DBH (diameter at breast height) of all trees >2 cm was measured in each plot in January 1995. Fifteen to 20 trees were randomly chosen for measurement of tree height by range finder in each plot. The relationship between DBH and tree height was fitted by regression for each species. Mean tree height at each site was determined for all trees in each plot based on this regression.

To assess nutrient availability in surface soils without a canopy (less vegetation effect), a canopy gap less than 30 m from the intact forest plot in sites S1, S3, and S4 was used for comparisons. The gap in S1 was apparently caused by a lightning strike, while the gaps in S3 and S4 were associated with storm-related treefall. The sizes of gaps in S1, S3 and S4 were 502 m^2, 48 m^2 and 37 m^2, respectively. The ages of gaps were estimated to be at about three yrs based on ages of seedlings under the gaps (Duke and Pinzón 1992).

Soil property determination

The timing of three sampling trips was based on seasonal climatic and hydrological regimes. January represents the dry season with low rainfall and fewer tidal inundations. August represents the wet season with high rainfall and high tidal flooding frequencies. May corresponds to a transient season between dry and wet seasons. Three randomly chosen stations in each intact forest plot and canopy gap were marked in August 1994 for repeated measures of soil properties and mineralization rates in August 1994, January and May 1995. Soils were collected with a 5.0 cm diameter corer at each site from surface to 40 cm depth.

Soil samples at 10 cm interval were stored on ice in polyethylene bags in the field, and stored at 4°C in the laboratory prior to analysis. Recognizable plant litter and coarse root material were removed. Subsamples of soils were oven-dried to constant weight at 60°C and ground with a Wiley Mill to pass through a 250 μm mesh. Cores with a 15.2 cm diameter were used to estimate soil bulk density since the wider diameter eliminated compaction. Carbon (C) and N contents were determined on two replicates of each sample with a LECO CHN analyzer using standard protocols. Total P was extracted from soils with 1N hydrochloric acid after ignition at 550°C (Aspila et al. 1976) and determined using molybdenum blue, and ascorbic acid as reducing agents (Parsons et al. 1984). Extractable PO_4-P (P_{ext}) was determined by dilute acid-fluoride extraction of fresh soil samples (Olsen and Sommers 1982). The extract was analyzed colorimetrically for soluble reactive phosphorus. Amount of P extracted by this method is generally used as the available P index in plant ecology (Vitousek and Denslow 1986, Lajtha and Schlesinger 1988, Binkley and Vitousek 1989, Walbridge 1991).

N and P mineralization

Numerous techniques for measurements of soil mineralization have been developed, but no one method provides accurate estimates of N and P, thus all methods should be considered an index of nutrient availability for comparative purpose (Binkley and Vitousek 1989). The potential problems caused by field measures are that net mineralization may reflect treatment differences in microclimate rather than differences in the quality or quantity of soil organic matter (Wedin and Pastor 1993). Laboratory incubation can provide information on the amount of mineralizable N and P at the time of sampling. I used an anaerobic incubation of soil cores in the laboratory to determine net N and P mineralization. This allows a comparison of soil quality across a range of sites in the mangrove land-margin ecosystem under comparable

conditions. Intact soil cores were collected in glass tubes to maintain soil structure, which can be an important factor that influences soil microbial activity (Robertson et al. 1988). Glass tubes (2.5 cm diameter and 10 cm length) were placed in a soil recovery probe and driven into the soil. The end of each tube was capped with a rubber sleeve immediately after collection to avoid aeration, and the tube was stored on ice in a cooler. Paired tube samples at each depth of 0-10 and 10-20 cm intervals were collected at each sampling station. After samples were transported to the laboratory, one tube from each pair was anaerobically incubated in the dark in an environmentally controlled chamber at 25°C for 15 d. The other tube was kept at 4 °C until extracted with 1 mol/L KCl within 7 d of collection.

Soils were extracted with 1 mol/L KCl (1:10 mass/volume). The extract was centrifuged and analyzed for NH_4-N by colorimetric method (Parsons et al. 1984), and for NO_x-N and PO_4-P with an ALPKEM autoanalyzer using standard techniques. Ammonium and nitrite+nitrate extracted from initial soils was treated as extractable ammonium (NH_4-N) and extractable nitrite+nitrate (NO_x-N), respectively. Rates of net nitrification, ammonification and P mineralization for each soil depth were determined by subtracting the initial concentration of respective nutrients (NO_x-N, NH_4-N, and PO_4-P) from concentrations at the end of the incubation period. Mineralization rates were converted to a soil area basis with respective bulk density values.

P fractionation

The sequential extraction scheme selected was developed by Hieltjes and Lijklema (1980) and a modification of P fractionation scheme has been successfully used to characterize P in Everglades wetland soils (Koch and Reddy 1992, Gale et al. 1994) and estuarine sediment (Zwolsman 1994). Soil samples for P fractionation were collected in August 1994. Fresh soil

samples were sequentially extracted with 1 mol/L KCl (1:10 w/v) with 2 h of shaking at 250 rpm; 0.1 mol/L NaOH with 16 h of shaking; and 0.5 mol/L HCl with 24 h of shaking. After each step, the suspensions were centrifuged and the supernatants were analyzed colorimetrically for inorganic P (soluble reactive phosphate) using an ascorbic acid reduction method (Parsons et al. 1984). A subsample of the NaOH extract was digested by the Kjeldahl procedure (US EPA 1979) to determine total P in the extract. The portions of P in extractions with KCl, NaOH and HCl solution are defined respectively as: labile P, Fe-Al bound P, and Ca-bound P (Gale et al. 1994). Organic P determined as the difference between total P and inorganic P in the NaOH-extract is defined as hydrolyzable organic P. Residual P is the difference between the total P as determined by ignition-acid extraction method (Aspila et al. 1976) and the sum of P extracted.

Statistical analysis

My primary objectives were to compare substrate quality of mangrove soils along the longitudinal gradient of the Shark River estuary and to determine the effect of substrate quality on soil nutrient availability. I used linear regression models to test the dependencies of total soil C, N and P pools at four mangrove forests on distance from the mouth of the estuary. A repeated-measures ANOVA was used to analyze the effects of site and season on P_{ext}, NH_4-N, NO_x-N, ammonification and P mineralization in soils from intact forests. I also used one way ANOVA to test the effect of site on NH_4-N, NO_x-N and P_{ext} pools, net N and P mineralization, and P fractionation at each sampling date. In these ANOVAs of soil parameters, I restricted the tests for the effects of site along the estuary to soils taken under intact mangrove forests. When a main effect was significant, tests based on the ANOVA model were used to make multiple comparisons of means using Tukey's test. I also used t-

tests to look for the effect of vegetation (canopy gap vs. intact forest) on P fractions at each site and a repeated-measures ANOVA on other nutrient variables. All statistical tests were done by using either original data or log-transformed data in order to meet assumptions of parametric analysis. I used SAS (SAS 1989) to perform all statistical tests.

RESULTS

Tree height, salinity and soil nutrient content

Mean water salinity of three sampling days in Shark River estuary increased from 1.4 g/kg in S6 to 27.2 g/kg in S1 (Fig. 2.2). Mean tree height of the even-aged mangrove forests in the land-margin transition increased from 5.4 m at S6 to 10.1 m at S1 (Fig. 2.2). The correlations between salinity, tree height and distance from the mouth of the estuary were highly significant. Both total C and N concentrations in the top 40 cm of mangrove soils showed a significant linear decrease along the Shark River estuary from S6 (C=43.3%, N=2.33%) to S1 (C=14.3%, N=0.7%) (Table 2.1). However, P concentrations showed an inverse relation with distance from the estuary mouth, increasing from 0.06% in S6 to 0.11% in S1 (Table 2.1). When nutrient pools were expressed as mass per unit area, C and N pools were not correlated with distance along the estuary (Fig. 2.3). However, P pools exponentially increased from 26.3 g/m^2 in S6 to 152.2 g/m^2 in S1 along the estuary (r^2=0.95, P<0.05). The total P pool in mangrove soil was six times greater in S1 than in S6 (Fig. 2.3). The consistent relation between C and N concentrations in these mangrove soils was reflected in atomic C:N ratios between 22:1 and 25:1 along the entire longitudinal axis of the estuary. Atomic N:P ratios exponentially increased with distance from the estuary mouth from 15:1 at S1 to 102:1 at S6 (r^2=0.99, P<0.05).

Soil N and P availabilities along the estuary

Extractable N and P pools. - The repeated measures ANOVA showed significant effects of site on the amount of NO_x-N without showing season effects (Table 2.2). Multiple comparisons of means in each sampling season showed a significant site effect on NO_x-N only for January (Fig. 2.4). Results of NH_4-N and NO_x-N extracted by KCl indicated that most of the inorganic N in these mangrove soils was dominated by NH_4-N (Fig. 2.4). The repeated measures ANOVA showed significant effects of site and season on the amount of NH_4-N with a significant interaction factor (Table 2.2). Amounts of NH_4-N were generally high at S1 during all three sampling seasons (Fig. 2.4). Mean NH_4-N pools within the 0-20 cm soil for three seasons increased significantly along the estuary at 0.35, 0.36, 0.55 and 0.97 g/m^2 from the oligohaline to marine sites (Fig. 2.5).

The repeated measures ANOVA showed significant effects of site and season on the amount of P_{ext} with a significant interaction factor (Table 2.2). This site difference for P_{ext} was more pronounced in January 1995 with less site differences in August 1994 (Fig. 2.4). The P_{ext} pool was significantly greater in S1 for all sampling dates, but not significantly different between S4 and S6 at August and May samplings (Fig. 2.4). Mean P_{ext} pools within the 0-20 cm soil for all three seasons were 1.60, 0.98, 0.48 and 0.42 g/m^2 in S1, S3, S4 and S6, respectively. Thus both P_{ext} and NH_4-N pools exhibited an increase from the oligohaline to marine zones in this mangrove land-margin ecosystem (Fig. 2.5).

Nitrogen mineralization. - The production of NO_3-N from the remineralized NH_4-N in the soil incubations was negligible for all sites and seasons (data are not shown). Repeated ANOVA tests of ammonification indicated significant effects of site and sampling season with significant

interactions (Table 2.2). Multiple comparisons of means in each sampling season revealed significant site effects only in January and May (Fig. 2.6). Net NH_4-N production occurred in January and May, but net immobilization was found in August for all sites. Mean daily net ammonification rates within the 0-20 cm depth for three seasons decreased exponentially with distance from the downstream (182 $mg \cdot m^{-2} \cdot d^{-1}$ in S1 and 135 $mg \cdot m^{-2} \cdot d^{-1}$ in S3) to intermediate and upstream sites (46 $mg \cdot m^{-2} \cdot d^{-1}$ in S4 and 17 $mg \cdot m^{-2} \cdot d^{-1}$ in S6) (Fig. 2.5). Therefore soils in S1 can potentially supply more than 10 times the amount of NH_4-N mineralized in S6.

P mineralization.- Net P mineralization rates measured as the difference in extractable P (by KCl) during an incubation period were more variable than N mineralization (Fig. 2.6). There was a significant effect of site in January with a significantly higher net P mineralization in S4 and S6 (Fig. 2.6). Repeated measures ANOVA showed that the season effect on P mineralization was significant (Table 2.2). Mean daily rates of net P mineralization averaged over the three seasons within the 0-20 cm soil were positive at S4 (4.78 $mg \cdot m^{-2} \cdot d^{-1}$) and S6 (1.28 $mg \cdot m^{-2} \cdot d^{-1}$), compared to negative values reflecting immobilization at S1 (-1.43 $mg \cdot m^{-2} \cdot d^{-1}$) and S3 (-0.04 $mg \cdot m^{-2} \cdot d^{-1}$).

P fractionation.-There were significant differences in absolute amounts of labile-P, Fe/Al-bound-P, hydrolyzable-organic-P, Ca-bound-P and residual P at 0-20 cm depths at sites along the estuary (Table 2.3). The amount of labile P was significantly higher in S1 than other sites and was not significantly different among S3, S4 and S6 (Table 2.3). Labile P never exceeded 2% of the total amount of P among all sites within the 0-20 cm depth, and the percent of labile P was higher in S6 (1.9 %) than in S3 (0.7%) and S1 (0.8%) (Fig. 2.7).

Fe/Al-bound-P pools increased from S6 (1.24 g/m^2) to S1 (5.58 g/m^2) (Table 2.3). However, the percent of Fe/Al-bound-P in the total P ranged from 8.2% to 10.5% and did not exhibit a significant trend along the estuary (Fig. 2.7). The amount of hydrolyzable-organic-P ranged from 2.39 to 7.64 g/m^2 and was significantly higher in S1 and S3 then in S4 and S6 (Table 2.3). The highest percent of hydrolyzable-organic-P fraction of the total P was in S4 (21%), and this contribution was similar among S1, S3 and S6 (Fig. 2.7). Except in S1, hydrolyzable-organic-P was the second largest pool of P in these mangrove soils.

Ca-bound-P pools ranged from 0.50 to 21.33 g/m^2 and had the most significant increase from S6 to S1 in the estuary, which indicated there was 40 times more Ca-bound-P in S1 than in S6 (Table 2.3). The percentage of Ca-bound-P also increased significantly, from 3.3% in S6 to 32.6% in S1 (Fig. 2.7). Ca-bound-P pool was larger than Fe-Al-bound P pool in S1 and S3, while Fe-Al-bound P pool was larger than Ca-bound-P pool in S4 and S6. Residual P was the largest P fraction in all sites, with a significant increase in percentage from 45% in S1 to 70% in S6 along the estuary (Fig. 2.7). However, the amount of residual P increased significantly from S6 toward S1 (Table 2.3).

Soil N and P availabilities in canopy gaps and forests

The repeated ANOVA indicated a significant vegetation effect on P_{ext} with a mean of 1.31 g/m^2 in canopy gaps compared to 1.02 g/m^2 in the intact forests (Fig. 2.3, Table 2.4). The repeated ANOVA also showed there was a significant effect of vegetation and season with interaction factor for NO_x-N. Mean NO_x-N was 20.9 mg/m^2 in the intact forests compared to 12.4 mg/m^2 in the canopy gaps (Fig. 2.3, Table 2.4). There were no significant differences in NH_4-N, net ammonification and P mineralization rates between canopy gaps and forests. Paired comparisons revealed that there were no significant effects of vegetation on any of the P

fractions in sites S1, S3 and S4 (Table 2.3).

DISCUSSION

The effect of vegetation on N and P availabilities

Amounts of extractable soil P, nitrate and nitrite were higher in canopy gaps than intact forests in this study. Vitousek and Denslow (1986) have reported that P availability was slightly higher in crown-fall zones than in intact forests of a lowland tropical rainforest. Mladenoff (1987) also found higher soil P concentrations in canopy gaps of a northern hardwood-hemlock forest and suggested that the higher P content in gaps was due to the reduced uptake of N. Loss of vegetation in gaps also may directly reduce the uptake of P by plants. Mangrove vegetation can transport oxygen through roots into soil and enhance soil redox potential (McKee 1993). Therefore oxidized soil may promote transformation of ammonium to nitrate+nitrite. Overall, canopy gaps had no effect on N and P mineralization (Table 2.4). The laboratory incubation method for mineralization in this study did not reflect the effects of environmental factors such as changes of temperature and moisture, which are influenced by absence of a forest canopy. These results only compare the effect of an absence of plant biomass on substrate quality. Although large scale disturbances such as hurricanes can dramatically increase the detrital pool in mangrove forest (Smith et al. 1994), the effect of small gaps on nutrient availability may depend on gap age, gap size and vegetation structure (Vitousek and Denslow 1986, Mladenoff 1987, Zhang and Zak 1995). The size of gaps in this study ranged from 37 to 502 m^2. In addition, tidal flooding in mangrove wetlands may reduce the gap effects on nutrient availability by redistributing detritus in mangrove forests.

Landscape trends and control of N availability

Total soil N (0.7 to 2.3%) in the mangrove land-margin ecosystem studied here is higher than global estimates of total N concentrations in mangrove soils, which range from 0.02 to 0.4% (Alongi et al. 1992). In contrast to soil P concentrations, soil N concentrations decreased from 2.3% at the oligohaline site to 0.7% at the marine site of the estuary. However, the soil N pool per unit area was fairly constant across this mangrove land-margin at about 1.0 kg/m^2 within 0-40 cm depth. The tendency of soil N concentrations along the estuary associated with total C concentrations suggests that there is an accumulation of recalcitrant organic matter that is resistant to decomposition. Walbridge (1991) suggested that soil organic N accumulates as soil P availability decreases in P-deficient systems. Two possible mechanisms may involve this biogeochemical process. P mineralization from organic matter is often the direct result of phosphatases produced by plants and microbes without the microbial oxidation of organic matter and associated N (McGill and Cole 1981). The selective reabsorption of P relative to N by plants during leaf senescence reduces the relative uptake of P compared to N and accelerates the cycling of N between soil and plants (Walbridge 1991). In addition, the higher bulk density in the marine zone of the Shark River estuary may dilute N concentration.

In this study, N existed mostly as organic N, with the small amount of inorganic N comprised primarily of ammonium. This is consistent with other studies of mangrove soils showing that the extractable nitrate+nitrite pool is a small proportion of the total amount of inorganic N (Boto and Wellington 1984, Rivera-Monroy et al. 1995). However, nitrate can be an important source of inorganic N for mangrove growth (Boto et al. 1985).

Seasonal changes in ammonification rates can be the result of variation in substrate quality. This study showed that net ammonification was negligible with evidence of

immobilization in August; however, net ammonification rates in January (35-239 $mg \cdot m^{-2} \cdot d^{-1}$) and May (18-70 $mg \cdot m^{-2} \cdot d^{-1}$) are comparable to other macrophyte systems such as subtropical seagrasses (28-294 $mg \cdot m^{-2} \cdot d^{-1}$) (Boon et al. 1986), tidal freshwater marsh (44 $mg \cdot m^{-2} \cdot d^{-1}$) (Bowden 1984), and marine sediment (24-106 $mg \cdot m^{-2} \cdot d^{-1}$) (Blackburn and Henricksen 1983). In all of these studies net ammonification rates were measured under controlled conditions. In a case study measuring seasonal variation of ammonification in coastal wetlands, Abd. Aziz and Nedwell (1986) also found that the ammonification rate under controlled condition was minimal during summer. They suggested that seasonal changes in the rates were related to the variation in available mineralizable organic N. The latter accumulates during winter due to low temperature and is gradually depleted from spring to summer with increased mineralization rates.

The mineralizable organic N is a small proportion of the total N in mangrove soils, not only due to higher annual temperature, but also to the temporal pattern in litter production and export. Litter production in south Florida generally peaks during August to October (Pool et al. 1975, Twilley et al. 1986). Surface litter mass on the forest floor in a basin mangrove forest of southwestern Florida remains high from October or November to May, and is significantly lower from July to September (Twilley et al. 1986). This temporal pattern of litter mass on the forest floor is coincident with the tide flooding frequency (Twilley 1985). There are less than eight tides per month in a Florida basin mangrove forest from December to April, compared to over 30 when seasonal sea level peaks exceed mean sea level in September (Twilley 1985). Thus, litter mass is accumulated after peak litter production because of the decreasing tidal flooding frequency and relatively low temperature. The higher soil ammonification rate in January under controlled conditions corresponds to the accumulation of potential mineralizable organic N during this period. When tidal flooding frequency and

temperature increase starting in late spring, fresh organic matter is exported by tidal exchange and consumed by microbial decomposition.

Mangroves have a maximal growth during summer in Florida (Gill and Tomlinson 1971). Plant roots are able to absorb almost all available N from soil, which causes a strong competition between plants and microbes for inorganic nutrients. When live roots are excluded from sampling cores under controlled conditions, microbial communities can absorb the N released from mineralization. Immobilization occurs when there is insufficient mineralizable organic N due to depletion by microbes and tidal export during spring to summer. This suggests that mangrove growth in this region may be more limited by N availability in summer than in the other seasons.

The method of core-sampling with glass tubes to measure ammonification rates under controlled laboratory conditions provides an estimate of net NH_4-N production. N mineralization was not correlated with either total C and N pools or C:N ratios (Table 2.5). This suggests that ammonification rates in this mangrove region are independent of the total N concentration. Mean rates of net ammonification were significantly correlated with initial extractable phosphate and ammonium pools, while being negatively related to N:P ratios (Table 2.5), suggesting that N mineralization is regulated by phosphate and ammonium supply. Highly significant correlations of microbial activity with P components in New Guinea mangrove muds indicate that microbial activity is probably P-limited in mangrove soils, which then may limit N mineralization (Alongi et al. 1993). Pastor et al. (1984) also found inorganic N and P supply limiting N mineralization in terrestrial forests.

Relative N mineralization (N mineralization per unit of total N) is a useful index to compare overall substrate quality as a factor determining N mineralization rates (Schimel et al. 1985, Pastor et al. 1987, Hart and Gunther 1989, Polglase et al. 1992). Relative N

mineralization decreased exponentially with distance from the mouth of the estuary (Fig. 2.8). This indicates that the proportion of recalcitrant organic N in mangrove soils increases rapidly with distance from the Gulf of Mexico to inland mangrove-marsh ecotone. A decrease in rates of N mineralization associated with declines in organic matter quality with increasing soil age has been observed in a prairie (Schimel et al. 1985) and old fields (Pastor et al. 1987).

In addition to the composition of soil organic matter, the species composition of forests has been suggested as an important factor influencing soil N mineralization through quality and quantity of litterfall (Pastor et al. 1987, Hart and Gunther 1989). Wedin and Tilman (1990) have experimentally demonstrated that differences in the tissue N concentration, below ground lignin concentration and below-ground biomass of grass species resulted in differences in annual net N mineralization. There are only three mangrove species in the study area, however their distribution is distinct among sites with *L. racemosa* and *A. germinans* dominating in the downstream location and *R. mangle* dominating in the intermediate and upstream locations (Chapter 3). It is well documented that *Avicennia* litter decomposes more quickly than that of other species due to high nutritive quality and lower concentration of tannin (Twilley et al. 1986, Alongi et al. 1992). *R. mangle* leaves are have higher concentrations of condensed tannins than *A. germinans* and *L. racemosa* (McKee 1995*a*, *b*). Tannin and other polyphenolic compounds can inhibit microbial activity in mangrove soils (Benner et al. 1986, Alongi et al. 1992). Lacerda et al. (1995) found that there is an increase in the contribution of carbohydrates and amino acids to the soil organic pool in *Avicennia* soils but not in *Rhizophora* soils. They further suggested that organic matter associated with *Avicennia* soil is more degradable than with *Rhizophora*. Thus, P availability, substrate and litter quality can potentially control the spatial gradient of N availability in mangrove soils. In addition, spatial trends in soil P gradients coupled to N availability could in turn strongly influence mangrove

forest development and composition.

Landscape trends and control of P availability

The concentrations of total P (0.06-0.12%) in the mangrove soils along the Shark River estuary are within the values (0.01-0.16%) for mangrove soils in the world (Alongi et al. 1992). However, more than half of the total P in this study area existed in a residual form. Available source of inorganic P to mangrove soils include mineralization of organic P matter, solubilization of mineral-P, and external flooding of tidal waters (Alongi et al. 1992). Mangroves absorb these pools of inorganic P and return them as organic-P through litterfall to the forest floor. Anaerobic mangrove soil limits the oxidation of organic matter by microorganisms and a greater proportion of P remains in the residual P pool. This pool of organic P becomes chemically recalcitrant and is not available for mangrove utilization (Boto 1991).

Rates of net P mineralization measured in this study are based on the net change in the concentration of the labile P pool. This net change is a balance between P release from the mineralization of organic P and dissolution from minerals, and uptake by microbes and adsorption by minerals during the incubation. The 1 mol/L KCl solution used in this study mildly extracts labile P, which constitutes less than 2% of the total P pool in these mangrove soils. The results revealed a small release of P from soil mineralization in the mesohaline and oligohaline sites, but no net P mineralization in the sites close to the mouth of the Shark River estuary. These data suggest that strong immobilization of labile P occurs in mangrove soils with higher rates of N mineralization. Bacteria in mangrove soils are highly productive and they can sequester much of the labile nutrients in sediment (Alongi et al. 1993, Robertson and Phillips 1995). Microbes are able to immobilize almost all of the labile P produced from

organic mineralization in acid organic soils (Walbridge and Vitousek 1987, Walbridge 1991). Rapid immobilization of amended inorganic phosphorus (30 mg/kg) suggests that P adsorption by minerals in mangrove soils can strongly immobilize soluble reactive phosphate (Hesse 1962, 1963). Adding 400 kg P/ha to mangrove soils in Australia increased the concentration of extractable P to only ~65 μg/g above ambient levels of 20-30 μg/g (Boto and Wellington 1983, Alongi et al. 1992). Higher Ca-bound-P was found in the marine sites than in the oligohaline site along the Shark River estuary, indicating the relative influence of carbonate processes at the mouth of the estuary. It has been demonstrated that carbonate can rapidly adsorb the inorganic P released from mineralization of organic matter (DeKanel and Morse 1978, Binkley and Vitousek 1989). Therefore, both the carbonate fixation of P and microbial immobilization may contribute to the absence of net P mineralization at the downstream mangrove sites in the Shark River estuary. KCl extraction is too mild to desorb phosphate adsorbed by Ca, Fe and Al minerals, but P in these minerals may be partly available to mangroves. Thus, P mineralization rates in this study probably underestimate the concentration of biologically available P in mangrove soils.

Changes in the chemical forms of P can be a function of soil development as demonstrated in soils of desert (Lajtha and Schlesinger 1988) and Hawaiian islands (Crews et al. 1995). In both case studies, Ca-bound-P decreased with increasing soil age, but residual P showed a reverse trend. In my study, sequential extractions of P indicate a significant increase in Ca-bound-P and decrease in residual-P as percentage of total P from the oligohaline to marine sites of the estuary. This landscape trend in P distribution is probably not related to soil age, since known mangroves have existed in this region for more than 3000 yrs (Scholl 1964*a, b*). Forms of soil P in mangroves with open nutrient cycles may depend on the source of P input. A significantly higher Ca-bound-P as the percentage of total P near the mouth of the

estuary suggests that the greater bulk density concentration of P in the marine sites may be related to the deposition of carbonate sediment from the Gulf of Mexico. Upstream mangroves at the head of the estuary receive less mineral sediment and show a greater proportion of organic P.

Geomorphology, topography and hydrology play important roles in determining the spatial gradient of P availabilities. The environmental setting in this mangrove land-margin ecosystem was identified by Thom (1984) as a mainland carbonate platform, in which terrestrial sediment supply is low but calcareous sediment production dominates. Mangrove soils in the study area consist of mangrove residuals and carbonate sediment (Scholl 1964*a, b*), and thus weathering of minerals in parent rock material is not an important source of nutrients (Fourqurean et al. 1993). The other external sources of phosphorus in this carbonate setting are water and sediment from the Everglades and the Gulf of Mexico, or precipitation. Upstream marshes in the Shark River Slough effectively reduce surface water P concentrations to levels near detection limits, which leads to relatively low P inputs to the Everglades National Park, despite the increased loading of P into marshes (Davis 1994). The results from the Shark River estuary indicate that tidal water and suspended sediments from the Gulf of Mexico represent a major source of nutrients to the mangroves. When a tide transports dissolved and suspended P from the Gulf of Mexico into the Shark River estuary, the availability of this imported P to the mangroves will depend on the tidal elevation relative to the topography of the mangroves. There is no direct measurement of P flux in this mangrove wetland, but other studies on the exchange of P between vegetated coastal wetland and adjacent waters have suggested that marsh (Wolaver and Spurrier 1988) and mangroves (Boto and Wellington 1988) are a sink of P. Long-term P accumulation is linked with external inputs in mangrove wetlands (Lynch et al. 1989, Twilley et al. unpublished manuscript), saltmarsh (DeLaune et al. 1981)

and fresh-water wetlands (Craft and Richardson 1993*a*,*b*, Reddy et al. 1993). Lynch et al. (1989) found higher accretion rates in riverine and fringe mangroves than in basin mangroves of Florida and Mexico. P accumulation was negatively correlated with distance from upland inflows in the Everglades fresh-water wetlands (Craft and Richardson 1993*a*,*b*, Reddy et al. 1993). Total P and available P in mangrove soils had a significant landscape trend with an increase from oligohaline to marine zones along the Shark River estuary. These results support the hypothesis that the major source of P in mangrove wetlands distributed along an estuary in a carbonate mainland environment is from the marine source of the estuary, and not directly from terrestrial runoff. The hypothesis that freshwater sources of nutrients control the supply of P in mangrove estuaries is specific to those geomorphological settings with terrigenous sediments (Thom 1982).

Table 2.1. Soil C, N and P concentrations and bulk density along the Shark River estuary. Data are means of three seasons ± SE. Correlation coefficients are between respective soil variables for each site and distance from the mouth of the Shark River estuary (* $P<0.05$, ** $P<0.01$).

Variables	Sampling position	S1	S3	S4	S6	Correlation coefficient (r)
Distance from the estuary mouth (km)		1.8	4.1	9.9	18.2	
Total C (%)	Forest	14.3 ± 0.3	22.2 ± 1.2	32.5 ± 1.5	43.3 ± 1.1	0.985*
	Gap	20.0 ± 0.7	22.9 ± 1.2	33.3 ± 1.7		
Total N (%)	Forest	0.70 ± 0.07	1.15 ± 0.09	1.55 ± 0.07	2.33 ± 0.10	0.990**
	Gap	0.97 ± 0.07	1.26 ± 0.04	1.59 ± 0.10		
Total P (%)	Forest	0.11 ± <0.01	0.12 ± <0.01	0.09 ± <0.01	0.06 ± <0.01	-0.960*
	Gap	0.09 ± <0.01	0.10 ± <0.01	0.09 ± <0.01		
Bulk density (g/cm^3)		0.462	0.212	0.148	0.135	-0.751

Table 2.2. Summary of F statistics from repeated measures ANOVA of site and season effects on nutrient availability. Statistical tests were conducted using univariate tests. Effect of sampling station was not significant ($P>0.05$).

Sources	df	NH_4-N	P_{ext}	NO_x-N	Ammonification	P mineralization
Site	3,8	26.85***	108.5***	8.15**	7.53*	4.10*
Season	2,16	17.28***	10.88***	2.68	75.70***	8.38**
Site*season	6,16	3.84*	4.10*	1.91	7.88***	8.83***

*$P\leq0.05$, **$P\leq0.01$, or ***$P\leq0.001$

Table 2.3 Phosphorus fractionation at 0-20 cm depth in sediments from intact mangrove forests and canopy gaps. Data are means ± SE (n=3). The superscript letters indicate significant differences (Tukey's $P<0.05$) among sites in P components under intact forests.

Sampling Position	Site	Soil P components (g/m^2)				
		Labile-P	Fe/Al-bound-P	Hydrolyzable organic-P	Ca-bound-P	Residual P
Forest	S1	0.54^{a} ±0.04	5.58^{a} ±0.21	7.64^{a} ±0.39	21.33^{a} ±1.60	30.36^{a} ±5.68
	S3	0.26^{b} ±0.06	3.32^{b} ±0.37	6.55^{a} ±0.52	5.87^{b} ±1.21	23.32^{ab} ±2.28
	S4	0.30^{b} ±0.03	2.66^{b} ±0.34	5.40^{b} ±0.40	0.92^{c} ±0.04	16.14^{ab} ±2.07
	S6	0.29^{b} ±0.02	1.24^{c} ±0.03	2.39^{c} ±0.16	0.50^{c} ±0.03	10.69^{b} ±0.59
Site effect $P=$		0.003	<0.001	<0.001	<0.001	0.013
Canopy gap	S1	0.84 ±0.13	5.61 ±0.60	6.64 ±0.24	16.74 ±2.67	20.92 ±1.66
	S3	0.34 ±0.02	3.26 ±0.28	5.33 ±1.00	8.03 ±0.97	17.26 ±1.69
	S4	0.24 ±0.02	2.36 ±0.12	4.57 ±0.43	0.81 ±0.04	15.55 ±1.69
Vegetation effect $P=$		ns	ns	ns	ns	ns

Table 2.4. Summary of F statistics from repeated measures ANOVA of vegetation (intact forest vs canopy gap) and season effects on nutrient availability. Statistical tests were conducted using univariate tests. Effect of sampling station was not significant ($P>0.05$).

Sources	df	NH_4-N	P_{ext}	NO_x-N	Ammonification	P mineralization
Vegetation	1,4	1.74	41.3**	37.0**	0.88	0.44
Season	2,44	1.47	2.69	3.66*	37.09**	5.85**
Vegetation*season	2,44	2.25	0.33	5.41**	0.22	1.42

*$P\leq0.05$, **$P\leq0.01$, or ***$P\leq0.001$

Table 2.5 Linear correlations among N mineralization (N_{min}), P mineralization (P_{min}) and other soil properties within the 0-20 cm depth in mangrove forests and gaps. (Mean values over three seasons were used for correlative analysis). (* $P \leq 0.05$, ** $P \leq 0.01$, *** $P \leq 0.001$).

	N_{min} mg·m^{-2}·d^{-1}	P_{min} mg·m^{-2}·d^{-1}	NH_4-N g/m^2	P_{ext} g/m^2	Total C kg/m^2	Total N g/m^2	Total P g/m^2	Atomic C:N
P_{min}	-0.700							
NH_4-N	0.853*	-0.716						
P_{ext}	0.926**	-0.668	0.960***					
Total C	0.332	-0.393	0.770*	0.623				
Total N	0.314	-0.390	0.698	0.610	0.918**			
Total P	0.883**	-0.757*	0.906**	0.852*	0.563	0.431		
C:N	0.270	-0.321	0.576	0.379	0.671	0.328	0.626	
N:P	-0.876*	0.472	-0.672	-0.727	-0.146	0.030	-0.826*	-0.449

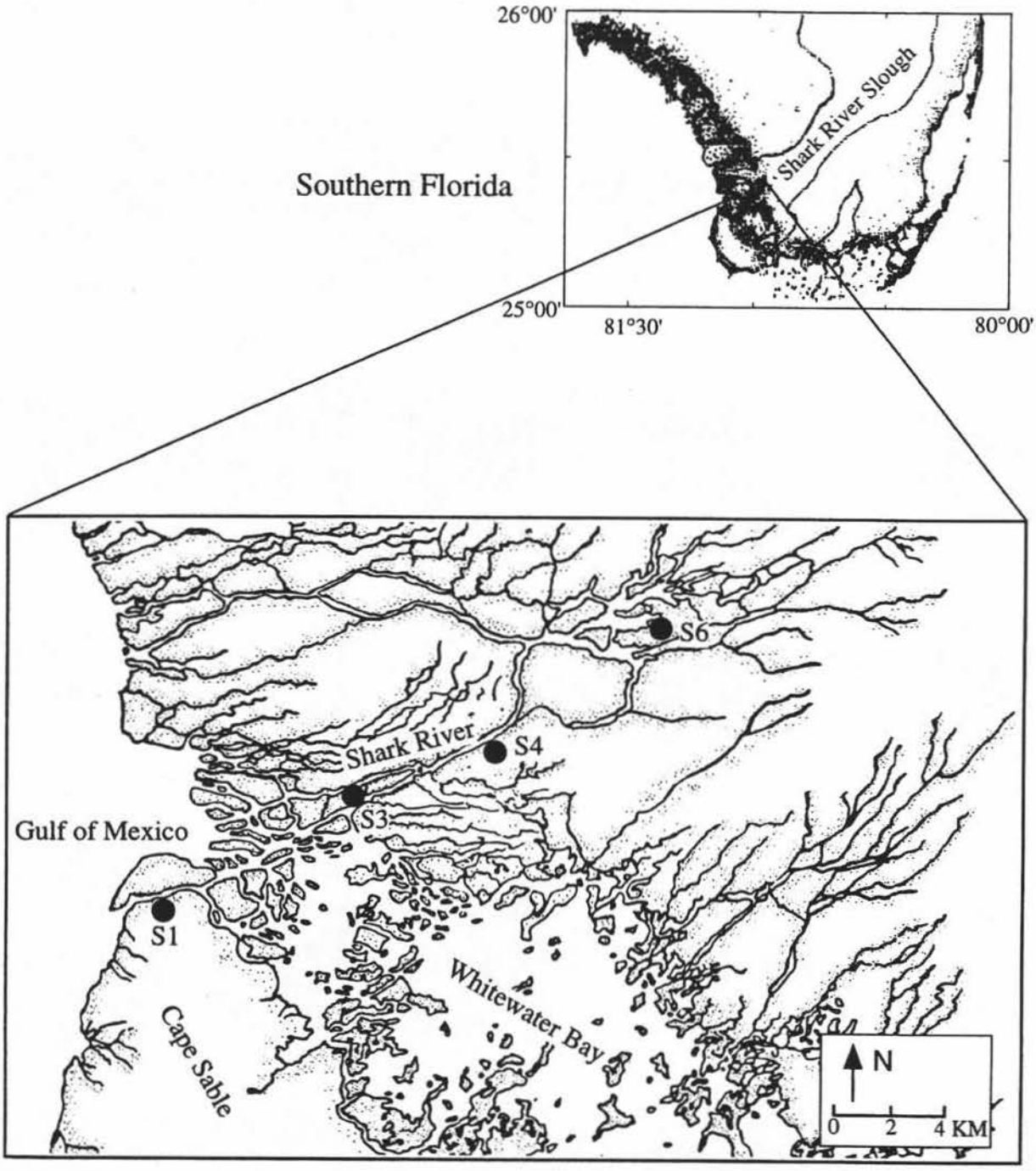


Figure 2.1. Study site locations along the Shark River estuary in the Everglades National Park.

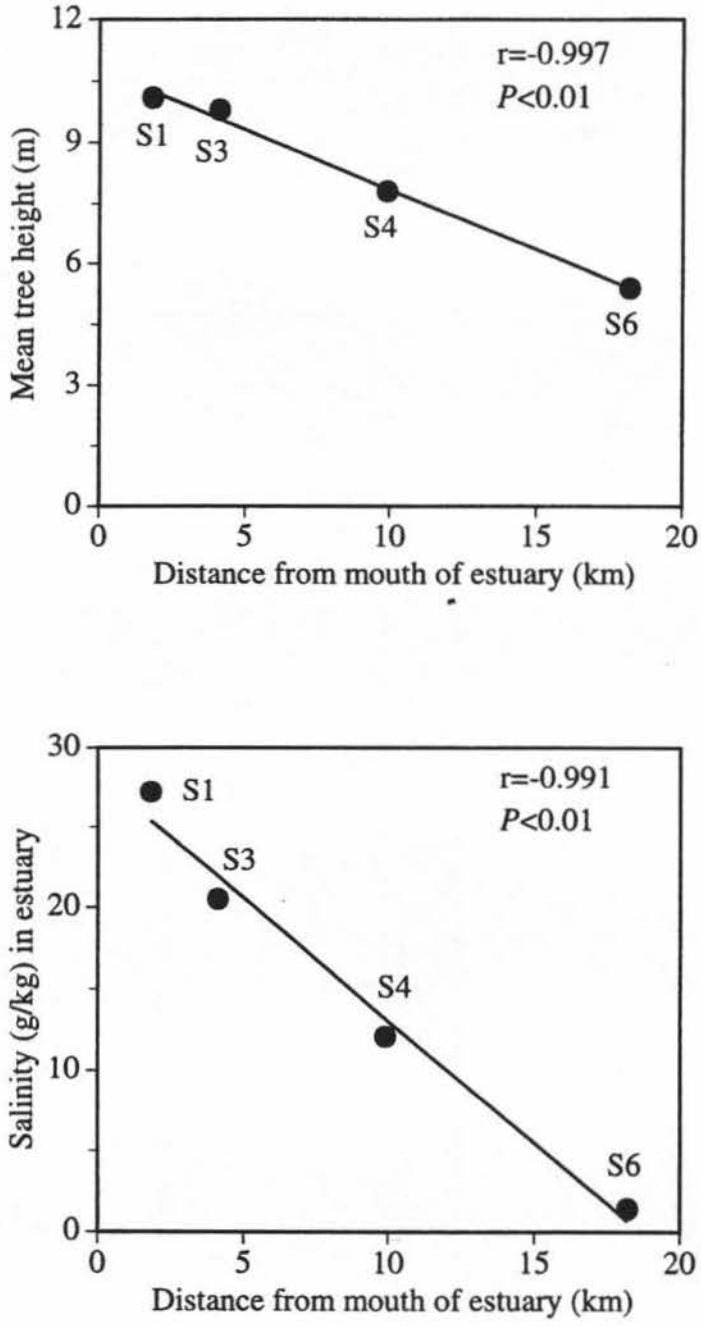


Figure 2.2. Changes of mean tree height of mangrove forests and salinity from the marine site (S1) to the oligohaline site (S6) along the Shark River estuary of the Everglades National Park.

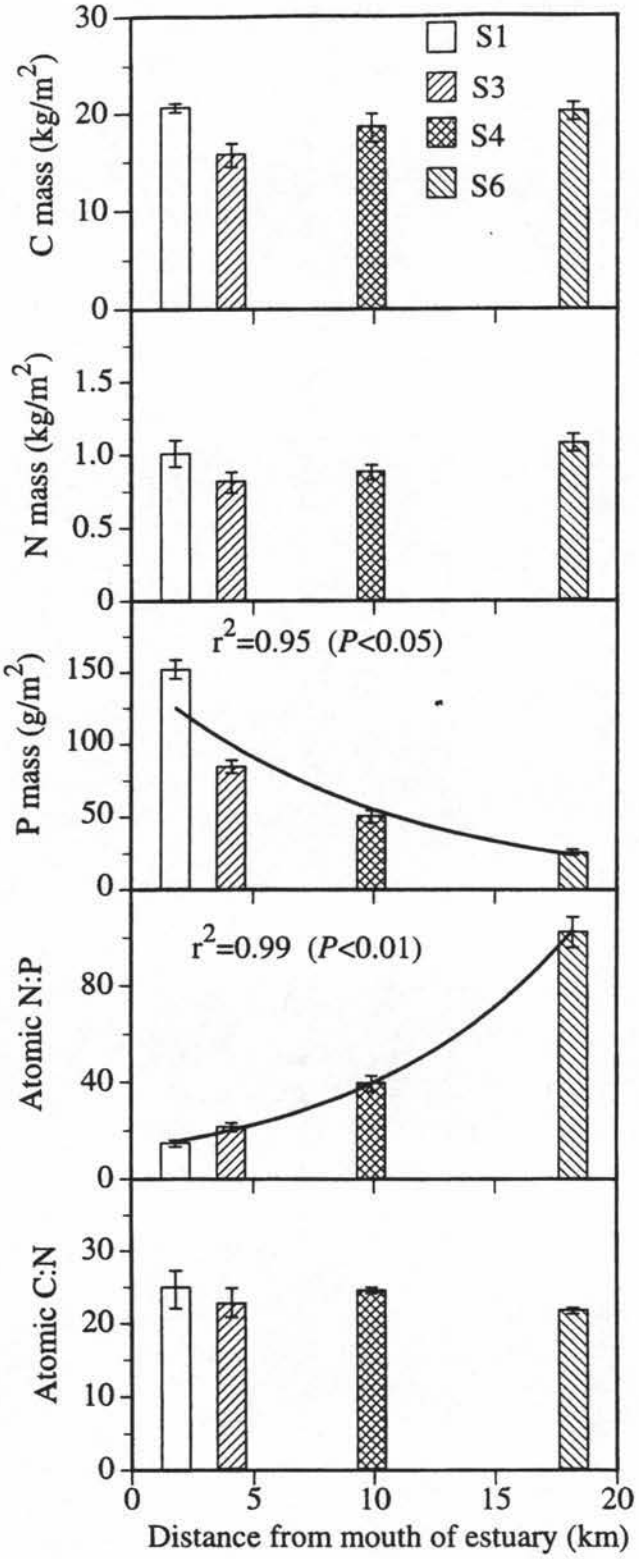


Figure 2.3. Changes of soil C, N and P within 0-40 cm soil in mangrove forests from the marine site (S1) to the oligohaline site (S6) along the Shark River estuary of the Everglades National Park. Data are mean of three seasons ± SE.

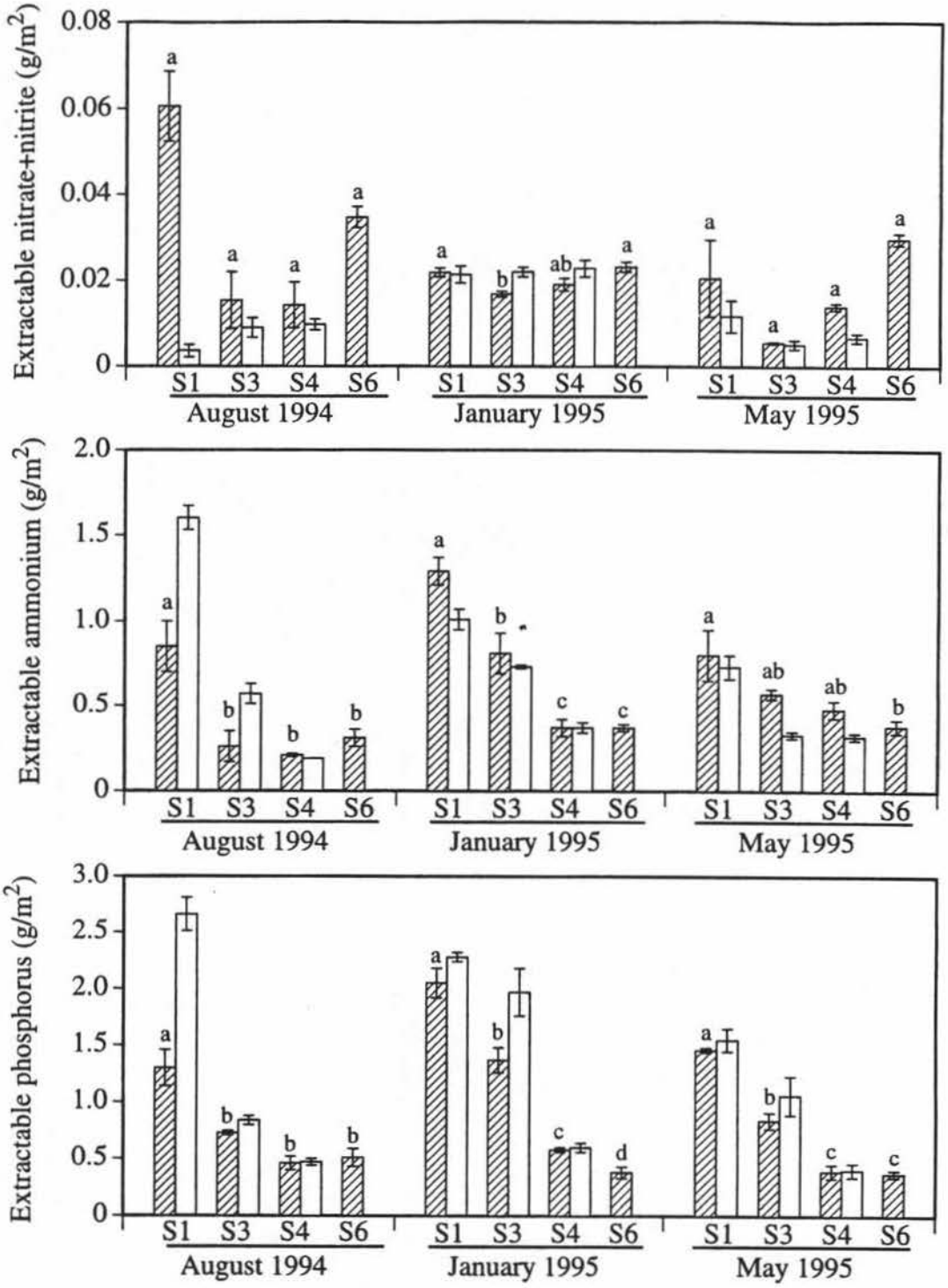


Figure 2.4. Extractable nitrate+nitrite, ammonium and phosphorus within the 0-20 cm soil at four mangrove sites along the Shark River estuary in August 1994, January and May 1995. Hatched bar and open bar represent sampling stations under intact forests (S1 - S6) and under canopy gaps (S1 - S4), respectively. Each value is the mean (±SE) of three stations. The values for intact forests from different sites at each sampling date with the same letter are not significantly different ($P>0.05$; Tukey's test).

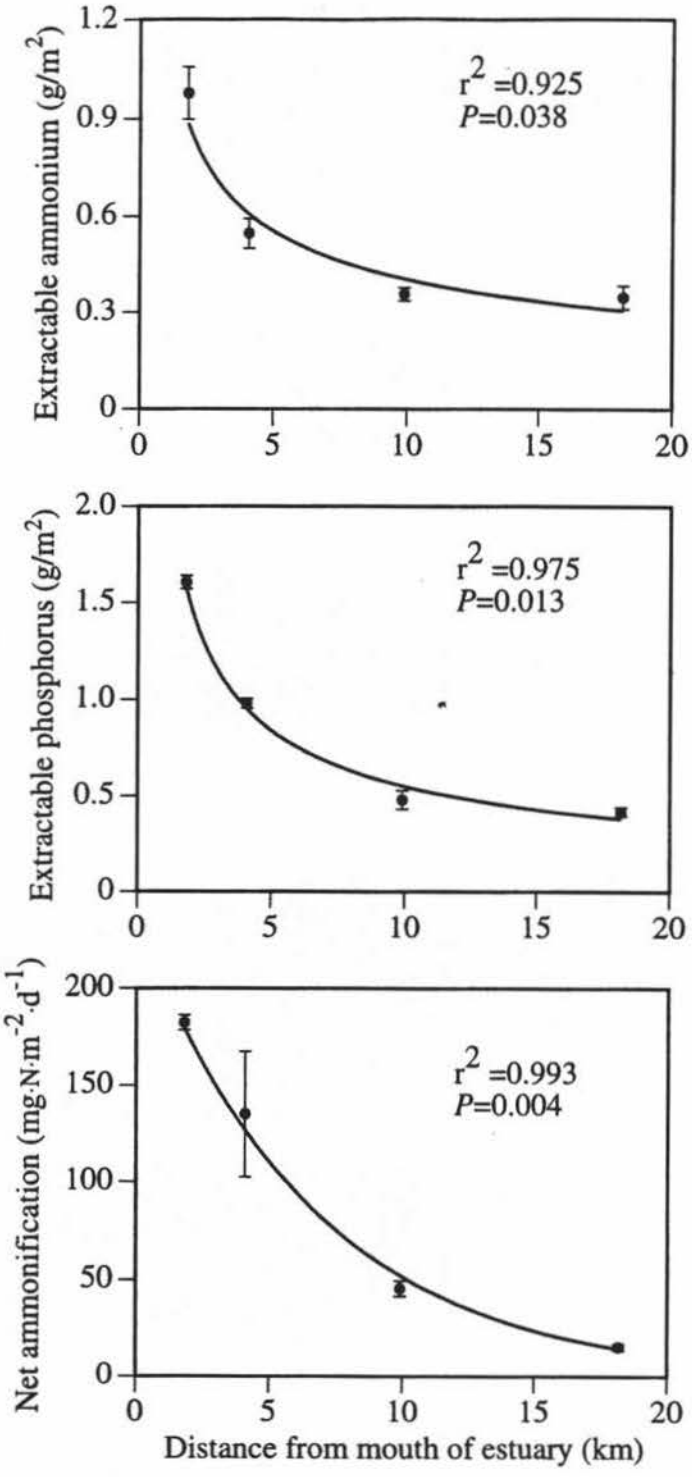


Figure 2.5. Relationship between mean extractable ammonium, extractable phosphorus, net ammonification, and the distance from the mouth of the Shark River estuary. Values are mean ±SE (n=3). Curves have been fitted to the relationship: $y = ax^b$ for extractable ammonium and phosphorus; $y = exp(a+bx)$ for net ammonification.

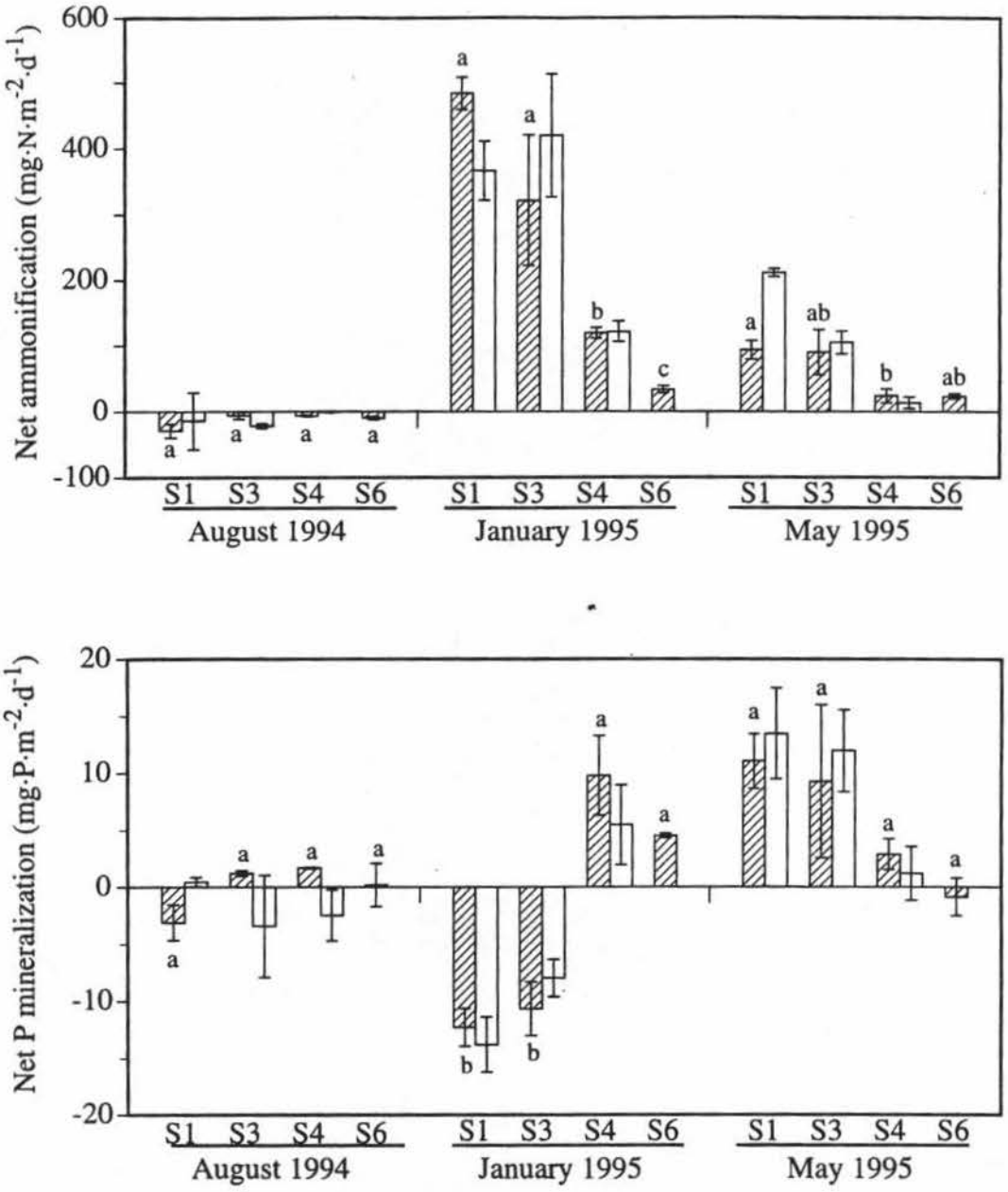


Figure 2.6. Net ammonification and phosphorus mineralization within the 0-20 cm soil at four mangrove sites along the Shark River estuary in August 1994, January and May 1995. Hatched bar and open bar represent sampling stations under intact forests (S1 - S6) and under canopy gaps (S1 - S4), respectively. Each value is the mean (±SE) of three stations. The values for intact forests from different sites at each sampling date with the same letter are not significantly different ($P>0.05$; Tukey's test).

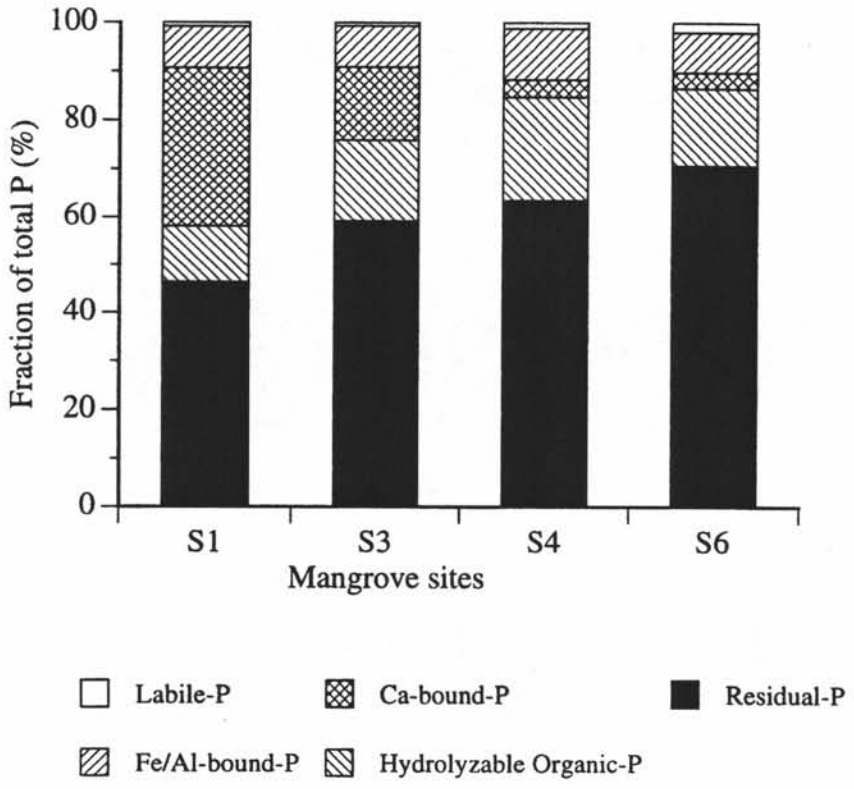


Figure 2.7. Changes in P fractionations in percent of total P within the 0-20 cm soil at four mangrove sites along the Shark River estuary.

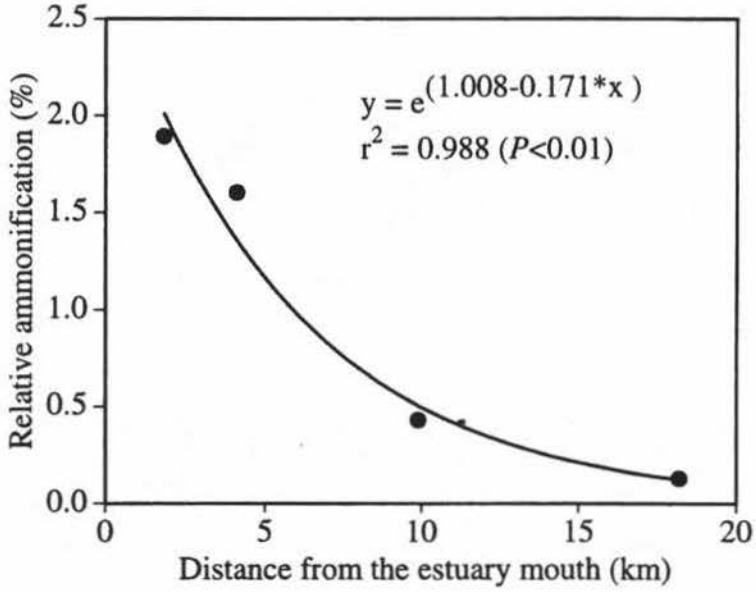


Figure 2.8. The relative ammonification rate of mangrove sediments in relation to the spatial gradient of the Shark River estuary. Relative ammonification is calculated as the net total amount of ammonium mineralized (0-20 cm) during three periods of 15-d incubation as a percentage of mean total N present initially.

CHAPTER 3

LANDSCAPE PATTERNS OF MANGROVE FOREST STRUCTURE AND SOIL CHARACTERISTICS ALONG THE SHARK RIVER ESTUARY, FLORIDA

ABSTRACT

Mangrove forest structure, growth, soil nutrient resources and pore water stressors were examined along the longitudinal gradient of the Shark River estuary in the Everglades National Park. Patterns of forest structure were based on 34 yrs of growth since Hurricane Donna destroyed most of the mangrove resources in this region in 1960. Forest basal area increased from lower values at the upstream and intermediate locations of the estuary (19.61 and 20.72 m^2/ha, respectively) to nearly double these values at two downstream locations (40.36 and 39.67 m^2/ha) near the mouth of the estuary. Tree density with dbh >10 cm was 1900/ha in the downstream location, which indicated a more mature stand than in the upstream location where only 334 trees/ha were >10 cm dbh. *Laguncularia racemosa* had a higher importance value in the downstream location, whereas *Rhizophora mangle* dominated in the intermediate and upstream locations. Biomass increments were higher at the downstream sites (10.73 and 11.96 $Mg \cdot ha^{-1} \cdot yr^{-1}$) than at the lower stature forest in the upstream and intermediate sites (3.23 and 4.20 $Mg \cdot ha^{-1} \cdot yr^{-1}$). Pore water salinities in mangrove soil were < 35 g/kg at all three sampling seasons and sulfide concentrations were generally < 0.15 mmol/L. There was no spatial trend of total C and N contents per unit soil volume, nor in C:N ratios among the sites. However, total P, extractable P and extractable ammonium contents increased from the upstream sites to the sites at the mouth of the estuary. Soil properties in the downstream marine region of the Shark River estuary include high levels of nutrient resources and low concentrations of toxic stressors supporting a region of optimum growth of mangroves. A regression of mangrove basal area on concentrations of soil total P per unit volume suggest that the landscape gradient of mangrove forest development is associated with soil P resources along this subtropical estuary.

INTRODUCTION

Global trends of mangrove structural complexity and biomass show a decrease toward higher latitude, however, above ground biomass among mangrove forests can vary greatly within a specific latitude (Twilley et al. 1992, Saenger and Snedaker 1993). Variation in forest structure among mangroves can be linked to the geophysical processes and geomorphology of a regional setting. Factors influencing variation in mangrove stature among specific geomorphic settings have been proposed to include the distribution of toxic stressors (such as salinity and hydrogen sulfide) and resources (such as nutrients and light) within the intertidal zone. In areas of increasing soil salinity mangroves may be considered as an ecosystem under stress due to the limitation of hypersaline soils on the growth of mangroves (Lugo and Snedaker 1974), changes in species composition, and increasing scrubbiness (Macnae 1968). Cintrón et al. (1978) correlated the specific decrease in basal area and tree height with increased soil salinity in mangroves among the dry coasts of Puerto Rico. As a result of strong salinity gradients (35-300 g/kg), mangroves along the dry Pacific coasts of Central America exhibited significant differences in structural development within the same forest region (Jiménez 1990). In contrast, hypersaline soils have less effect on mangrove forest development along humid tropical coasts where rivers provide a source of freshwater to dry coastal environments (Blasco 1984)

The growth of mangroves is not only constrained by variations in soil salinity, but also by highly toxic compounds such as hydrogen sulfide. Hydrogen sulfide is transformed from sulfate in reduced soil. Concentrations of sulfide exceeding 3 mmol/L have been recorded in mangrove soils (Nickerson and Thibodeau 1985, McKee 1993), and sulfide is considered a factor limiting growth and distribution of mangrove species. Boto and Wellington (1984)

found that above ground biomass of mangroves decreased at sites with more reduced soils in an Australian mangrove forest. In a greenhouse study, McKee (1993) demonstrated that reduced soil conditions caused a 20 to 40% decrease in total biomass of *Avicennia germinans* seedlings relative to drained soil controls.

Nitrogen (N) and phosphorus (P) have been implicated as the nutrients most likely limiting primary productivity of mangrove ecosystems (Twilley 1995). Based on field observations, Lugo and Snedaker (1974) hypothesized that dwarf mangroves in Florida suffer from nutrient limitation because they usually occur in an environment lacking obvious external nutrient sources. Biomass and productivity increased as nutrient inputs were increased in simulations of an ecosystem model of mangrove wetlands (Lugo et al. 1976). Surveys of forest structure and soil characteristics among natural mangrove communities in Australia indicated that above ground biomass was positively correlated with extractable P (Boto and Wellington 1984). Day et al. (1987) observed that riverine forests in Términos Lagoon had much greater biomass and productivity than fringe and basin mangroves along a tidal creek, Estero Pargo. The first direct evidence that nutrients may influence the structure and productivity of mangrove wetlands was by Onuf et al. (1977), who measured the growth of overwash mangroves naturally enriched by bird guano in Florida. They found greater leaf production and branch growth in those mangroves relative to those at sites without bird guano. Field fertilization studies by Clarke and Allaway (1993) showed that higher nutrients enhanced the growth and survival of seedlings in gaps and under the canopy of forests in Australia. Furthermore, Feller (1995) and Twilley (1995) manipulated nutrient levels in organic soils of a dwarf mangrove in Belize and revealed that *Rhizophora mangle* trees responded quickly and grew vigorously following fertilization with P.

More than 50 yrs ago, Davis (1940) suggested that mangrove forests in the

downstream region of the estuaries in southwestern Everglades are "probably the optimum growth of mangroves in the Americas". However, this hypothesis has not been tested with synoptic surveys of forest structure and environmental factors in this specific land-margin ecosystem. Coastal forested wetlands in the southwestern Everglades of south Florida extending from the Whitewater Bay region to Ten Thousand Islands include one of the greatest mangrove areas in the Gulf of Mexico (Davis 1940, Smith et al. 1994). Mangrove wetlands extend about 10-20 km inland bordering several estuaries that drain the Everglades, such as the Shark River Slough. Several studies of mangrove forests have been carried out in this region including zonation (Davis 1940), hurricane disturbances (Craighead and Gilbert 1962, Craighead 1971, Smith et al. 1994, Wanless et al, 1994, Doyle et al. 1995), organic export and trophic dynamics (Heald 1969, Odum and Heald 1972), and structure and litter production of ecological types (Pool et al. 1975, 1977). However, the landscape gradient of mangrove forests along the estuary as a function of environmental conditions has received far less attention. It has been observed that mangrove forest stature along the more marine regions of the estuary is about 25 m, and tree height decreases toward the mangrove-marsh transition zone (Davis 1940, Smith et al. 1994, Chapter 2). Specifically, it has not been shown whether these changes in forest structure are associated with either increased stressors or reduced nutrient resources.

In this paper, I described patterns of mangrove forest structure relative to distribution of soil resources and toxic stressors along the Shark River estuary in the Everglades National Park. This study was undertaken 34 yrs after Hurricane Donna destroyed most of the mangrove resources in this region in 1960 (Craighead and Gilbert 1962). The objective of this study was to investigate the relationships between landscape gradients of mangrove forest structure and soil characteristics. I quantified the structure and biomass increments of

density, tree height and basal area along the Shark River estuary. The sites were located between 25°19'N, 81°08'W and 25°25'N, 80°58'W at about 1.4 (S1), 4.1 (S3), 9.9 (S4) and 18.2 (S6) km inland from the mouth of the estuary (Fig. 2.1). Following the terminology of Duke (1992), mangrove habitats in S1 and S3 sites are categorized as downstream locations of the Shark River estuary, while S4 is intermediate and S6 is an upstream location. This region consists of 1-4 m deep peats accumulating above a mainland carbonate Oolite platform, which is unique among geomorphological groups of mangroves (Davis 1940, Scholl 1962 a,b, Thom 1984, Woodroffe 1992).

Permanent plots were established at each of the four sites to study dynamics of mangrove vegetation along the estuary. A 20 x 20 m plot about 10 to 20 m inland from the estuary was divided into four 10 x 10 m quadrats at sites S1, S3 and S4. A smaller plot 10 x 15 m plot about 5 m inland from the estuary was divided into three 10 x 5 m quadrats at S6 due to the restricted band of mangrove vegetation along the estuary in this upstream region. Three stations were randomly selected in each forest plot and marked in August 1994 for repeated measures of soil and pore water properties in August 1994, January and May 1995.

Forest structure and growth

All trees with diameter at breast height (dbh) > 2 cm in each plot were tagged and measured in January 1995 and remeasured in February 1996. I also measured dbh of dead trees in January 1995. Fifteen to 20 trees were randomly chosen in each plot for the measurements of tree height using a range finder. I also measured tree height and dbh in a disturbed mangrove forest at the mouth of Broad River, which is recovering from Hurricane Andrew in 1992, to analyze the relationship between tree height and dbh. Regression between dbh and tree height was estimated for each species.

mangrove forests, soil and pore water nutrient pools, and pore water salinity and sulfide concentrations along the longitudinal gradient of the Shark River estuary. Understanding spatial patterns of soil nutrient resources and stressors is crucial to the interpretation of mangrove forest dynamics in the face of natural disturbance, such as hurricanes. In addition, these environmental constraints on forest structure and function are linked to human land-use patterns in the Everglades watershed, particularly those associated with the Shark River Slough.

MATERIALS AND METHODS

Study area

The study sites are located along the Shark River estuary on the west coastal plain of the Everglades National Park (Fig. 2.1). An elevation gradient of the coastal Everglades region of only 2.8 cm/km (SFWMD 1992) along with a low-energy environment results in the development of extensive mangrove wetlands. Three mangrove species, *Rhizophora mangle* L., *Avicennia germinans* (L.) Stearn. and *Laguncularia racemosa* (L.) Gaertn., form a continuous band of forested wetlands that extend from the Gulf of Mexico to the inland limit of periodic salt water influence. *Conocarpus erecta* L. is also found in this coastal region where the salinity is lower than 10 g/kg and soils are frequently inundated. This study area was previously destroyed by Hurricane Donna in 1960, with an instant mortality of mangroves reported at 50 to 70%, but the eventual tree mortality was higher (Craighead and Gilbert 1962). Because tree destruction in this region by Hurricane Donna was so widespread, mangrove forests at each site along the Shark River estuary are considered to be approximately even aged.

Four sites of mangrove forests were selected for measurements of species composition,

Total above-ground biomass of *R. mangle* and *L. racemosa* was calculated using published allometric equations from Cintrón and Schaeffer-Novelli (1984) and of *A. germinans* from Day et al. (1987). Annual net biomass growth was estimated as the difference between the initial and final biomass of each individual tree using species-specific equations. The sum of these differences was used to estimate biomass production for each plot. There is no allometric equation for *C. erecta* so I used the allometric equations of *L. racemosa* as a reference to estimate biomass of *C. erecta* because their growth forms are similar at this site.

Pore water analyses

Pore water samples were collected at the three soil stations in each plot using a plastic siphon with syringe as described by McKee et al. (1988). I was able to collect pore water at 20 cm depth using this method in May 1995 and August 1994, but collections were at 40 - 50 cm in January 1995 due to lower water level. One aliquot of pore water was assayed for salinity using a portable Labcomp Instruments Model SCT analyzer and for pH using a HANNA H19025 pH meter. A second aliquot of the pore water sample was filtered and immediately added to an equal volume of antioxidant buffer in the field, then brought to the laboratory to be analyzed for sulfide concentrations with a LAZAR Model IS-156 sulfide sensing electrode (McKee et al. 1988). A third aliquot of pore water was used to measure nutrient concentrations by filtering through a GF/F filter and storing the sample frozen until assayed for inorganic nutrients. Ammonium concentrations were measured by colorimetric method (Parsons et al. 1984). Nitrite, nitrate and phosphate in pore water samples were determined by ALPKEM Autoanalyzer using standard techniques (Strickland and Parson 1972).

Soil nutrients

Soils were collected with a 5.0 cm diameter corer at the three stations to a depth of 40 cm. Soil samples at 10-cm intervals were stored on ice in polyethylene bags in the field, and stored at 4°C in the laboratory prior to analysis. Index of available P was determined by a dilute acid-fluoride extraction of fresh soil samples (Olsen and Sommers 1982). The extract was analyzed colorimetrically for soluble reactive phosphorus. Fresh soils were extracted with 1 mol/L KCl (1:10 mass/volume) to measure extractable ammonium. The extract was centrifuged and analyzed for NH_4-N by colorimetric method (Parsons et al. 1984). Recognizable plant litter and coarse root material were removed from soil samples prior to extractions. Soil subsamples were ovendried to constant weight at 60°C and ground with a Wiley Mill to pass through a 250 μm mesh. Total C and N content of two replicates of each sample were determined with a LECO elemental analyzer using standard protocols. Total P in soils was extracted from soils with 1N HCl after ignition at 550°C (Aspila et al. 1976) and determined by using molybdenum blue, and ascorbic acid as reducing agents (Parsons et al. 1984). Another 15.2 cm diameter soil core from each site was used to estimate soil bulk density. Nutrient concentrations were multiplied by bulk density to obtain nutrient contents expressed per unit soil volume.

Statistical analysis

Repeated measures ANOVAs were used to test the effects of site, depth and sampling date on soil C, N and P concentrations and contents. I also used repeated measures ANOVAs to test the effect of site and sampling date on pore water variables including salinity, sulfide and inorganic nutrients. One way ANOVA was used to test for differences in concentrations of pore water variables among the sites for each sampling date. All statistical tests were done by

using either original data or log-transformed data to meet assumptions for parametric analysis. SAS was used to perform all statistical tests (SAS 1989).

RESULTS

Forest structure and growth

The landscape patterns of mangrove forest structure along the Shark River estuary exhibited differential recovery from Hurricane Donna disturbance in 1960, assuming that these stands are even-aged. The highest density of trees among the four sites was 7333 trees/ha at S6, compared to 3725, 3600 and 2578 trees/ha at S1, S3 and S4, respectively (Fig. 3.1). However, density of trees >10 cm dbh increased significantly from 334 trees/ha at S6 to 1900 trees/ha at S1, with intermediate values of 850 and 1600 trees/ha at S4 and S3, respectively (Fig. 3.2). S6 was characterized by a high density of small trees (5534 trees/ha) with dbh <6 cm. Size class distribution of trees at S6 showed an exponential decrease of tree density with an increase in dbh, however, frequency of size-class distribution at S1 was bell-shaped (Fig. 3.2).

R. mangle, *A. germinans*, and *L. racemosa* were found in the plots at S1, S3 and S4, but *A. germinans* was replaced by *C. erecta* at S6. *R. mangle* was found in all sites and this species represented 35% to 90% of total tree density among the study sites. The dominance of *R. mangle* was restricted to the size-class <8 cm dbh, except at S4 where *R. mangle* dominated in all size-classes (Fig. 3.2). At S3, *L. racemosa* dominated in size-class >14 cm dbh, while no *R. mangle* above this size-class was found in the plot. All three species were co-dominant in size-class >14 cm at S1.

Basal areas were similar at S1 and S3 with values of 40.36 and 39.67 m^2/ha,

respectively. However, basal areas at S4 and S6 were only 20.72 and 19.61 m^2/ha, respectively, which was about half of the values at S1 and S3 (Fig. 3.1). Basal area indicated that the structural complexity of mangroves increased from the oligohaline zone to the marine sites of the estuary.

Mangrove forests were mixed-species communities at S1 and S3, where *L. racemosa* had the highest importance value (42.1 and 48.5%, respectively in S1 and S3) and *A. germinans* the least (Fig. 3.1). The S4 site was dominated by *R. mangle* with an importance percentage of 72%. *R. mangle* was co-dominant with *C. erecta* at S6.

Regression equations relating tree height and dbh were obtained for each species:

R. mangle - log(height) =0.2162+0.7434*log(dbh), (r^2 = 0.83, n=73);

L. racemosa- log(height) =0.2931+0.7465*log(dbh), (r^2 = 0.96, n=35);

A. germinans- log(height) =0.2069+0.746*log(dbh), (r^2 = 0.87, n=30).

Mean tree heights of mangrove forests in the four sites increased from 5.4 m in the oligohaline location (S6) to 10.1 m in the downstream location (S1). Tree heights at S4 and S3 were 7.8 and 9.8 m, respectively.

Biomass of individual trees was calculated with tree height and dbh using the species-specific allometric equations described above. Total above ground biomass at each of the four sites was estimated by summing the individual tree biomass values. Organic matter storage was higher in mangrove forests at S1 and S3 rather than S4 or S6. Total above ground biomass in 1994 was estimated at 245.7, 250.8, 127.4 and 78.7 Mg/ha in S1, S3, S4 and S6, respectively (Fig. 3.1). The contribution of each species to total biomass was similar to that of total basal area (Fig. 3.1). *L. racemosa* was the major component of total biomass in S1 and S3, whereas *R. mangle* was dominant in S4 and S6.

Average tree growth rates, calculated as an increase in basal area ($cm^2 \cdot tree^{-1} \cdot yr^{-1}$) and in

biomass ($kg \cdot tree^{-1} \cdot yr^{-1}$), varied among sites and species (Table 3.1). *A. germinans* had the greatest basal area increase and biomass production at S1, whereas *L. racemosa* growth rate exceeded those of the other species in S3, S4 and S6. The average tree growth rates of *R. mangle* were lower than those of *A. germinans* and *L. racemosa* in all sites.

Annual increments of total biomass in S1 and S3 were twice the levels of those in S4 and S6 during the interval from January 1995 to February 1996 (Table 3.1). Although average tree growth rate of *R. mangle* were low, this species contributed 78% and 87% of total biomass increment in S4 and S6, respectively, due to higher density of *R. mangle* in these sites. *L. racemosa* dominated total biomass increments at 46% in S1 and 86% in S3.

Pore water characteristics

There were significant effects of site and season on pore water salinity with a significant interaction of site * season (Table 3.2). Pore water salinity decreased from S1 to S6 at all sampling dates and peak concentrations at each station occurred during August (Fig. 3.3). The highest pore water salinity occurred at S1 in August at 33.5 g/kg, compared to 8.2 g/kg at S6 during this season. Pore water salinities were generally lower in January at 23.2 g/kg and 1.6 g/kg at S1 and S6, respectively. The sites with the greatest seasonal change in salinity were S3 and S4 that ranged from 8.2 and 4.4 g/kg in January to 26.1 and 26.5 g/kg in August, respectively.

There were significant effects of site and season on the pore water sulfide with a significant interaction of site * season (Table 3.2). Multiple comparisons of means in each sampling season exhibited a significant site effect only in August, with the highest concentration at S6 compared to no differences among S1, S3, and S4 (Fig. 3.3). No sulfide concentrations could be detected at any of the sites in January when the ground water level was

40 cm below the surface. The highest mean sulfide concentration was 0.46 mmol/L at S6 in August, compared to 0.15 mmol/L at the other sites. Pore water pH was near neutral at all sites with the mean of sites ranging from 6.6 to 6.9.

Nitrite and NO_3^- concentrations were <1 μmol/L and <0.5 μmol/L, respectively, at all sites during the three sampling seasons (Fig. 3.4). The repeated measures ANOVA showed significant effects of site and season on the pore water NO_2^- with a significant interaction (Table 3.2). Significant site effects were only observed in January with higher concentrations of NO_2^- at S6 and S4 than at S1 and S3 (Fig. 3.4). There were no significant site and season effects on NO_3^- (Table 3.2, Fig. 3.4). NH_4^+ concentrations were significantly different among sampling seasons (Table 3.2), with the highest mean in August and no difference in concentrations between January and May. However, there were no significant site effects on pore water NH_4^+ concentrations (Table 3.2). Mean PO_4^{3-} concentrations were <2 μmol/L at all sites during the three sampling seasons, except at S3 in January. There were significant effects of season and significant interaction between site and season, but there was no site effect on pore water PO_4^{3-} concentrations (Table 3.2).

Soil nutrients

There were significant effects of site, depth and season on contents of available P and extractable NH_4^+ expressed as per unit volume (Table 3.3). Available P contents usually decreased from surface to 40 cm depth. The spatial trend of available P contents was an increase from S6 to S1 along the estuary (Fig. 3.5). The decrease in extractable NH_4^+ contents with depth was more significant at S1 than other sites (Fig. 3.5). The mean NH_4^+ content was the highest at S1 in the 0-10 cm depth. Soil extractable NH_4^+ contents did not show a

significant spatial trend as measured in available P.

There were significant effects of site, depth and season on concentrations (per dry mass) of total soil C, N and P (Table 3.3). Significant interactions among site, depth and season precluded further statistical testing of site, season and depth effects on these soil variables. However, in general, landscape trends in nutrient concentrations were not similar for each nutrient. Total C and N concentrations showed a landscape trend with a decrease from S6 to S1 (Fig. 3.6). In contrast, total P concentrations decreased from S1 and S3 to S6 (Fig. 3.6). Generally, the concentrations of C, N and P decreased slightly with depth, however, the effects of depth on these nutrient concentrations were less than that of site (Table 3.3). Nutrient contents were calculated as a per unit volume and also compared among the sites. There were significant effects of site and season on contents of C, N and P (Table 3.3). C and N contents did not showed a landscape trend along the estuary, however, P contents increased significantly from S6 to S1 (Fig. 3.6).

There was a significant effect of site on C:N ratios. Overall mean atomic C:N ratio was 24.7, 22.9, 24.6 and 21.8 in S1, S3, S4 and S6, respectively, without a landscape trend with distance from the mouth of the estuary (Table 3.3, Fig. 3.6). N:P ratios decreased significantly from S6 to S1 with an overall mean atomic N:P ratio of 102.2 (S6), 39.5 (S4), 21.6 (S3) and 14.8 (S1) among sites (Table 3.3, Fig. 3.6). Like N:P ratios, overall mean atomic C:P ratios also decreased from S6 to S1 at 2224, 969, 487 and 355 in S6, S4, S3 and S1, respectively. N:P and C:P ratios decreased significantly with depth at S6.

DISCUSSION

Soil sulfide and salinity stress along the estuarine gradient

Previous studies report that mangrove and salt marsh sulfide concentrations in Florida are highest in late summer and lowest in winter (Carlson et al. 1983, Rey et al. 1992). Measurements of sulfide concentrations showed a similar pattern with highest values in August and undetectable concentrations in January along the Shark River estuary. Peak sulfide concentrations in summer have been attributed to higher inputs of organic detritus and high evapotranspiration (Rey et al. 1992). High inputs of organic detritus lead to higher oxygen consumption by microbes and enhanced evapotranspiration concentrates sulfide in pore water. Twilley (1985) reported maximum rates of evapotranspiration in August of a basin mangrove forest in southwestern Florida. Undetectable sulfide concentrations at all sites in January corresponded with a decrease in seasonal sea level (Provost 1973) and tidal flooding frequency (Twilley 1985), which enhances rates of oxygen diffusion into sediment and drains reduced pore water from upper soil strata (Rey et al. 1992).

Significant differences in sulfide concentrations among the sites were only found in August with the higher value in the upstream location. This pattern may result from several factors related to hydrology, soil texture and plant aeration. Tidal inundation can flush out sulfides in mangrove soils and contribute reactive iron (King et al. 1982); however, this effect may decrease with increased distance of the wetland from the Gulf shore. Significantly higher soil concentrations of C (43%) in the upstream site of the Shark River estuary may reduce water flow in mangrove soils given that lower water conductivity occurs in wetland soils with higher organic matter content (Mitsh and Gosselink 1993). Furthermore, mangrove roots can have a significant feedback effect on reduced mangrove soils by transporting oxygen to the

surrounding soil matrix (McKee 1993). The magnitude of this effect depends on plant biomass and root density (Boto and Wellington 1984, McKee et al. 1988). Although the above-ground mangrove biomass at S6 was only half of the amount at the downstream sites, implying a lower oxidation potential by roots into sediment, the relative amount of below-ground biomass among the sites was not clear.

The species-specific tolerance of mangroves to pore water sulfide concentrations has been associated with patterns of mangrove species zonation. Carlson et al. (1983) measured sulfide concentrations ranging from <0.01 mmol/L to 1.5 mmol/L in an east Florida mangrove. Nickerson and Thibodeau (1985) reported that values ranged from 0.68 to 4.1 mmol/L in Bahamian mangrove soils. McKee and her colleagues, using the same method as I did, found that pore water sulfide concentrations ranged from 0.24 to 3.36 mmol/L (McKee et al. 1988) and 0 to 2.46 mmol/L (McKee 1995*a*) in a Belizean mangrove, compared to 0.14 to 3.08 mmol/L in a southwestern Florida mangrove (McKee 1993). Mangrove soils along the Shark River estuary can be characterized as only slightly reducing with most concentrations of sulfide less than the lower range of these other studies. The lower concentrations of sulfide (0-0.46 mmol/L) compared to these other reported values indicate that this stressor is not responsible for the landscape gradient of decreased forest stature of mangrove wetlands in the Shark River estuary.

Hypersalinity has been frequently suggested as one of the major factors limiting mangrove forest stature and growth (Lugo and Snedaker 1974, Cintrón et al. 1978, Boto and Wellington 1984). Pore water salinity in mangrove wetlands along the Shark River estuary during both the dry and wet seasons did not exceed 35 g/kg, below the critical value that influences mangrove complexity (see Lugo et al. 1988). Heald (1969) and Powell (1989) also reported that salinities in the North River estuary and the Shark River estuary were lower than

30 g/kg in mangrove regions based on monthly measurements. There were increases to the marine zone in both the landscape gradients of pore water salinity and basal area of forest along the axis of the Shark River estuary, indicating that forest development along the estuary was not limited by soil salinity. Based on correlation of tree height and soil salinity, Cintrón et al. (1978) suggested that a soil salinity of 65 g/kg was a threshold above which would cause an increase in mangrove tree mortality in Puerto Rico. Day et al. (1987) found that mangrove structure and productivity in Mexico was not affected by salinities under 50 g/kg. Therefore, mangrove wetlands in the Shark River estuary are characterized as lacking any significant stress effects of either soil salinity or sulfide concentrations.

Soil N and P resources along the estuarine gradient

Concentrations of pore water ammonium and phosphate were lower in the study sites of the Shark River estuary compared to reported values for other mangrove soils. Pore water ammonium concentrations are lower than reported for mangroves in Florida Bay (Rosenfeld 1979*a*), Missionary Bay of Australia (Smith et al. 1991), Papua New Guinea (Alongi et al. 1993), and Belize (McKee 1995*a*), but are similar to those reported for mangroves in the Indian River of Florida (Carlson and Yarbro 1988) and dwarf mangroves in Belize (Feller 1995). Pore water phosphate values in the study sites of the Shark River estuary are lower than those reported by Rosenfeld (1979a), Carlson and Yarbro (1988), McKee (1995*a*) and Feller (1995) for mangroves in a carbonate setting and by Smith et al. (1991) for Australian mangroves, but are higher than those reported by Alongi et al. (1993).

The presence of detectable pore water NO_3^- and NO_2^- in the Shark River study sites over three sampling periods coincides with the significance of aerobic zones around mangrove roots that can enhance nitrification (Joye and Hollibaugh 1995), which may lead to lower

ammonium concentrations in pore water. It is interesting that NO_2^- was higher than NO_3^- during January at S3, S4 and S6, when ground water level was lowest and sulfide concentrations were undetectable. This suggests a seasonal coupling of nitrification with the hydrology of these forests mediated by increased aeration of the upper soil strata. In general, there was no consistent spatial gradient of pore water ammonium, nitrate, nitrite, and phosphate in the mangrove soils along the Shark River estuary. Factors controlling these pore water values are complex, including decomposition and mineralization (Chapter 2), adsorption and dissolution by mineral and organic matter (Rosenfeld 1979b), fluxes across the sediment-water interface (Alongi et al. 1993, Rivera-Monory et al. 1995a), plant uptake (Boto and Wellington 1984), microbe immobilization (Alongi et al. 1993), redox potential (Boto and Wellington 1984) and bioturbation (Smith et al. 1991). The interactions of these factors probably have more significant effects on pore water nutrients within mangrove sites than among sites along the estuary.

Alongi et al. (1992) reviewed concentrations of total soil N and P in mangrove wetlands around the world. Total N concentrations ranged from 0.02 to 0.4 % and most of P concentrations were between 0.011 to 0.067%, except in a mangrove in West Africa where total P ranged from 0.08 to 0.16%. Several recent studies in mangroves reported total soil N concentrations ranging from 0.03 to 1.7% and P concentrations ranging from 0.043 to 0.085% (Lynch 1989, Alongi et al. 1993, Alongi 1996). Compared with these data, mean concentrations of soil total N (0.7 to 2.3%) and P (0.06 to 0.12%) in mangrove wetlands along the Shark River estuary are higher than in most of the mangroves world-wide.

There is an increased concern that accelerated nutrient loadings, especially P, from anthropogenic sources can change the vegetation characteristics of oligotrophic regions of the Everglades. Intensive studies have been conducted on N and P distribution and accumulation

in soil and plants in Water Conservation Area 2A, adjacent to Everglades Agricultural Area, in the northern Everglades (Davis 1991, Koch and Reddy 1992, Craft and Richardson 1993a,b, Reddy et al. 1993, DeBusk et al. 1994). Results of these studies showed that there was a spatial gradient of soil P decreasing from areas proximal to surface inflows to regions south in WCA2A. Surface soil concentrations of total P in the nutrient enrichment area occurred at levels of 0.12-0.16% (DeBusk et al. 1994) and 0.14-0.16% (Craft and Richardson 1993a), compared to about 0.05% in areas south of the enrichment in WCA2A to 0.07% in WCA3 (Craft and Richardson 1993b). Both southern areas are in the immediate vicinity of the upstream extent of the Everglades National Park. Total P concentrations in the oligohaline mangrove site (0.057%) of the Shark River estuary are similar to reported concentrations in WCA2A and WCA3, upstream of the Shark River Slough. However, P concentrations near the mouth of the estuary (0.12%) are similar to the upper limits of total soil P in the marsh adjacent to areas of agriculture effluent. If bulk density is taken into consideration, P contents per unit volume soil in the downstream locations (0.212 and 0.381 mg/cm^3 in S3 and S1, respectively) are even higher than those in the enriched area in WCA2A where P contents are < 0.12 mg/cm^3 (Koch and Reddy 1992), 0.2 mg/cm^3 (Reddy et al. 1993), and 0.16 mg/cm^3 (Craft and Richardson 1993a). These comparisons indicate that increased loading of P to the northern Everglades marsh from the agriculture area has not yet affected mangroves in this study area, because upstream marshes in the Shark River Slough effectively reduce surface water P concentrations which leads to relatively low P inputs to the Everglades National Park (Davis 1994).

Total C and N concentrations increased from the mouth of the Shark River estuary to oligohaline site, resulting in similar ratios of C:N; however, there was no landscape trend of total C and N contents per unit volume along the estuary. In contrast to the spatial trend in total

C and N concentrations, both total P concentrations (per unit dry mass) and contents (per unit volume) showed a reduction in mangrove soils from the mouth of the estuary to the oligohaline zone along the Shark River estuary. The gradient in soil P concentrations coincides with higher bulk densities at the downstream locations. Soil extractable P contents exhibited the same trend as total P content. The major source of freshwater to the estuary is the Shark River Slough, and the gradient of soil salinity along the estuary represents the relative importance of terrestrial runoff and Gulf water to the chemical composition of soils among the study sites. Increased contents of both total and extractable P with salinity suggests that the Gulf of Mexico is the major source of P for mangrove growth. Fourqurean et al. (1992) reported higher P availability in the northwest region of Florida Bay and hypothesized that P is transported in dissolved and suspended forms to this region from the Gulf of Mexico to Florida Bay. Therefore, P from the Gulf source appears to have a stronger impact on mangroves along the Shark River estuary than freshwater input from the Shark River Slough, at least in the recent time scale.

Forest structure

It has been suggested that mangrove wetlands in south Florida can recover from large scale disturbances, such as hurricanes, and achieve maturity in 20-30 yrs (Lugo and Snedaker 1974, Lugo et al. 1976, Lugo 1980). Such large scale disturbances have a significant impact on the structure and function of mangrove ecosystems throughout the Caribbean (Craighead and Gilbert 1962, Roth 1992, Smith et al. 1994, Wanless et al. 1994, Doyle et al. 1995). On September 10, 1960, Hurricane Donna passed throughout the Shark River region with a wind speed at 220 km/hr and gusts higher than 288 km/hr (Craighead and Gilbert 1962). The initial mortality of mangroves caused by the hurricane was 50 to 70% (Craighead and Gilbert 1962),

however, mortality probably was higher due to delayed mortality (Smith et al. 1994). After 34 yrs of regeneration, mangrove forests in the downstream locations of the estuary have grown into a mature forest with the highest basal area among mangrove forests in Florida and Puerto Rico (Table 3.4). Mangrove forests in Florida and Puerto Rico lie in the hurricane tracking zone, whereas mangrove forests in Mexico and Costa Rica are less influenced by hurricanes and these forests have a lower density but larger trees and higher basal area (Pool et al. 1977).

The bell-shaped pattern of size-class distribution of mangroves in S1 represents a relative mature forest, compared to distributions in S6 and S4 that have a much higher density of smaller trees. Since mangroves in this region regenerated from the disturbance of Hurricane Donna, I assume that all sites are of similar age with a possibility that the forest in S6 is older than in S1, given that the central path of Hurricane Donna was located in the downstream region of the estuary (Craighead and Gilbert 1962). Thus, size-class distribution, an index of age structure, of mangrove forests in these study sites may be related to the gradient of nutrient resources.

Davis (1940) recorded that the relative abundance of three mangrove species in the downstream zone of the Shark River was 60% for *R. mangle*, 30% *A. germinans* and 10% *L. racemosa*. Results indicate that forests in the downstream locations (S1 and S3) are mixed-species community with a relative higher importance value of *L. racemosa*. *L. racemosa* had a greater growth rate and dominated in the larger size (dbh>8 cm) cohort in sites with high P availability (S1 and S3). This implies that *L. racemosa* recovers faster than *R. mangle* and can dominate the mangrove canopy in fertile sites. McKee (1995b) compared the growth characteristics of seedlings under the control of light intensity and nutrient availability, and suggested that the order of success of three mangrove species was *L. racemosa* > *A. germinans* > *R. mangle* at either higher nutrient or light availability. Not only can *L. racemosa* have a

higher growth potential under high light and nutrient availability, this species may become dominant in the downstream locations of the estuary because it recovers rapidly by trunk sprout after stem damage (Wadsworth 1959). In my study plots, *A. germinans* were the largest specimens of live and dead trees with dbh > 30 cm in all plots. These trees are survivors from Hurricane Donna in 1960 and this species may be the most resistant to hurricane disturbance. Smith et al. (1994) surveyed the mortality of mangroves in south Florida after Hurricane Andrew in 1992 and also found that *A. germinans* had significantly less mortality than the other two mangrove species. The widespread occurrence of *R. mangle* through the study area and its dominance in the smaller tree cohort (dbh <8 cm) indicate that *R. mangle* has a relatively higher tolerance to shade and nutrient stress. The density of dead trees of *L. racemosa* was the highest at 83% in S1, 72% in S3 and 69% in S6 for total dead trees, with an exception in S4. The closed canopy and self-thinning of forest will probably replace *L. racemosa* with *R. mangle* due to the lower tolerance of *L. racemosa* to shading (Ball 1980). Therefore, hurricane disturbance may have an impact on the species richness of a region by resetting the processes of mangrove succession.

Forest biomass accumulation in relation to nutrient limitation

Biomass production of mangroves in my study sites increased from the oligohaline to marine zones along the Shark River estuary. Biomass production at two downstream locations (S1 and S3) was 10.73 and 11.96 $Mg \cdot ha^{-1} \cdot yr^{-1}$, which is comparable with that of a riverine mangrove (12.06 $Mg \cdot ha^{-1} \cdot yr^{-1}$) and higher than a fringe mangrove (7.7 $Mg \cdot ha^{-1} \cdot yr^{-1}$) in Laguna de Términos, Mexico (Day et al. 1987). The annual increment of biomass was lower at the intermediate and upstream locations of the estuary dominated by *R. mangle* and similar to an estimate (3.07 $Mg \cdot ha^{-1} \cdot yr^{-1}$) of *Rhizophora* forests in Puerto Rico (Golley et al. 1962).

However, these values are higher than that of a basin (0.68 $Mg \cdot ha^{-1} \cdot yr^{-1}$) and a fringe mangrove (1.2 $Mg \cdot ha^{-1} \cdot yr^{-1}$) in southwestern Florida (Warner 1990). In the absence of a toxic stress, soil nutrient availability is often implicated as the principle factor determining variation in forest structure and biomass production. Comparative analysis of mangrove forests and soil characteristics in Australia revealed that concentrations of extractable P decreased with tidal height and extractable P was one of the major factors limiting annual biomass accumulation (Boto and Wellington 1984). P fertilization resulted in a positive leaf production in elevated mangrove areas (Boto and Wellington 1983). Experimental additions of P to dwarf mangroves in Belize significantly stimulated the growth of trees, which increased biomass accumulation (Feller 1995, Twilley 1995). Silver (1995) further pointed out that soil P availability is important to humid tropical forest functions, such as litterfall production. My study shows that the landward decline of forest structure among even-aged mangrove forests can be associated with a decrease in soil P concentration, suggesting that P availability is a major factor influencing the gradient of forest development in the Shark River estuary. In addition, the mean N:P ratio of mangrove soil varied along the estuary from <10 in the downstream locations, 18 in the intermediate zone, to >40 in the upstream location. This gradient in relative availability of N and P indicates the importance of P as a limiting nutrient in the oligohaline zone of this estuary.

A study of mangrove productivity and soil characteristics in tropical Australia and Papua New Guinea showed that forests with lower productivity were associated with soils that have decreased concentrations of P (Boto et al. 1984). Boto (1991) further suggested that tropical mangroves in Australia are P-limited. I used a Monod model (Bridgham et al. 1995) to analyze the specific nature of P-limitation of mangrove forest development in Florida and the Caribbean. The relationship between forest development and nutrient resource availability in

mangroves was examined by the following model (Bridgham et al. 1995):

$$PR = \frac{(R_{ac} - R_{min})PR_{max}}{R_{ac} - R_{min} + \alpha}$$

where PR is production, PR_{max} is the maximum production, R_{ac} is the amount of resource acquired, R_{min} is nutrient availability at zero production and α is half-saturation constant with respect to R_{ac} (see Bridgham et al. 1995 for details). To apply this Monod model to results in this study, I used basal area as an index of biomass production and total P (per unit area soil) as an estimate of nutrient availability (Bridgham et al. 1995). Basal area is a more direct estimate of forest production than biomass, because errors can be introduced by different allometric equations used to calculate biomass in different geographical areas (Day et al. 1987). Basal areas were regressed against respective contents of soil P using the Monod model above and a nonlinear fitting technique (SAS 1989) by minimizing residual sum of squares. There was a significant range in total P concentrations among the mangrove sites, and basal area was strongly correlated with total soil P (Fig. 3.7). The fit of the Monod model was significant (r^2=0.80), and R_{min} was positive with an optimum soil P content of 36.3 g/m^2 to a depth of 40 cm. The half-saturation constant of soil P based on the nonlinear model was 29.3 g/m^2.

These data suggest that basal area increased asymptotically with soil P content among these even-aged mangrove forests along the Shark River estuary. Lower soil P resources in the oligohaline zone of the estuary limit the basal area development of mangrove wetlands. Basal area development approached the asymptote in the marine zone near the mouth of the Shark River estuary where maximum soil P concentrations exist. These results suggest that the landscape pattern of mangrove forest recovering from hurricane disturbance may depend on availability of soil P resources. Therefore, results in this study indicated that soil properties in the marine region of the Shark River estuary can be characterized as lacking any effects of

stress in terms of either nutrient resource or toxic compounds (salinity and sulfide). Thus Davis's (1940) hypothesis that the coastal forest in this region is the optimum growth of mangroves in the Americas can be related to these soil attributes.

Table 3.1 Average basal area (BA) increment and biomass increment per tree, and total annual basal area increment and woody growth per unit area of mangroves along the Shark River estuary, the Everglades National Park.

	S1	S3	S4	S6
Average BA increment ($cm^2 \cdot tree^{-1} \cdot yr^{-1}$)				
Avicennia germinans	5.57	7.16	0.57	-
Laguncularia racemosa	3.84	10.90	12.07	1.94
Rhizophora mangle	3.19	0.94	1.51	1.32
Conocarpus erecta	-	-	-	0.39
Average biomass increment ($kg \cdot tree^{-1} \cdot yr^{-1}$)				
Avicennia germinans	4.03	4.81	0.37	-
Laguncularia racemosa	3.09	9.17	8.59	1.15
Rhizophora mangle	2.35	0.60	1.04	0.69
Conocarpus erecta	-	-	-	0.11
BA increment ($m^2 \cdot ha^{-1} \cdot yr^{-1}$)				
Avicennia germinans	0.24	0.06	0.01	-
Laguncularia racemosa	0.65	1.11	0.09	0.04
Rhizophora mangle	0.51	0.12	0.36	0.71
Conocarpus erecta	-	-	-	0.07
Total	1.40	1.29	0.46	0.83
Total woody growth ($Mg \cdot ha^{-1} \cdot yr^{-1}$)	10.73	11.96	3.23	4.20

Table 3.2. Summary of F statistics from repeated measures ANOVA of site and season effects on pore water chemistry. Statistical tests were conducted using univariate tests. Effect of sampling station was not significant ($P>0.05$).

Sources	df	Sulfide	Salinity	NH_4^+	NO_2^-	NO_3^-	PO_4^{3-}
Site	3, 8	31.62***	167.8***	NS	12.2**	NS	NS
Season	2, 16	50.82***	445.7***	30.3***	33.4***	NS	5.17*
Site*season	6, 16	13.30***	28.9***	NS	7.3***	NS	2.93*

*$P\leq0.05$, **$P\leq0.01$, or ***$P\leq0.001$, NS no significance.

Table 3.3 Summary of F statistics from repeated measures ANOVA of site, depth and season effects on soil C, N and P. Statistical tests were conducted using univariate tests for between-subject factors (site, depth) and multivariate tests for within subject factors (season, season*site, season*depth, season*site*depth). Effects of season*depth, season*site*depth were not significant ($P>0.05$).

Variables	Sources				
	Between subject (F-values)			Within subject (Wilks' value)	
	Site	Depth	Site*Depth	Season	Site*Season
df	3, 32	3, 32	9, 32	2, 31	6, 62
Available P ($\mu g/cm^3$)	270***	88.7***	8.4***	0.47***	NS
Extractable NH_4^+ ($\mu g/cm^3$)	72***	73.0***	2.7*	0.39***	0.33***
C(%)	2317***	24.2***	6.3***	0.30***	0.63*
N(%)	1637***	21.6***	7.8***	0.22***	0.21***
P(%)	205***	9.5***	9.3***	0.60***	0.62*
C (mg/cm^3)	22***	NS	NS	0.36***	NS
N (mg/cm^3)	22***	3.1*	NS	0.24***	0.20***
P (mg/cm^3)	501***	3.5*	3.7**	0.78*	0.63*
C:N	20***	NS	3.6**	0.14***	0.12***
N:P	372***	14.0***	21.8***	0.69**	0.63*
C:P	375***	15.3***	21.6***	NS	0.61*

*$P\leq0.05$, **$P\leq0.01$, or ***$P\leq0.001$, NS=no significance

Table 3.4 Structural characteristics of mangrove forests of southern Florida, Puerto Rico, Mexico and Costa Rica.

Site	Latitude (N)	Number of trees >2.5 cm	Basal area (m^2) >2.5 cm	Reference
		Florida		
Shark River (S1)	25°20′	3725	40.4	This study
Shark River (S3)	25°21′	3600	39.7	This study
Shark River (S4)	25°22′	2575	20.7	This study
Shark River (S6)	25°24′	7333	19.6	This study
Ten Thousand Islands	25°50′	4000	38.5	Pool et al. 1977
	25°50′	2800	23.5	Pool et al. 1977
	25°50′	1800	15.0	Pool et al. 1977
Rookery Bay	25°55′	5900	20.3	Pool et al. 1977
	25°55′	2600-9400	12.9-35.5	Lugo et al. 1980
Turkey Point	25°25′	25030	6.0	Pool et al. 1977
		Puerto Rico		
Piñones	18°27′	1380-3210	15.8-21.6	Pool et al. 1977
Vacia Talega	18°27′	1890	20.9	Pool et al. 1977
Ceiba	18°15′	5690	16.7	Pool et al. 1977
Mona Island	18°06′	2930	35.0	Pool et al. 1977
Aquirre	17°57′	3670	22.6	Pool et al. 1977
Jobos Bay	17°57′	11650-47330	14.3-15.5	Pool et al. 1977
Punta Gorda	17°57′	1780	6.9	Pool et al. 1977
		Mexico		
Roblitos	22°31′	2240	29.6	Pool et al. 1977
Isla La Palma	22°35′	2360	60.8	Pool et al. 1977
Isla Roscell	22°30′	1480	28.5	Pool et al. 1977
El Calón	22°44′	3120	15.2	Pool et al. 1977
Rio de las Cañas	22°31′	1790	57.8	Pool et al. 1977
Laguna de Términos	18°40′	3360	34.2	Day et al. 1987
Laguna de Términos	18°40′	7510	23.3	Day et al. 1987
		Costa Rica		
Moin	10°00′	1370	96.4	Pool et al. 1977
Boca Barranca	09°58′	1100	32.9	Pool et al. 1977
Santa Rosa	10°45′	1050	23.2	Pool et al. 1977

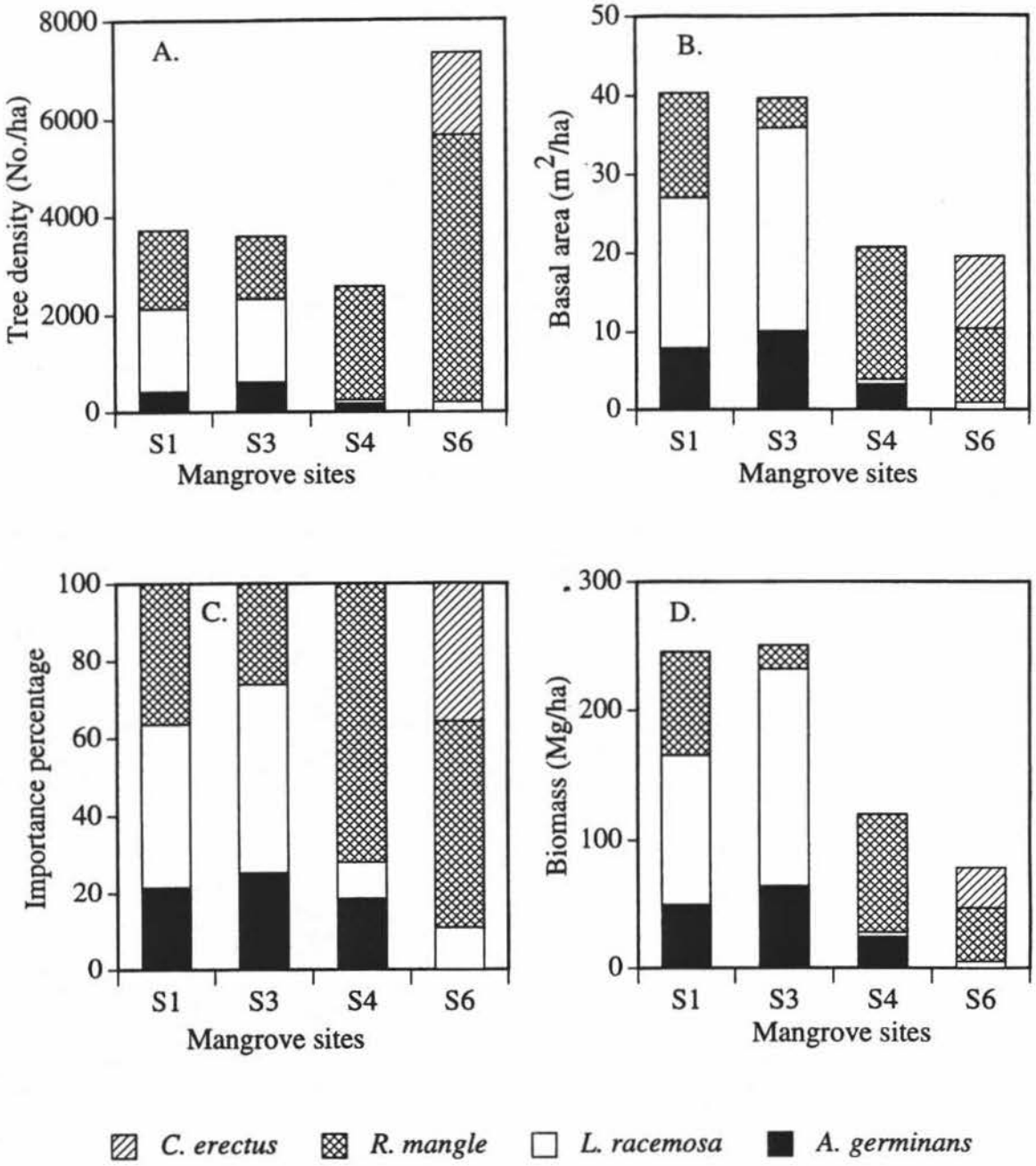


Figure 3.1 Mangrove forest structure by species at sites along the Shark River estuary from the downstream location (S1) to the upstream location (S6) including: A) Density, B) Basal area, C) Importance values, and D) Biomass.

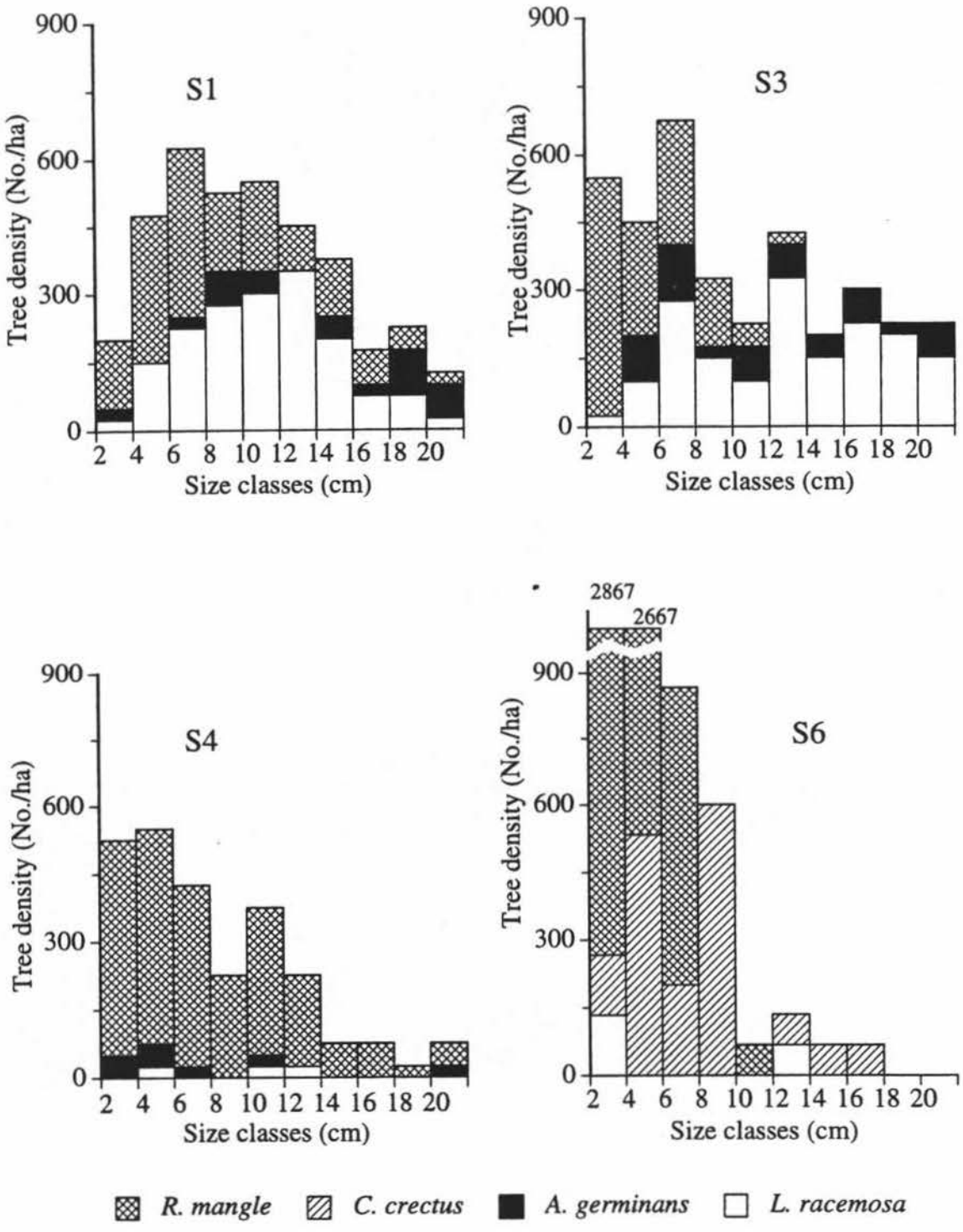


Figure 3.2 Size class distribution of mangroves by species along the Shark River estuary from the downstream location (S1) to the upstream location (S6).

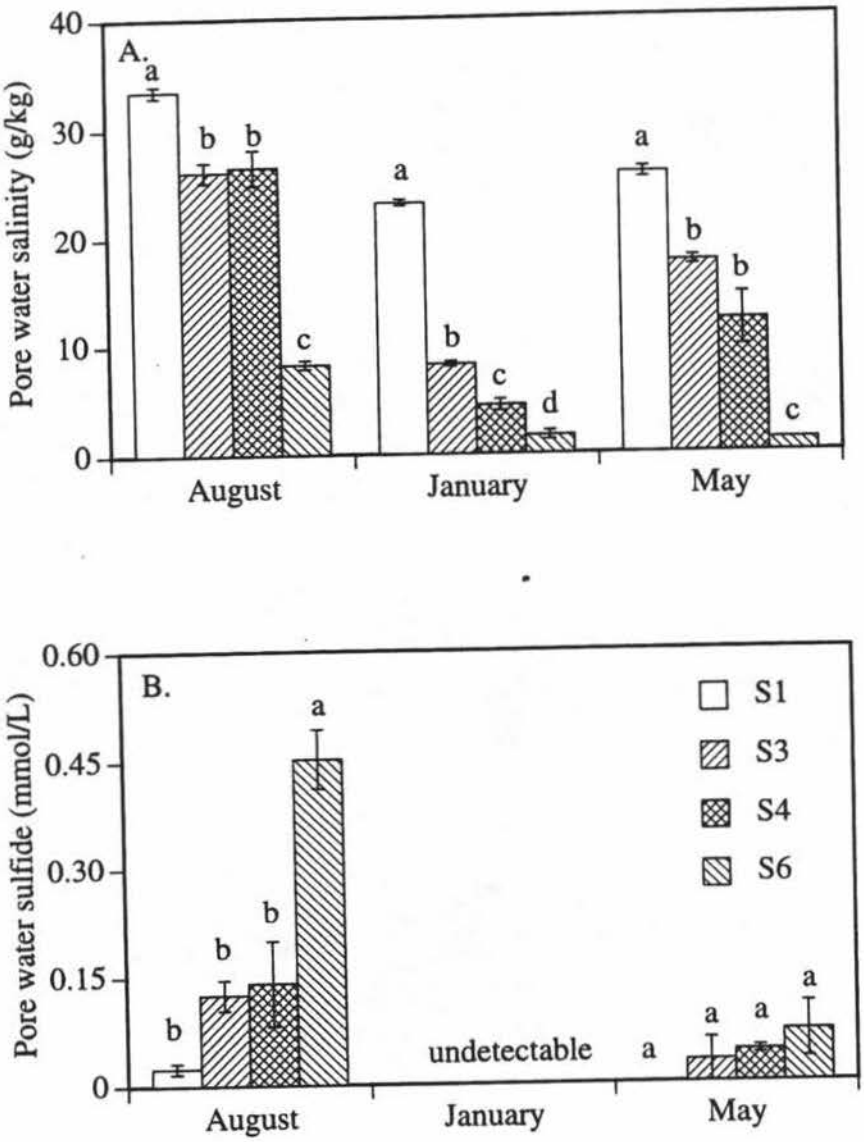


Figure 3.3 Spatial and temporal variation in pore water stressors including salinity (A) and sulfide (B) measured along the Shark River estuary during August 1994, January and May 1995. The values at each sampling date with the same letter are not significantly different ($P>0.05$; Tukey's test). Values are mean ± SE (n=3).

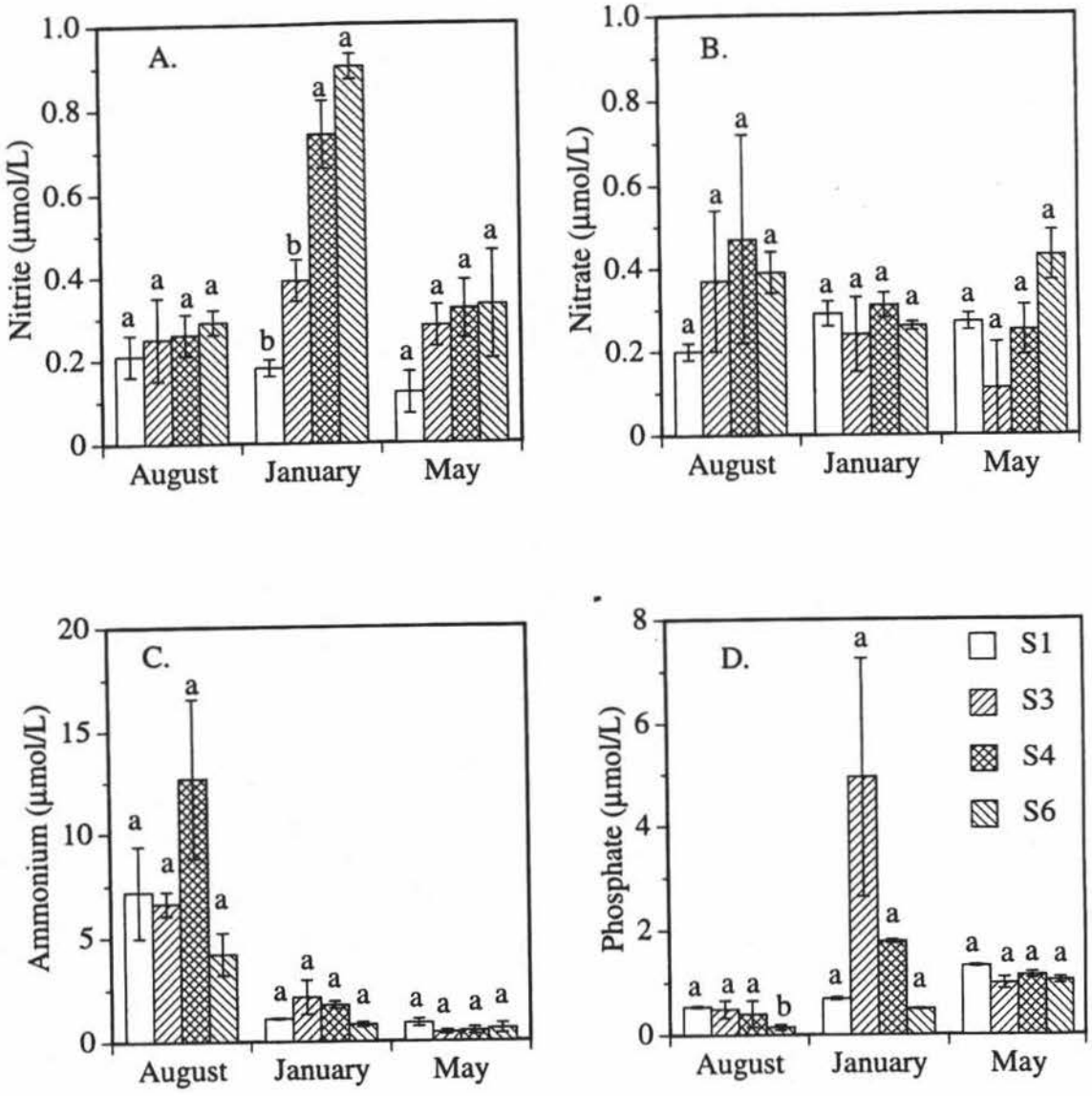


Figure 3.4 Spatial and temporal variation in pore water nutrients including nitrite (A), nitrate (B), ammonium (C) and phosphate (D) measured along the Shark River estuary during August 1994, January and May 1995. The values at each sampling date with the same letter are not significantly different ($P>0.05$; Tukey's test). Values are mean ± SE (n=3).

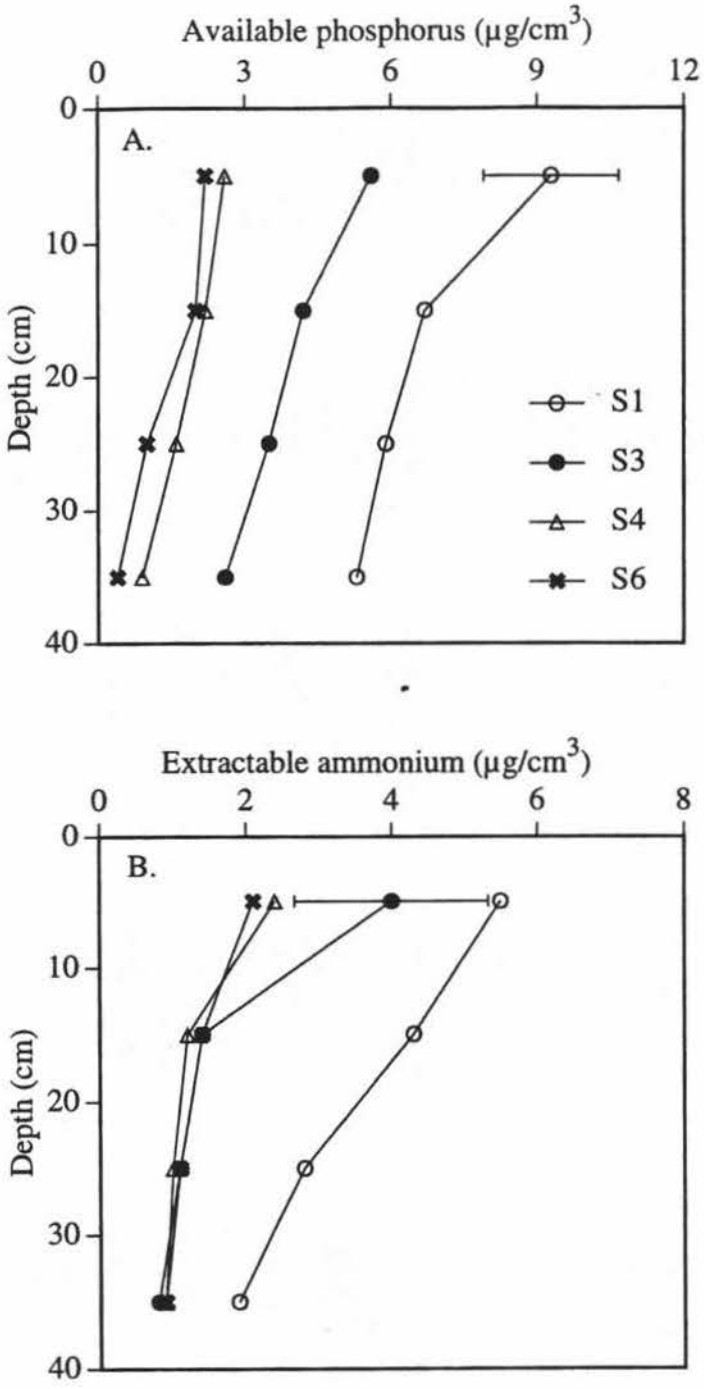


Figure 3.5 Vertical profiles of available phosphorus and extractable ammonium in mangrove soils along the Shark River estuary. Values are expressed as mean of three sampling seasons. Error bars represent the largest standard error of the mean in the data.

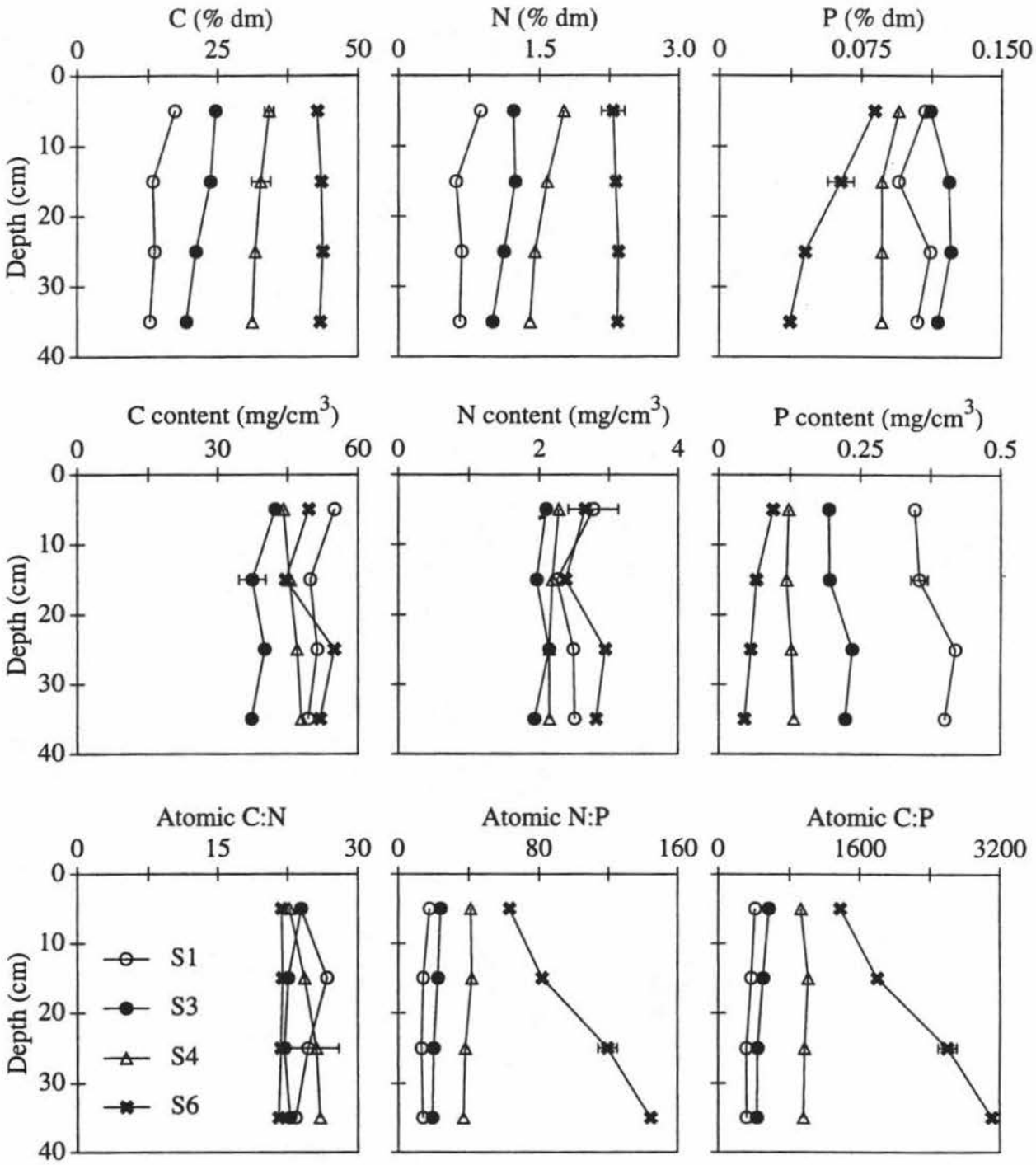


Figure 3.6 Vertical profiles of C, N and P in mangrove soils along the Shark River estuary expressed as percent dry mass (% dm), contents per unit volume of soil (mg/cm3) and atomic ratios of nutrients. Values are expressed as mean of three sampling seasons. Error bars represent the largest standard error of the mean in the data set.

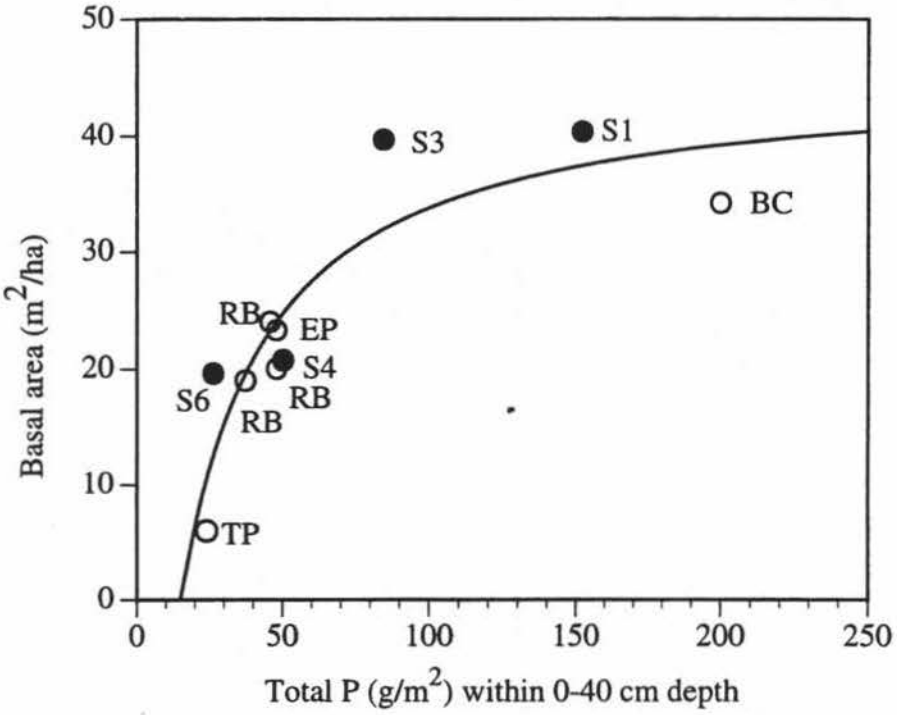


Figure 3.7 Basal area of mangrove forests relative to total phosphorus in mangrove soils. Line is prediction from Monod model (see text).
RB= Basin mangroves, Rookery Bay, Southwest Florida (Warner 1990, Lynch 1989); TP= Dwarf mangroves, Turkey Point, Southeast Florida (Pool et al. 1977, Snedaker and Brown 1981); BC= Riverine mangrove, Boca Chico, Laguna de Términos, Mexico (Day et al. 1987, Lynch 1989); EP= Fringe mangrove, Esterno Pargo, Laguna de Términos, Mexico (Day et al. 1987, Lynch 1989).

CHAPTER 4

MODELING THE VERTICAL DISTRIBUTIONS OF ORGANIC MATTER, NITROGEN AND PHOSPHORUS IN MANGROVE SOILS

ABSTRACT

The vertical distributions of organic matter, nitrogen and phosphorus in mangrove soils were investigated with a mechanistic and process-based model. The nutrient mangrove model (NUMAN) was developed from the SEMIDEC and CENTURY soil organic matter models and parameterized with data from four mangrove sites along the Shark River estuary. The soil characteristics in the four mangrove sites varied greatly in both concentrations and profiles of soil C, N and P. Organic matter, expressed as percentage of ash free dry weight, decreased from 82% in the upstream locations to 30% in the marine sites. Comparisons of the simulated and observed results demonstrated that the landscape gradient of soil characteristics can be adequately modeled by accounting for plant production, litter decomposition and export, and allochthonous input of inorganic materials. The results illustrated that the increase in organic matter content and decrease in soil bulk density from mangrove sites at the mouth of the estuary to those at upstream locations was controlled mainly by variation in allochthonous inputs of inorganic material and mangrove root production. Model simulations showed that the greatest change in organic matter, N, and P occurred in the soil surface, but changes were also evident at depths ranging from 1 cm to 5 cm at some of the sites. The rapid decomposition of labile organic matter was responsible for this decrease in organic matter. Simulated mineralization rates of nitrogen decreased quickly with depth, which corresponded with the decrease of labile organic matter. Fitting the simulation results of the model to observed nutrient profiles indicated that N and P dynamics are tightly linked to organic matter retention. In the future, NUMAN will be modified and linked to a mangrove forest gap model to simulate the feedback mechanisms of soil nutrient recycling, which controls development of the mangrove wetlands.

INTRODUCTION

Long-term geomorphic and hydrologic processes along with primary plant production largely control the formation, physical properties and chemical compositions of mangrove soils (Thom 1982). These soil characteristics have been suggested as significant controls of mangrove productivity (Boto and Wellington 1984), and soil formation has also been considered an important process contributing to biogenic carbon sinks and vertical accretion (Twilley et al. 1992, Parkinston et al. 1994). Soil formation in mangrove wetlands, as in other intertidal wetlands, is the combination of several ecological processes including organic matter production (above and belowground components), export, decomposition, and burial; as well as sedimentation of allochthonous inorganic materials. Organic matter dynamics are also tightly coupled to the biogeochemical cycles of nitrogen (N) and phosphorus (P) by the processes of decomposition, mineralization and plant uptake. Quantifying these processes can provide insights into the biogeochemistry of mangrove soils and the feedback of nutrient recycling on mangrove forest development. However, the temporal scale of soil formation in mangrove wetlands is at hundreds to thousands of years (Scholl 1964a, b). Therefore, biogeochemical models that reconstruct sediment profiles can be used to estimate the relative significance of these processes to the accumulation of organic matter and nutrients in wetland soils.

The biogeochemistry of mangrove soils was studied by modifying the SEMIDEC simulation model developed for soils in tidal marsh wetlands (Morris and Bowden 1986) and the CENTURY model developed for grasslands (Parton et al. 1987). The SEMIDEC model integrates the effects of both aboveground and belowground production, decomposition of organic matter and mineralization, and sedimentation of allochthonous inorganic materials. A

specific combination of these processes successfully predicts the profiles of organic matter, N, P and rates of N mineralization in a tidal marsh wetland.

The objectives of this study were to: (1) modify the SEMIDEC model to examine the effects of forest production, exportation, decomposition and sedimentation on C, N and P distribution in mangrove soils; (2) validate the model with measurements of spatially explicit variables along the Shark River estuary of the Everglades National Park; (3) identify key ecological processes from model simulations that account for the spatial differences among mangrove soils within this geomorphic setting; and (4) provide a soil nutrient model linked to a mangrove forest gap model, to simulate the feedback mechanisms of soil nutrient recycling.

MATERIALS AND METHODS

Soil cores were collected along the Shark River estuary in Everglades National Park in June 1994. Coring consisted of driving 15.2 cm diameter polyvinyl chloride tubing to a depth of 60 cm, compaction was minimized because of the wide diameter core. One core was taken from each site at S1, S3, S4 and S6 (Fig. 2.1). Each core was sectioned at 2 cm intervals, dried at 65°C to constant weight, and weighed for dry bulk density. Each section was ground in a grinding mill and sieved through a 20 mesh screen. Organic content, total N, and total P concentrations were determined on each section. Organic content (% ash free dry weight, AFDW) was determined by combusting each sample at 480°C for 6 h. Three randomly chosen stations in each site were marked for repeated measures of soil mineralization rates in August 1994, January and May 1995 (Chapter 2). Besides measures of mineralization rates in the 0-10 and 10-20 cm depth described in Chapter 2, I also sampled soils from 20-30 and 30-40 cm intervals. Determinations of total N, P and N mineralization rates were described in Chapter 2.

MODEL DESCRIPTION

Soil organic matter dynamics

A mangrove soil nutrient model (NUMAN) was adapted from a mechanistic and process-based model, SEMIDEC (Morris and Bowden 1986), which simulates the vertical distribution of organic matter, N, P, and mineralization in marsh sediments. The SEMIDEC model partitions soil organic matter into pools based on resistance to decomposition, assuming that each pool decomposes simultaneously and independently. Models using multiple compartments of soil organic matter have been used for terrestrial forests (LINKAGE, Pastor and Post 1986; VEGIE, Aber et al. 1991) and grasslands (CENTURY, Parton et al. 1987, Parton et al. 1988). Two pools of soil organic matter in a marsh are distinguished in the SEMIDEC model. One is the labile organic matter (LOM), with relatively rapid decay, which is analogous to the 'active' fraction of soil organic matter in the CENTURY model (Parton et al. 1987). The other pool is refractory organic matter (ROM), with slow decay, which is conceptually similar to the 'passive' fraction of soil organic matter in the CENTURY model.

A unique characteristic of the SEMIDEC model compared to other soil organic models is the calculation of the vertical profile of organic matter and nutrients. The SEMIDEC uses a life-history approach to describe the dynamics of soil organic matter and treats soil horizons as year-class cohorts, which are modified by root production and decomposition of organic matter over time as they are buried. A successful feature of the SEMIDEC model is the simulation of diagenesis for a single year cohort of sediment within a specific unit surface area, including calculations of organic matter, N and P contents in the year-class cohort. The input rates of organic and inorganic matter to the sediment are assumed to be constant.

Modifications of the SEMIDEC model were required to include some of the

biogeochemical processes that are unique to coastal forested wetlands including forest production and decomposition (Fig. 4.1). Litter fall production can be the major input of organic matter to the soil surface. Annual litter production (LP) is expressed as a direct function of forest basal area (BA):

$$LP(Mg \cdot ha^{-1} \cdot yr^{-1}) = a + b \cdot BA(m^2/ha); \quad [1]$$

where a and b are constants and were obtained by regressively fitting data collected from 17 mangrove forests in Florida, Puerto Rico and Mexico (data from Pool et al. 1975, Pool et al. 1977, Heald et al. 1979, Twilley et al. 1986, Day et al. 1987). Besides litter fall, dead trees also contribute organic matter to the forest floor (Robertson and Daniel 1989, Gong and Ong 1990). Not all of this organic matter can enter the soil, some of it is exported by tides and runoff, or consumed by animals (Heald 1969, Boto and Bunt 1981, Twilley 1985). The net accumulation of litter into mangrove soil surface was calculated as:

$$NLP = fl \cdot LP \cdot (1.0 - k_e); \quad [2]$$

$$NTP = (1.0 - fl) \cdot LP \cdot (1.0 - k_e); \quad [3]$$

$$NWP = k_m \cdot AMASS \cdot (1.0 - k_e); \quad [4]$$

where NLP, NTP, NWP are annual net accumulation of leaf litter, twigs and dead wood in mangrove soil surface, respectively. LP is expressed as $g \cdot cm^{-2} \cdot yr^{-1}$, fl is a ratio of leaf litter to total litter, and other parts of litter were treated as twigs. k_e is a site specific constant related to disappearance of standing litter, which is a function of hydrology, topography, activity and frequency of consumers. k_m is the turnover rate of wood biomass and AMASS is aboveground biomass (g/cm^2).

Net deposition of leaf litter is partitioned directly into pools corresponding to labile and refractory soil organic matter, which is based on the lignin content (lc) of leaf litter. The lignin fraction in leaf litter flows into the refractory pool, and the other fraction flows into the labile

pool. The compartments of standing dead wood and twigs have a specific decay constant, k_w and k_t, respectively. Losses of dead wood and twig litter are separated between microbial respiration and transfer to refractory organic matter. The first stage of decay for both dead wood and twig litter is respiration that represents a mass loss of 45% (k_0), which is similar to that in the CENTURY model for decomposition of structural organic matter. The contribution of aboveground litter to LOM and ROM at the surface (t=0) was calculated as:

$$LOM(0)=NLP\cdot(1.0-lc)(1.0-k_5); \quad [5]$$

$$ROM(0)=\{NLP\cdot lc+(1-k_0)[k_t\cdot NTP+k_w\cdot NWP]\}(1.0-k_5); \quad [6]$$

where k_5 is ash content of litter.

The distribution of mangrove roots is an exponential function with depth (Komiyama et al. 1989) as follows:

$$R=R_0\cdot\exp(-k_1\cdot D); \quad [7]$$

where R is root mass (g/cm2) at depth D (cm) and R_0 is root mass at the surface (g/cm2), k_1 is attenuation rate of root mass with increasing depth (D) from the surface. Root biomass within a soil cohort was calculated as in the SEMIDEC model:

$$R(t)=R_0\int_{D_b}^{D_t}\exp(-k_1 D)dD=R_0[\exp(-k_1 D_b)-\exp(-k_1 D_t)]/-k_1 \quad [8]$$

where D_b and D_t are the upper and lower depths (cm) of the soil cohort, respectively. Lacking direct information for the study sites along the Shark River estuary, I estimated annual fine root production (FRP) (g·cm-2·yr-1) and large root production (LRP) (g·cm-2·yr-1) in the soil cohort from aboveground litter production and from aboveground wood turnover rate (k_m), respectively:

$$FRP(t)=LP\cdot R(t)/RMASS; \quad [9]$$

$$LRP(t)=k_m \cdot R(t); \quad [10]$$

where RMASS is total belowground biomass (g/cm^2). Upon their death, roots also contribute to the labile and refractory organic matter pools of the soil. Organic matter input and decomposition in each year cohort of soil were modified from Morris and Bowden (1986). The mass of labile organic matter in a soil cohort is:

$$LOM(t+1)=LOM(t)-k \cdot LOM(t)+[(1-fc_1) \cdot FRP(t)+(1-fc_2) \cdot LRP(t)](1.0-k_5)$$
$$+ROM(t) \cdot k_2 \cdot (1-k_0); \quad [11]$$

where k is the decay constant of labile organic matter, fc_1 and fc_2 are fractions of fine roots and large roots that are refractory organic matter, respectively. k_2 is the decay constant of refractory organic matter.

Inputs of refractory organic matter include the refractory fraction of roots and residue from the decomposition of labile organic matter. This pool of ROM decays at a slow rate described by the equation:

$$ROM(t+1)=ROM(t)-k_2 \cdot ROM(t)+[fc_1 \cdot FRP(t)+fc_2 \cdot LRP(t)](1.0-k_5)$$
$$+k \cdot (1.0-k_0) \cdot k_3 \cdot LOM(t); \quad [12]$$

where k_3 is a proportion of decomposing LOM that enters ROM. Total soil organic matter (TOM) in a soil cohort is equal to the sum of two organic pools and root organic matter expressed as:

$$TOM(t)=LOM(t)+ROM(t)+R(t) \cdot (1.0-k_5). \quad [13]$$

Inputs of inorganic material to soil surface include allochthonous inorganic material and release of minerals from decomposing litter. I assumed that root uptake of inorganic material is restricted to the soil surface, because this is where most of the fine absorbing roots in mangroves soils are found (Clough 1992). The model also assumed that the uptake of

inorganic material for root growth is balanced by release of inorganic material from dead roots. Annual amounts of inorganic material absorbed by roots to support aboveground growth are equal to the sum of inorganic material in litter and wood production. Therefore, the amount of inorganic material within a soil cohort under the surface cohort was assumed constant with depth. The amount of inorganic material in the surface can be calculated as:

$$Wi(0)=k_4+k_5\cdot(NLP+NTP+NWP)-k_5\cdot(LP+k_m\cdot AMASS); \quad [14]$$

where Wi is the amount of inorganic material. k_4 is the annual deposition of inorganic material ($g\cdot cm^{-2}\cdot yr^{-1}$) from allochthonous sources.

The volume of a soil cohort was calculated as:

$$V(t)=[LOM(t)+ROM(t)+R(t)]/b_o+Wi(t)/b_i; \quad [15]$$

where b_o and b_i are the bulk density of organic matter and inorganic material (g/cm^3) within the soil cohort, respectively. For organic soils, the inorganic term in the above equation [15] is eliminated in the SEMIDEC model. Each soil cohort in the model represents 1 yr of organic and inorganic matter accumulation per unit area (cm^2) of soil. The volume of a soil cohort is its vertical height (cm), therefore

$$D_b=D_t+V(t); \quad [16]$$

where D_b was solved numerically corresponding to the new cohort depth based on the volume of organic and inorganic matter in that cohort (for a full description of these calculations see the SEMIDEC model, Morris and Bowden 1986). Then this new depth was used to calculate root biomass within the soil cohort. The overall bulk density (BD, g/cm^3) of that soil cohort is the sum of labile and refractory organic matter, root biomass and inorganic material divided by height of the cohort using:

$$BD(t)=(LOM(t)+ROM(t)+R(t)+Wi(t))/(D_b-D_t). \quad [17]$$

Notice that this model does not account for the effect of compaction on soil formation.

Soil nitrogen and phosphorus

The nitrogen model was different from that used in the SEMIDEC model, because of the uncertainty in identifying several parameters. Instead I used the CENTURY model as an approach to simulate nitrogen dynamics by assuming that soil N is bonded to C. In the NUMAN model, C:N ratio of LOM is 8 and of ROM is 20, and both remain fixed during the simulations. The C:N ratio of LOM is the same as active soil organic fraction in the CENTURY model. The C:N ratio of ROM was based on C:N measurements of mangrove soils in this study. Thus, the amount of total N in LOM (NLOM) and ROM (NROM) was calculated as:

$$NLOM(t)=LOM(t)/(2 \times 8); \quad [18]$$

$$NROM(t)=ROM(t)/(2 \times 20); \quad [19]$$

$$TN(t)=NLOM(t)+NLOM(t)+k_6 \cdot R(t); \quad [20]$$

where the factor 2 is the ratio of organic matter to C based on measurements in this study, k_6 is the N concentration of roots, and TN is total N amount in that soil cohort. N flows were assumed to be related to organic matter flows. N mineralization occurs by the decomposition of LOM and ROM:

$$N_{min}(t)=k \cdot NLOM(t)+k_2 \cdot NROM(t); \quad [21]$$

where $N_{min}(t)$ is the gross mineralization rate within the cohort ($gN \cdot cm^{-2} \cdot yr^{-1}$). Nitrogen loss from mangrove soil occurs as a result of plant uptake, immobilization, leaching, ammonia volatilization, and denitrification. The model calculated gross N mineralization, but did not trace the loss of N. Total annual N mineralization from the soil (TN_{min}, $g \cdot cm^{-2} \cdot yr^{-1}$) between the surface (at t=0) and a given depth for a specific time interval (n) is calculated by summing

the mineralization in each soil cohort at the depth range as follows:

$$TN_{min} = \sum_{t=0}^{n} N_{min}(t) \quad [22]$$

Inputs of P into mangrove soils include organic P from decomposing litter and mineral P deposition on the surface. Losses of P were assumed to be a function of gross N mineralization from organic matter. That is:

$$P(0) = p_0 + k_7 \cdot (NLP + NTP + NWP); \quad [23]$$

$$P(t+1) = P(t) - m \cdot N_{min}(t+1); \quad [24]$$

where k_7 is the concentration of P in litter, p_0 is the annual deposition of allochthonous P ($gP \cdot cm^{-2} \cdot yr^{-1}$) on the soil surface, and m is ratio of losses of N mineralization to P.

MODEL PARAMETERIZATION

Many of the parameters in the NUMAN were based on field results from the mangrove sites along the Shark River estuary, whereas others represent published data in the mangrove literature (Table 4.1). Litter bag studies of leaf degradation were used to derive decay constants as estimates for decomposition of LOM. Numerous studies have been conducted on decomposition of mangrove leaves. The average decay constant of *Rhizophora mangle* and *Avicennia germinans* leaves was 0.62 yr^{-1} in a mangrove wetland of southwestern Florida using 1 mm mesh litter bags (Twilley et al. 1986), which is similar to a decay constant of 0.624 yr^{-1} for *Laguncularia racemosa* leaves in a Mexican mangrove forest (Flores-Verdugo et al. 1987). Similar values of 0.54 and 0.64 yr^{-1} were found for *Avicennia marina* in an Australian mangrove (Van der Valk and Attiwill 1984). Heald (1969) studied decomposition of *Rhizophora mangle* leaves in brackish, predominantly fresh and dry conditions,

respectively, in the North River using 2 mm mesh bags. Fitting his data with a negative exponential function showed decay constants of 2.80, 1.47 and 0.93 yr^{-1}. Large mesh size allows greater losses of detritus from litter bags which are not completely decomposed. The decay of LOM in the NUMAN model occurs in the surface and sub- surface strata of mangrove soils. Therefore, estimating a decay constant from experiments using litter bags with a smaller mesh is better. Experiments that measure the decomposition of wood litter in mangrove wetlands are limited, but results show that decay constants for wood and twigs are low at 0.083 and 0.276 yr^{-1}, respectively (Robertson and Daniel 1989).

Parameters in the model including fc_1, fc_2, k_4 and k_e are unknown from the literature on mangrove ecology. I assumed that the fraction of fine roots contributed to the pool of ROM was the same fraction as for leaf litter (fc_1=0.15). However, I used fc_2=0.3 for the refractory fraction of other roots assuming that larger roots have a higher proportion of structural material.

Profiles of organic matter and bulk density are controlled by k_e and k_4 and these coefficients were determined by a model-tuning procedure, where the parameters were adjusted to fit observed soil profiles (Parton et al. 1987). The coefficient, k_4, represents sediment accretion, which can be determined directly by measuring a profile of ^{210}Pb in sediment (Lynch et al. 1989). If this coefficient was known, then k_e could be estimated independently. A best fit of measured and simulated concentrations of organic matter content and bulk density was accomplished by adjusting k_4 and k_e. An increase of k_4 or k_e will lead to higher values of bulk density but lower concentrations of organic matter. Heald (1969) measured organic matter export in a well-developed *Rhizophora mangle* forest in the North River, near the Shark River estuary, and found that 42% of leaf litter was exported to the estuary. I used k_e=0.4 as a reference parameter and adjusted k_e and k_4 to produce the best fit profile of nutrients. This

model-tuning technique using field estimates for one of the parameters is a constraint that keeps k_4 and k_e within a reasonable range.

Site specific parameters, such as aboveground biomass and basal area, were based on values obtained from the field sites (Chapter 3). Distances of the four study sites from the mouth of the estuary were 1.8, 4.1, 9.9 and 18.2 km. Aboveground biomass was higher in S1 and S3 than in S4 and S6 (Table 4.2). The model assumed that forest structure at all sites was in steady state and thus no changes in biomass and basal area were calculated during the simulations. The decrease in forest stature from the marine to the oligohaline zone of the estuary has been observed for more than half a century (Davis 1940). The turnover rate for wood (k_m,) was calculated as an average value for the four mangrove sites based on the relationship between woody production and aboveground biomass (Aber et al. 1991). The biomass and productivity of the belowground component of mangrove wetlands are poorly understood. Two *Rhizophora* forests in Puerto Rico and Panama have an average ratio of belowground to aboveground biomass of 0.74 (Golley et al. 1962, 1975), which was used to calculate belowground biomass. The depth of root distribution was assumed to be 150 cm from the sediment surface.

RESULTS AND MODEL CALIBRATION

The model was calibrated by simulating steady state production of the four mangrove sites along the Shark River estuary, which represent a landscape and salinity gradient from the oligohaline to marine soil conditions. Soil conditions in the downstream location (S1 and S3) were considered optimal for the growth of mangrove wetlands in Florida (Chapter 3). The observed soil profile of organic matter, bulk density, N and P varied significantly among the

four study sites. Average concentrations of organic matter (% AFDW) to a depth of 60 cm decreased from the oligohaline to marine sites with values of 82%, 62%, 45% and 30% at S6, S4, S3 and S1, respectively. In contrast to AFDW, bulk density increased from S6 to S1 with a value of 0.142, 0.187, 0.221 and 0.438 g/cm^3 as a result of decreased organic matter content. Like organic matter content, soil N concentrations declined from S6 (2.01%) to S1 (0.52%), whereas S4 and S3 had intermediates value of 1.40 and 1.08%, respectively. Higher P concentrations were found at S3 (0.097%) and S1 (0.085%) than at S4 (0.069%) and S6 (0.041%). Except in S1, vertical profiles of organic matter and bulk density in mangrove soils exhibited no clear differences with depth. N profiles varied with site, S1 and S4 had a relatively constant vertical distribution; whereas, N concentrations decreased to a depth of 40 cm in S3 and S6. P concentrations decreased from the surface to 40 cm in S3, S4 and S6, however, concentrations varied irregularly at the top 30 cm in S1.

The major source of freshwater to the estuary is from the Shark River Slough, and a gradient of salinity in mangrove soils along the estuary represents the relative importance of terrestrial runoff and Gulf water to the soil profile at a particular location. Tidal flooding increases and the influence of fresh water decreases from the upstream sites to those near the mouth of the Shark River estuary. Values of forest biomass at each respective site were used as initial conditions in the model to simulate soil nutrients profiles. The NUMAN model assumed that the loss of litter (parameter k_e) and allochthonous inorganic input (parameter k_4) were related to the spatial locations of the four sites along the estuary. The parameters k_e and k_4 were assumed to increase systematically from the oligohaline site (S6) to the marine site (S1) to produce a best fit profile (Table 4.2), since rates of organic matter export and sedimentation are higher in mangrove sites nearer the gulf coast.

The simulated concentrations of AFDW were within 12 percent of the observed

concentrations in S3, S4 and S6 below depth 10 cm, however, measured concentrations of AFDW varied significantly with depth in S1 with a minimum AFDW of 15.8% at depth 16-18 cm (Fig. 4.2). Generally, the model predicted a quick decrease of AFDW at the surface, because of the rapid decomposition of LOM. The predicted depth of rapid organic matter decomposition varied among sites, ranging from 1 cm at S6 to 5 cm at S1. Simulations showed that AFDW at S4 and S6 increased slowly below the rapid decomposition layer, which was an excellent fit to the observed profile below the top 10 cm. In contrast, the model did not predict an increase in AFDW below the rapid decomposition layer at S1, but showed a relatively constant concentration with depth. The discrepancies in AFDW profiles among the downstream (S1), intermediate (S4) and upstream (S6) sites were due to higher deposition rates of allochthonous inorganic materials at the sites near the mouth of the estuary. The simulated profiles of bulk density showed a reverse trend as AFDW among the sites and a good fit was observed in S3, S4 and S6 (Fig. 4.3). Observed bulk density in S1 indicated a peak value of 0.622 g/cm^3 at 16-18 cm depth, with some variance through the whole core.

The simulated N concentrations were within the extreme concentrations of observed profiles at each site, except at surface soil in S1 and S3 (Fig. 4.4). The observed N profile in S1 was a S-shaped curve with depth, whereas simulated N concentrations were constant with depth at about the average value of the observed concentrations. The model predicted a slight increase in N concentrations following an initial decline in surface soils in sites S3, S4 and S6, which fits well with the observed N profile in S4. But this pattern of soil N is a poor fit of concentrations in S3 and S6, differences in slope of profiles at S3 and S6 were evident.

Daily rates of net N mineralization for each mangrove site were averaged from field measurements on three sampling dates (Chapter 2), and these average values were extrapolated to an annual rate, and compared to simulated gross mineralization rates (Fig. 4.5). Note that

the observed N mineralization rates were representative of 10 cm sections (to a depth of 40 cm), however, simulated values were calculated for each soil cohort section. Both the simulated and observed N mineralization rates in each study site decreased quickly with depth, except for the observed values in S1. Also, the simulated values were generally higher than the observed values. However, the observed profile of N mineralization in S1 did not decrease quickly in the top 30 cm, and this rate exceeded the simulated value below the top 10 cm section. Simulated rates of N mineralization were higher than observed values, which may be an artifact of the difference in field methods and operational definitions of this process within the model. The laboratory incubations of mangrove soil in my study provided an index of net N mineralization during the incubation period, including the consumption by microbes during organic matter mineralization. Therefore, it is reasonable that the estimate of N mineralization by the model was higher than the net mineralization rates measured in laboratory incubations. The model calculated the integrated gross N mineralization rate within 0-40 cm and showed an increase from the upstream to downstream sites along the Shark River estuary with values of 4.8 (S6), 5.3 (S4), 8.9 (S3), and 8.9 (S1) mg $N \cdot cm^{-2} \cdot yr^{-1}$.

Parameter p_0, the annual input of allogenic inorganic and organic P through deposition of sediment particles or adsorption from flooding waters, was adjusted to fit the P profile for each site (Table 4.2, Fig. 4.6). Compared to mean observed P concentration of 0.85% in S1, the simulated P concentration slightly decreased from 0.91% at depth 3 cm to 0.84 at depth 60 cm by assuming p_0=0.00019 $g \cdot cm^{-2} \cdot yr^{-1}$ or 1.9 $g \cdot m^{-2} \cdot yr^{-1}$. The observed P profile in S1 indicated a low P concentration of 0.037% at depth of 16-18 cm corresponding to a high value of bulk density at that depth. Both observed and simulated P concentrations in S3 decreased gradually below an initial increase. Predicted P concentrations increased rapidly in the top 1 cm of soil in S4 and S6, then decreased rapidly with depth. This decrease in P concentrations

in the model fit well with the observed P profile, which corresponded with a release of P from organic matter associated with N mineralization.

Profiles of N:P ratios varied markedly among the sites, not only in the magnitude of N:P ratios, but also in the trends of N:P ratios with depth (Fig. 4.7). S1 had a relatively constant N:P ratio of 6.1 with depth. Except at depth of 22-24 cm, where a maximum N:P ratio of 17 was measured, observed values in S3 showed a slight increase from 10 at 2 cm depth to 12 below 54 cm. The observed N:P ratios in S4 decreased from 29 at the soil surface to 16 at 6-8 cm, then increased to 32 at 60 cm. The observed N:P ratios in S6 increased significantly from 23 at the surface to 66 at 36 cm, then shifted to 107 at 38 cm and decreased to 79 at 60 cm. Simulated N:P ratios were an excellent fit with the observed N:P profiles in S1 and S3, except for a difference in the top 4 cm. Both observed and simulated N:P ratios in S4 indicated a decrease in the soil surface followed by an increase below that depth. The simulations of S6 correctly forecasted the significant increase of N:P ratio with depth.

DISCUSSION

The NUMAN model of mangrove soils was modified from the SEMIDEC and CENTURY models, and parameterized with independent field measurements in mangrove soils along the Shark River estuary. Comparisons of simulated and observed results demonstrated that significant landscape gradients of soil characteristics can be adequately modeled using plant production, loss rates of standing litter, decomposition of organic matter, and allochthonous inputs of inorganic material as key ecological processes. The NUMAN model simulates vertical distributions of organic matter, and N and P concentrations in mangrove soils as a

function of organic matter diagenesis in a coastal forested wetland. This model also predicts various rate processes, such as N mineralization, sedimentation and root turnover rate, based on the profiles of organic and inorganic matter.

I hypothesized that organic matter concentrations in mangrove soils would be elevated at those sites with low export rates of litter and low deposition rates of inorganic material from allochthonous sources. These processes are site-specific along the longitudinal axis of the Shark River estuary. Litter export rates used in the NUMAN model ranged from 0.4 to 0.6 for this estuary, which were based on several published data. For Florida mangroves, Heald (1969) estimated that 42% of the litter fall in a fringe mangrove was exported as leaf litter detritus in the North River, the similar result was found by Lugo and Snedaker (1975) that 41% of leaf litter fall was exported in a black mangrove forest of Rookery Bay. In Australian mangroves, Boto and Bunt (1981) calculated litter export rate was 81% of litter fall. Flores-Verdugo et al. (1987) observed 90% of the litter fall was exported to the adjacent lagoon in a white mangrove forest in Mexico.

Observed results in my study showed that soil organic matter concentrations among mangrove wetlands increased dramatically with increased distance from the estuary mouth, while bulk densities decreased, suggesting that sedimentation rates decreased along the axis of the estuary. The NUMAN model is able to simulate the spatial gradient of soil profiles by adjusting the amount of inorganic material input in a reasonable range as compared to recent studies of sediment accumulation among mangrove forests (Lynch 1989) (Table 4.3). Lynch (1989) used ^{210}Pb dating techniques to estimate the accretion rates in mangrove forests in southwest Florida and Mexico and found that accumulation of inorganic material varied significantly among ecological types of mangroves, ranging from 107 to 1404 $g \cdot m^{-2} \cdot yr^{-1}$. The model required an input of 1500 $g \cdot m^{-2} \cdot yr^{-1}$ of inorganic material to maintain a soil profile with

a bulk density of 0.438 g/cm^3 in S1. A riverine mangrove forest in Terminos Lagoon, Mexico, where rivers contribute large amounts of sediment, had a bulk density of 0.412 g/cm^3 and required 1404 g·m^{-2}·yr^{-1} of inorganic material accumulation. It is interesting to note that litter production for S1 calculated from the allometric equation in the NUMAN model was 13.1 Mg·ha^{-2}·yr^{-1}, which is close to the value of 12.5 Mg·ha^{-2}·yr^{-1} in the riverine mangrove forest at Terminos Lagoon (Day et al. 1987). This implies that a similar rate of organic matter production contributes to comparable rates of soil formation.

Inorganic material accumulation estimated by the model for S3 was similar to the measured rate for a fringe mangrove forest in Estero Pargo. However, the organic matter content is higher in S3 than in Estero Pargo (45.3% vs 32.4%), probably reflecting higher organic production in S3 as indicated by the difference in basal area of the two forests (39.7 vs 23.3 m^2/ha). Organic matter, bulk density and N concentration in soils in S4 are similar to those of a basin mangrove in Rookery Bay, where there has been extensive mangrove research (Lugo and Snedaker 1975, Twilley 1985, Twilley et al. 1986). Model simulations for S4 using a litter export rate of 45% of litter fall (k_e=0.45) required an input of 180 g·m^{-2}·yr^{-1} of inorganic material to fit the soil profile of bulk density at this site. This sedimentation rate was similar to the measured rate of inorganic sediment accumulation in Rookery Bay basin forest (107-179 g·m^{-2}·yr^{-1}). There are no literature values of sedimentation for a mangrove wetland representative of S6, which is a site with extremely high organic matter concentrations, yet it appears that an inorganic input rate of 76 g·m^{-2}·yr^{-1} is reasonable for this oligohaline site. The lack of inorganic sediment input is due to the presence of low concentrations of suspended sediment from the Shark River Slough, and increased distance from the Gulf of Mexico.

Patterns of organic matter and bulk density distributions based on simulation results assume that compaction is negligible. This assumption is suitable for the study sites because

observed organic matter and bulk density profiles of mangroves do not change markedly to a depth of 60 cm. However, changes in bulk density concentration with depth indicate that compaction in mangrove sediments can be significant (Lynch 1989).

Compared with P accumulation rates measured in the other mangrove forests, the model calculated a higher input of P for the downstream locations (S1 and S3), due to higher P concentrations in soils along the estuary (Table 4.3). In Water Conservation Area 2A in the freshwater Everglades, Davis (1991) estimated P retention of 1.1 to 1.4 $gP \cdot m^{-2} \cdot yr^{-1}$ and Reddy et al. (1993) reported P accumulation ranging from 0.11 to 1.14 $gP \cdot m^{-2} \cdot yr^{-1}$ depending on distance from inflow structure. These observed rates are similar to the estimates by the NUMAN model for S3, S4 and S6 at 1.2, 0.4, and 0.27 $gP \cdot m^{-2} \cdot yr^{-1}$, respectively.

In its present form, the model simulated N and P mineralization rates based on only the decomposition of labile organic matter which is set at a fixed rate. The model was able to produce reasonable rates of N and P mineralization, and N:P ratio profiles, compared to observed results. These simulations suggest that N and P dynamics in mangrove soils were tightly linked to C dynamics. N dynamics in mangrove soil are complex and involve microbial metabolism and chemical and physical processes, such as N fixation (Alongi et al. 1992), fluxes between overlying water (Rivera-Monroy et al. 1995a), ammonification (Chapter 2), nitrification and loss N through denitrification (Rivera-Monroy et al. 1995b, Rivera-Monroy and Twilley 1996). N mineralization rates were also related to other nutrient availabilities such as P, and varied dramatically with season (Chapter 2). Although P may exists with several minerals, organic P was the major component of this nutrient in mangrove soils among the study sites (Chapter 2). Further investigations into the effects of microbial activity on organic matter dynamics are needed for an accurate assessment of N and P mineralization.

One of the objectives of an ecosystem model is to identify those ecological processes

that are poorly understood and which may play an important role in the biogeochemical properties of an ecosystem. My study suggested that the rates of root production, which lacked any direct verification, are critical processes in controlling organic matter accumulation and the vertical distribution of organic matter in mangrove soils. Mangrove peat in south Florida consists mainly of mangrove rootlets (Davis 1940, Scholl 1964a,b), suggesting that underground litter production plays a critical role in forming peat of mangrove forest. However, direct measurements of root production in mangrove wetlands are difficult, especially in identifying dead and live roots, and the effect of depth on organic matter decomposition is also not clear. Therefore, these model simulations provide a valuable estimate of the potential contribution of these processes by fitting observed soil profiles with new parameters.

The ability of the model to simulate organic matter diagenesis in soil was limited by its assumption that driving variables are in steady state. ^{14}C dating techniques revealed that mangroves have developed in the Shark River region over the past 3000 yrs (Scholl 1964a,b). Mangrove rootlets have contributed significantly to the 1-4 m of peat that has developed during the late Holocene transgression (Davis 1940, Craighead 1971). However, hurricanes, which are one of major large scale and cyclic disturbances for mangroves in Florida (Lugo and Snedaker 1974), can destroy mangrove biomass and redistribute tremendous amount of sediments in mangrove wetlands (Smith et al. 1994). These processes can seriously influence model predictions based on steady state assumptions of ecological processes. Observed soil profiles in S1 exhibited obvious shifts in bulk density and organic matter with depth. These sharp gradients in soil profiles probably reflect different sedimentation rates in this site. Site S1 was the only site with a four cm thick layer located 15 cm below the surface soil which had a significantly higher bulk density of 0.62 $g \cdot cm^{-3}$ compared to the mean bulk density of 0.44

$g \cdot cm^{-3}$ within 0-60 cm at S1. This difference in bulk density may be related to large amounts of sedimentation caused by Hurricane Donna in 1960. It has been observed that Hurricane Andrew resuspended sediments from the Gulf of Mexico and deposited 1-10 cm thick layers of sediment in mangrove wetlands in the Everglades National Park (Smith et al. 1994). The hurricane-induced sedimentation may decrease with distance from the source of resuspended sediments at the mouth of the estuary. I did not observe a peak of bulk density at other sites along the Shark River estuary similarly to the one measured in S1.

The NUMAN model used a constant rate of mangrove litter production based on the basal area structure of the forest. However, forest production is constrained by environmental variables, such as soil nutrient availability, which is determined by nutrient mineralization from organic matter and inputs of allochthonous materials. For future applications, the model can be modified and linked to forest dynamics model as a subroutine to simulate the feedback mechanisms of nutrient cycling, which controls the development of mangrove ecosystems.

Table 4.1. Definition and values of parameters used in the NUMAN model.

Parameters	Definition	Unit	Values	Source
b_o	Bulk density of organic matter	g/cm^3	0.1154	This study
fc_1	Fraction of fine root that is refractory	g/g	0.15	estimated
fc_2	Fraction of large root that is refractory	g/g	0.3	estimated
fl	Ratio of litter leaves to total litter	g/g	0.70	Pool et al. 1975, Twilley et al. 1986
k_0	Proportion of microbial respiration during decomposition	g/g	0.45	Parton et al. 1987
k	Decay constant for labile organic matter	yr^{-1}	0.62	See text
k_1	A distribution parameter for root biomass	cm^{-1}	0.04	Komiyama et al. 1987
k_2	Decay constant for refractory organic matter	yr^{-1}	0.00067	Parton et al. 1987
k_3	Proportion of labile organic matter flowing into refractory organic matter after decomposition	g/g	0.03	Parton et al. 1987
k_4	Annual deposition of inorganic material	g·cm^{-2}·yr^{-1}	Table 4.2	
k_5	Ash concentration in litter	g/g	0.10	Benner et al. 1990
k_6	N concentration in roots	g/g	0.005	Stanford 1976
k_7	P concentration in litter	g/g	0.0002	Stanford 1976
k_e	Disappear rate of standing litter	yr^{-1}	Table 4.2	
k_m	Turnover rate of wood	yr^{-1}	0.425	Chapter 3
k_t	Decay constant of litter twigs	yr^{-1}	0.276	Robertson and Daniel 1989
k_w	Decay constant of dead root	yr^{-1}	0.083	Robertson and Daniel 1989
lc	Lignin content in litter leaves	g/g	0.15	Benner et al. 1990
LP	Litter production	g·cm^{-2}·yr^{-1}	Table 4.2	
m	Ratio of N mineralization to P loss	g/g	0.00672	Morris and Bowden (1986)
R_0	Total root biomass	g/cm^2	Table 4.2	
RMASS	Total root biomass	g/cm^2	Table 4.2	
p_0	Annual allochthonous deposition of P	g·cm^{-2}·yr^{-1}	Table 4.2	
AMASS	Total aboveground biomass	g/cm^2	Table 4.2	

Table 4.2. Site specific parameters for simulations of the NUMAN model.

Parameter	S1	S3	S4	S6	Methods and source
Aboveground biomass (g/cm^2)	2.5	2.5	1.27	0.787	Allometric method, Chapter 3
Belowground biomass (g/cm^2)	1.85	1.85	0.94	0.582	Ratio of below/aboveground biomass
Basal area (m^2/ha)	40.36	39.67	20.72	19.61	Field survey, Chapter 3
R_0 (g/cm^2)	0.074	0.074	0.0377	0.023	Allometric method
LP ($g \cdot cm^{-2} \cdot yr^{-1}$)	0.13	0.129	0.074	0.071	Regression method
k_4 ($g \cdot cm^{-2} \cdot yr^{-1}$)	0.15	0.06	0.018	0.0076	Best estimate
k_e (yr^{-1})	0.6	0.58	0.45	0.4	Best estimate
p_0 ($g \cdot cm^{-2} \cdot yr^{-1}$)	0.00019	0.00012	0.00004	0.000027	Best estimate

Table 4.3. Comparisons of mangrove forest structure and sediment characteristics.

	Rookery Bay[1]	Boca Chica[2]	Estero Pargo[2]	Shark River[3]			
				S1	S3	S4	S6
Distance from open water (m)	10-70	10	15	20	20	20	5
Basal area (m^2/ha)	20-25	34.2	23.3	40.4	39.7	20.7	19.6
Litterfall ($Mg \cdot ha^{-2} \cdot yr^{-1}$)	8.1	8.3	12.5	13.1[a]	12.9[a]	7.4[a]	7.1[a]
Bulk density (g/cm^3)	0.188-0.221	0.412	0.288	0.438	0.221	0.187	0.142
AFDW (%)	52.3-64.3	22.5	32.4	30.3	45.3	62.3	82.2
N (%DM)	1.4-1.73	0.32	0.57	0.52	1.08	1.40	2.01
P(%DM)	0.05-0.058	0.043	0.058	0.085	0.097	0.069	0.041
Accumulation rate of inorganic matter ($g \cdot m^{-2} \cdot yr^{-1}$)	107-179[b]	1404[b]	566[b]	1500[c]	600[c]	180[c]	76[c]
Accumulation rate of P ($g \cdot m^{-2} \cdot yr^{-1}$)	0.15-0.20[b]	0.78[b]	0.48[b]	1.9[c]	1.2[c]	0.4[c]	0.27[c]

1. Data source: basal area from Warner (1990), litterfall from Steyer (1988), other data from Lynch (1989);
2. Data source: basal area and litterfall from Day (1987), other data from Lynch (1989);
3. Data source: this study;
a. Based on allometric method;
b: based on ^{210}Pb dating techniques;
c: model best estimates.

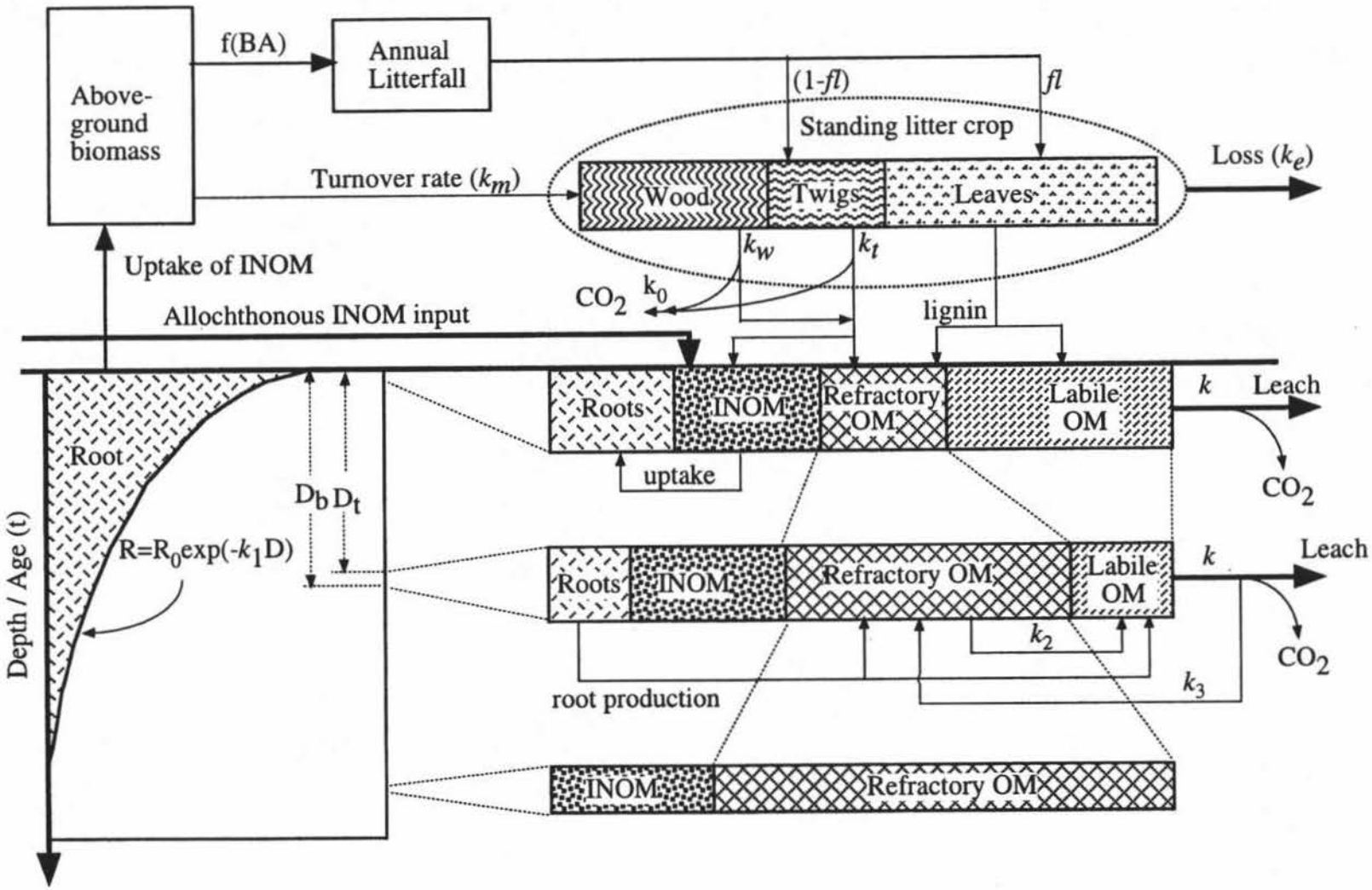


Figure 4.1. Conceptual diagram of the NUMAN model that simulates the biogeochemistry of sediment cohorts changing with depth in a mangrove ecosystem. (OM: organic matter; INOM: inorganic material).

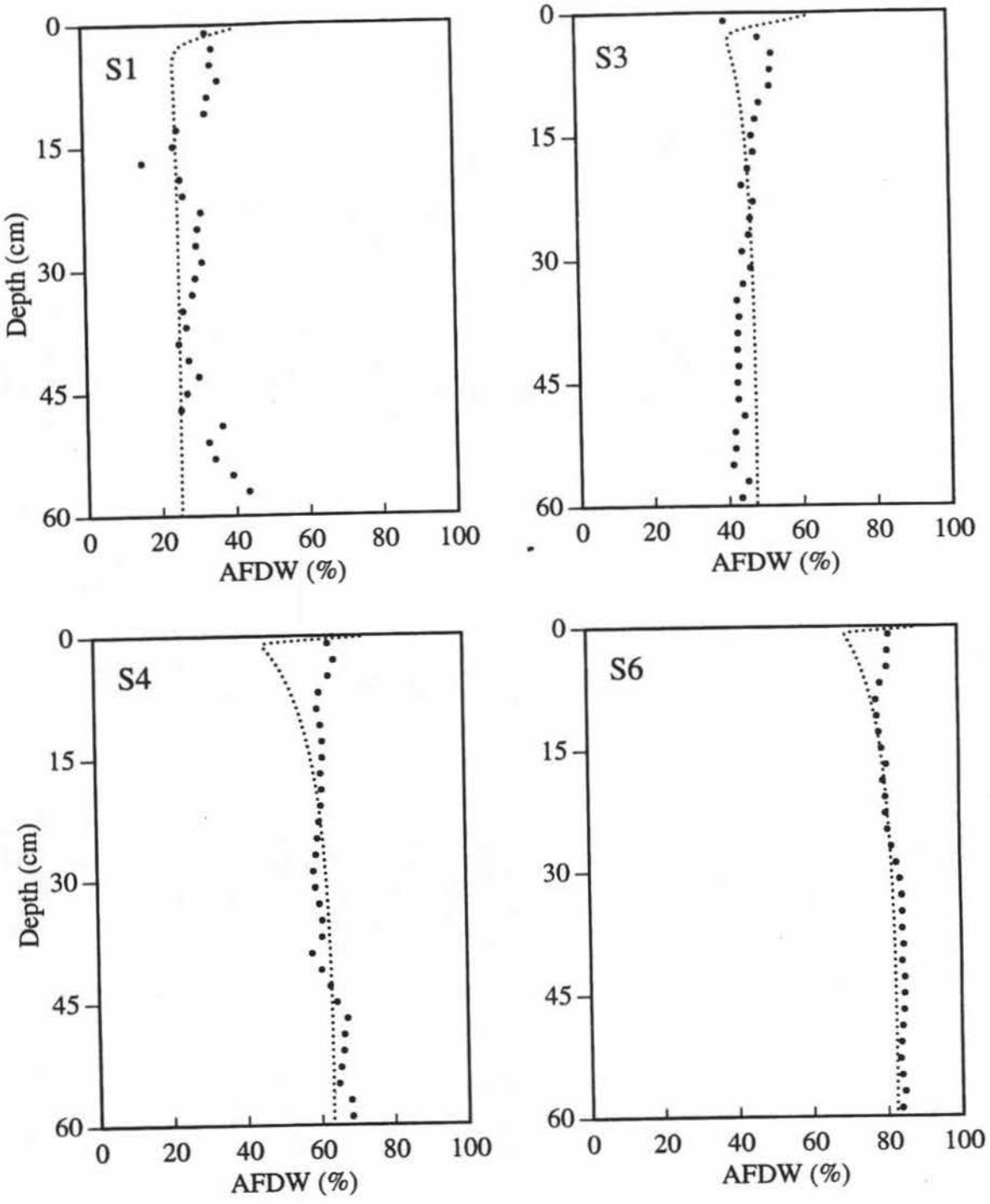


Figure 4.2. Comparison of observed concentrations of organic matter (AFDW %) (solid dot) and simulated concentrations (dashed line) in mangrove soils for the downstream (S1 and S3), intermediate (S4) and upstream (S6) sites along the Shark River estuary.

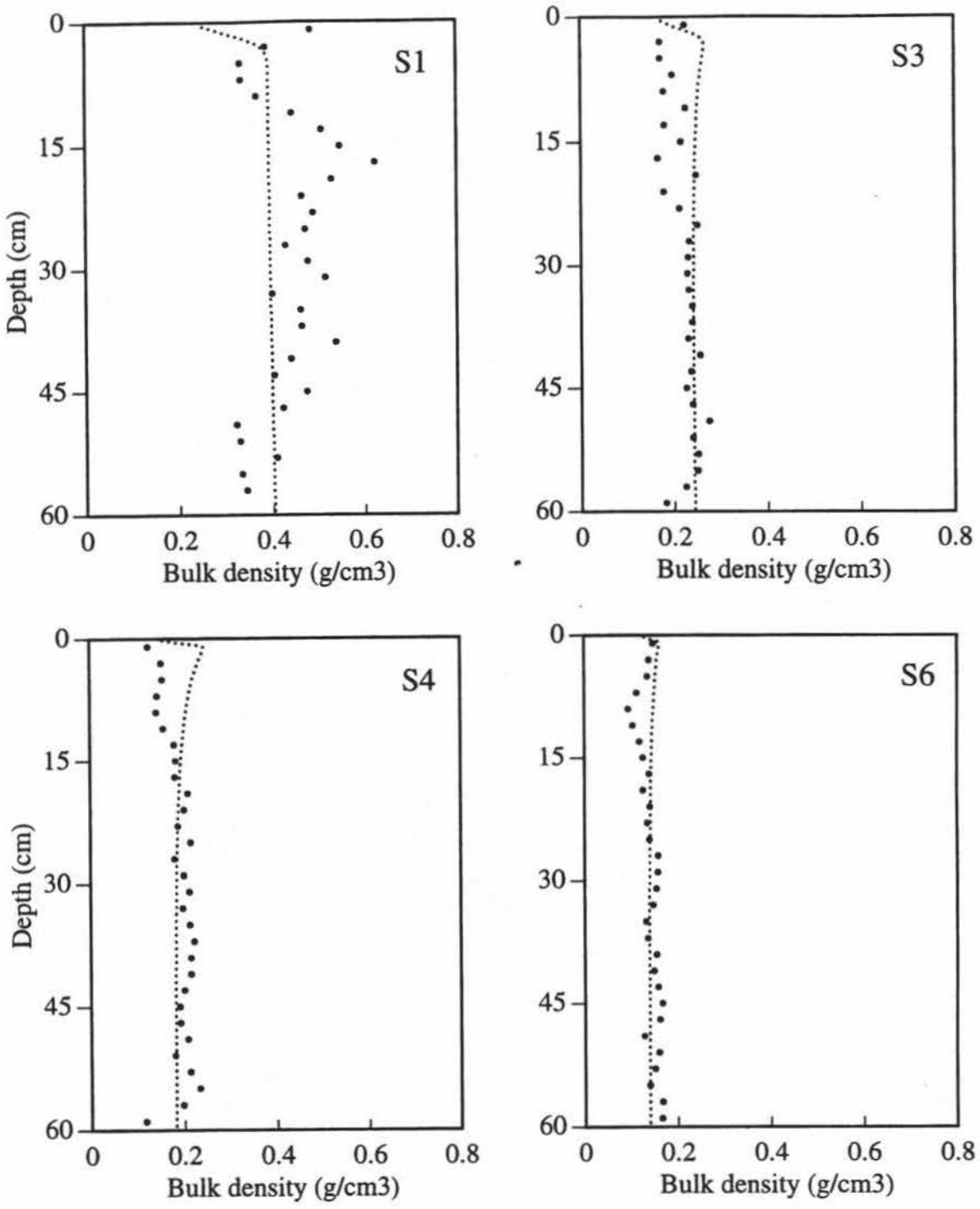


Figure 4.3. Comparison of observed (solid dot) and simulated (dashed line) bulk density in mangrove soils for the downstream (S1 and S3), intermediate (S4) and upstream (S6) sites along the Shark River estuary.

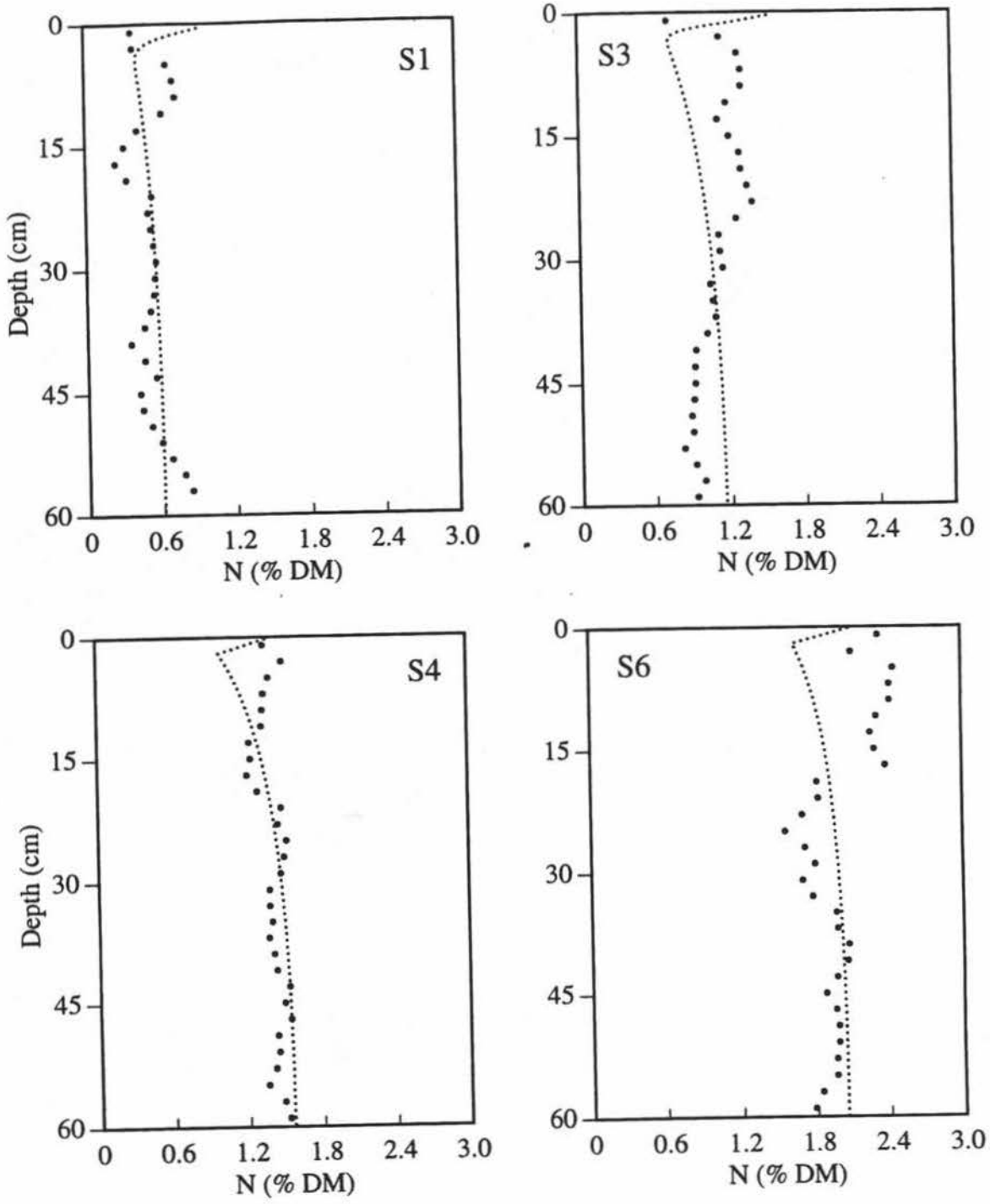


Figure 4.4. Comparison of observed concentrations of total nitrogen (solid dot) and simulated concentrations (dashed line) in mangrove soils for the downstream (S1 and S3), intermediate (S4) and upstream (S6) sites along the Shark River estuary.

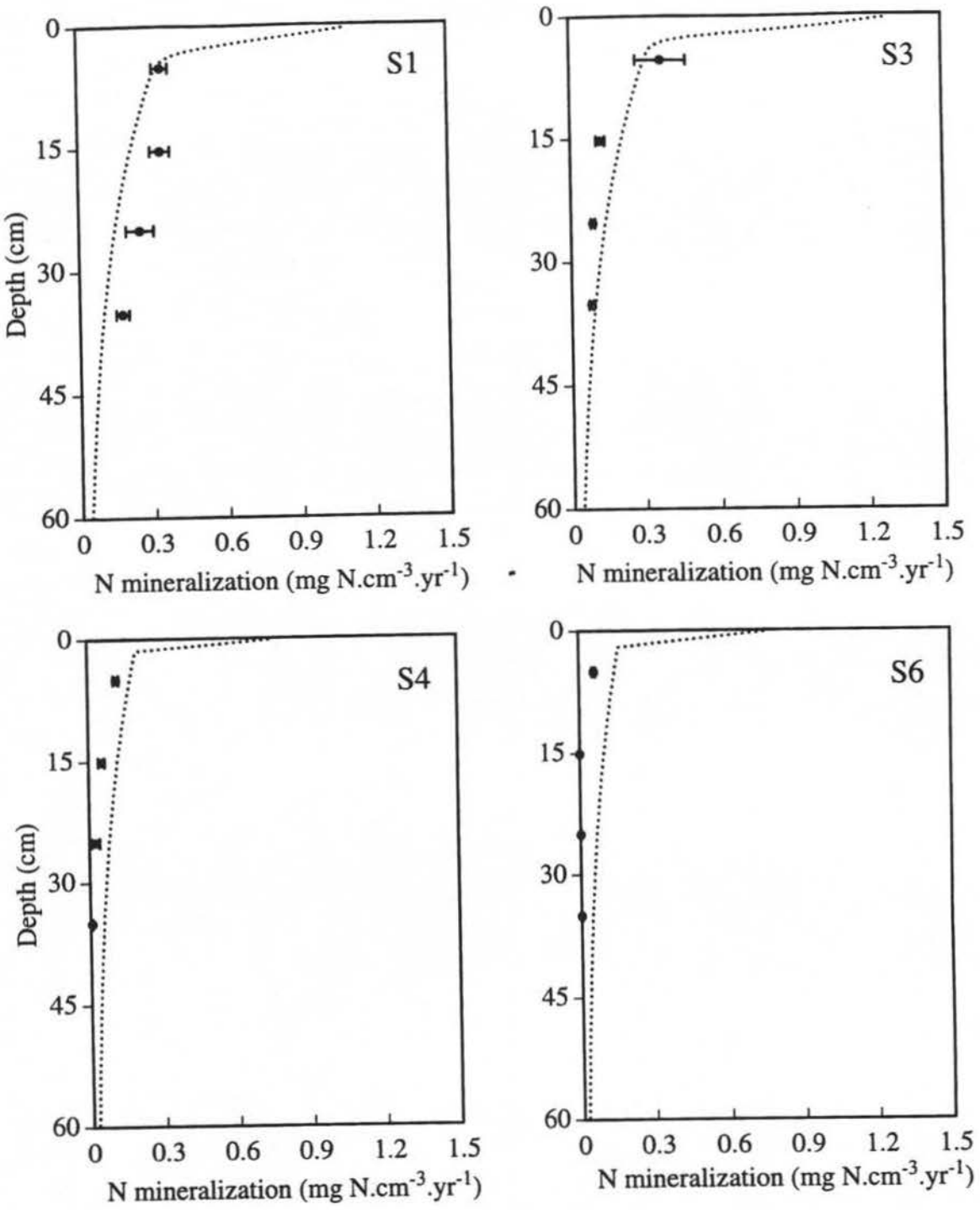


Figure 4.5. Comparison of observed (solid dot) and simulated (dashed line) nitrogen mineralization in mangrove soils for the downstream (S1 and S3), intermediate (S4) and upstream (S6) sites along the Shark River estuary. Observed values are mean ± SE (n=3).

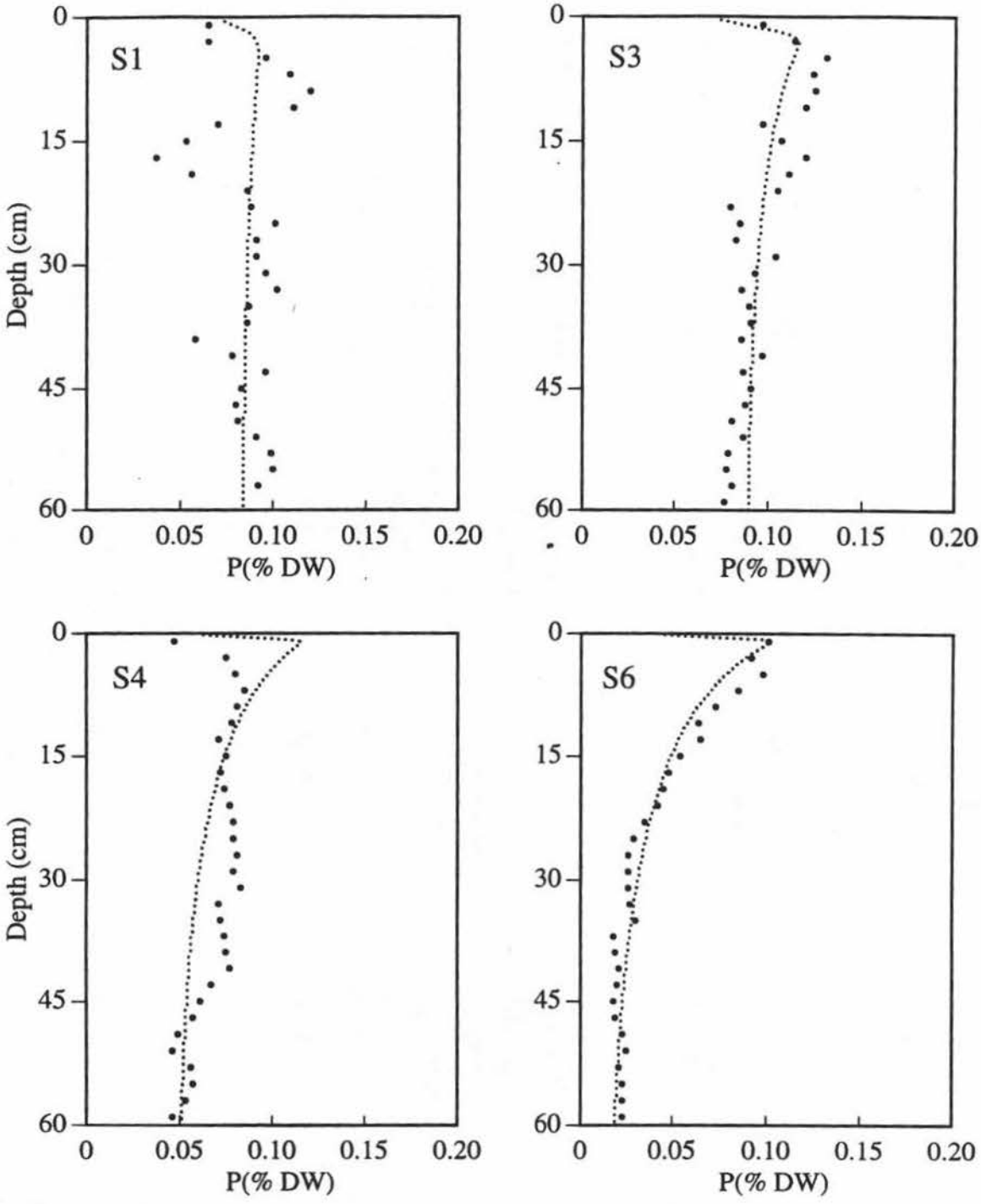


Figure 4.6. Comparison of observed concentrations of total phosphorus (solid dot) and simulated concentrations (dashed line) in mangrove soils for the downstream (S1 and S3), intermediate (S4) and upstream (S6) sites along the Shark River estuary.

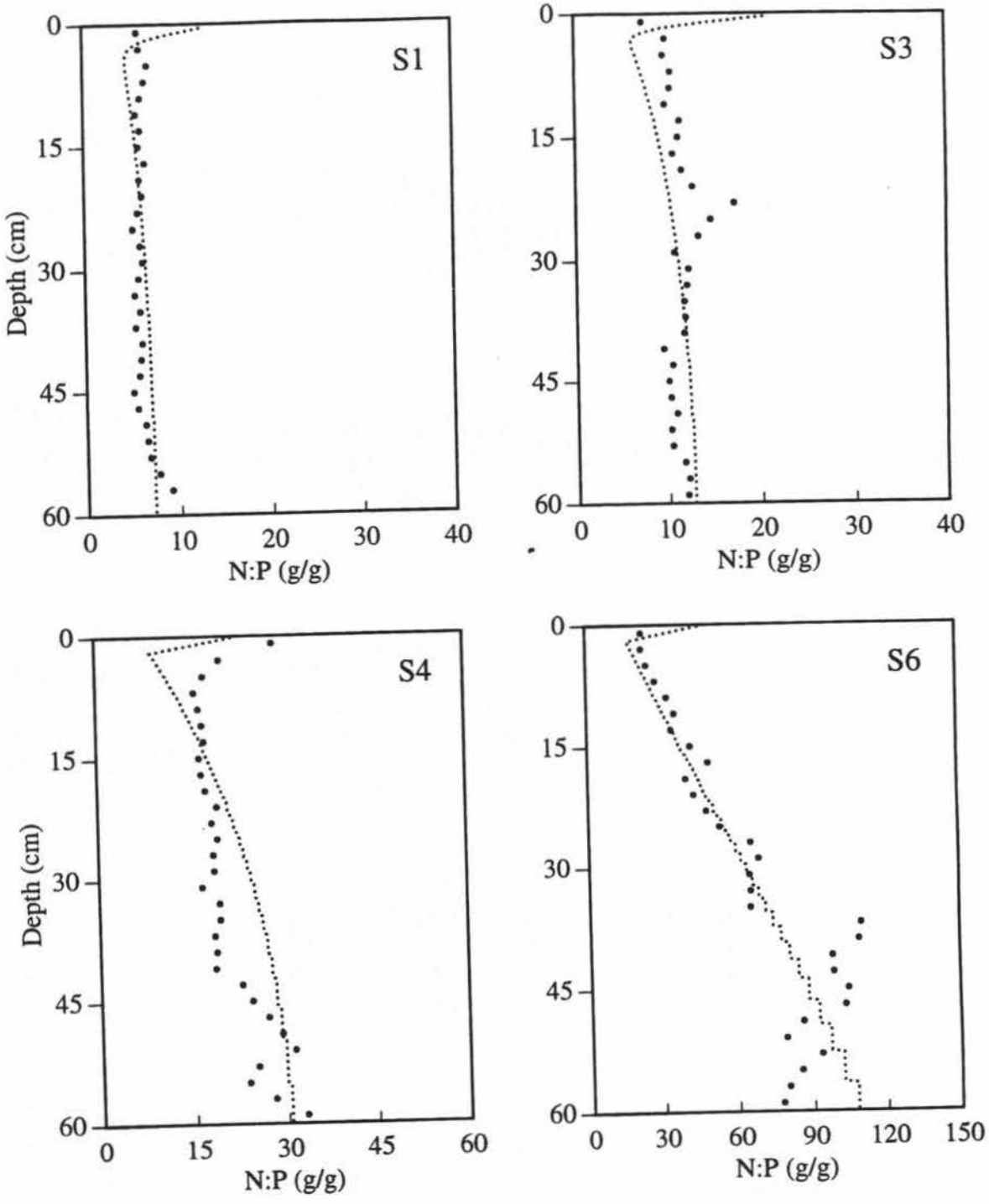


Figure 4.7. Comparison of observed ratios of N:P (solid dot) and simulated ratios (dashed line) in mangrove soils for the downstream (S1 and S3), intermediate (S4) and upstream (S6) sites along the Shark River estuary. Note that the scale for S1 and S3 is different from S4 and S6.

CHAPTER 5

MODELING THE DEVELOPMENT OF MANGROVE FORESTS ALONG SPATIAL GRADIENTS OF SOIL RESOURCE AVAILABILITY AND TOXIC STRESS

ABSTRACT

A computer model (MANGAL) derived from an individual-based gap model (FORMAN) and a soil organic matter model (NUMAN) was developed to investigate mangrove forest dynamics in relation to soil characteristics. Simulated forest structure was compared to that of three mangrove forests along the Shark River estuary, Florida, with a known disturbance history. Simulations of total and species-specific basal area of each mangrove site fit well with data from field surveys of the forests. Low nutrient availability in the intermediate site of the estuary limited the forest development. The measured size-class distribution of *Rhizophora mangle* showed higher frequencies for the smaller size classes, however, that of *Laguncularia racemosa* was bell-shaped. The model accurately tracked this pattern for each species. Mangrove succession was projected using the present stand condition of the downstream marine site in the estuary. Without disturbance, dominance of *L. racemosa* was eventually replaced by *R. mangle* or *Avicennia germinans*, depending on the recruitment rate of *A. germinans*. Simulated basal area of the three mangrove species along gradients of soil nutrient resource and salinity illustrated a change in competitive balance among the three species over time. *L. racemosa* dominated in fertile soils with low stress at early stages of recovery, but its abundance decreased while *A. germinans* increased in this region. The dominance of *R. mangle* was limited to regions with low nutrient availability and low salinity.

INTRODUCTION

A central question in mangrove ecology is the role that climatic, geomorphologic, hydrologic, edaphic, and biological factors play in the temporal and spatial patterns of abundance, distribution and species composition and zonation of coastal forested wetlands (Lugo and Snedaker 1974, Chapman 1976, Lugo 1980, Snedaker 1982, Woodroffe 1983, Thom 1982, Thom 1984, Twilley 1995). On broad geographical scales, the major variable governing the distribution of mangrove species is climate (Blasco 1984, Woodroffe and Grindrod 1991). On a regional scale, climate is much less variable, while soil can be quite heterogeneous because many edaphic characteristics depend on geomorphologic setting and hydrology (Thom 1982). The effect of hydrologic condition is primarily on the chemical and physical aspects of soil condition, which, in turn, affect the structure and function of a mangrove ecosystem (Lugo and Snedaker 1974).

Soil factors that exhibit resource and toxic stress gradients have repeatedly been shown to affect the structure and function of mangroves. Nutrient limitation (Onuf et al. 1977, Boto and Wellington 1984, Feller 1995, Twilley 1995) and hypersalinity (Lugo and Snedaker 1974, Cintrón et al. 1978) are among soil factors that have been suggested to be the most important mediators of the structure of mangrove wetlands. Quantifying the spatial and temporal variation in structure and composition of forest communities as a result of complex interactions among biotic populations and their soil environment can provide insights into how landscape patterns of forest will develop under different environmental settings and disturbance events. Simulation models are necessary for landscape analysis of patterns because it is difficult for experiments to be conducted across multiple scales in time and space (Turner 1989). In these circumstances, models provide a useful tool to describe,

quantify and project forest dynamics.

Compared with modeling of other wetland ecosystems, ecological modeling of mangroves is very primitive to nonexistent (Mitsch et al. 1988), although these wetlands dominate most of the tropical and subtropical intertidal regions of the world. Several process-based models have been developed using different approaches and different objectives in mind. Miller (1972) developed a model with a series of equations that predict primary productivity and transpiration of the mangrove forest canopy at an hourly time scale. The model predicted net and gross primary productivity, respiration, and transpiration, and was tested on data from a *Rhizophora* mangrove in Florida. Lugo et al. (1976) applied the concepts of energy and material flows to simulate the effects of upland runoff and tidal flushing on production and biomass in an overwash mangrove ecosystem. They found the time required to reach steady state levels of mangrove biomass was similar to the average time between tropical hurricanes, about 20 yrs. Their model also predicted that reductions in upland runoff caused a decrease in the productivity of mangrove wetlands. The impacts of tropical storms, herbicides and nutrient enrichment on mangrove ecosystems were simulated by Sell (1977) using a model similar to the model used by Lugo et al. (1976). The model suggested that complete mangrove recolonization of areas sprayed with herbicides may take 55 yrs to more than 100 yrs.

With the introduction of computer simulation techniques and better information about the growth and reproduction of different tree species, an individual-based simulation model can provide more realistic assessments of forest development (Huston et al. 1988). Individual-based gap models track the growth of each tree on a plot of defined size on the basis of species-specific life history traits and limitations of resource availability on the individual (Shugart 1984, Botkin 1993). This approach has been used to model various

types of forests and has become a major means to simulate terrestrial forest dynamics (Shugart et al. 1992, DeAngelis and Gross 1992, Liu and Ashton 1995, Pacala et al. 1996). Although the individual-based gap model originated from studies on temperate forests (Botkin et al. 1972), it has been successfully applied to simulate the dynamics of forested wetlands (Phipps 1979, Pearlstine et al. 1985) and tropical rain forests (Shugart et al. 1980, Doyle 1981). The individual-based model has been extended to include selected ecosystem-level processes, such as dynamics of edaphic nutrient availability in forest succession. Feedback effects of nutrient resource distribution, especially nitrogen, through decomposition of litter have been linked within the design of gap models (Aber et al. 1982, Weinstein et al. 1982, Pastor and Post 1986).

The primary objective of this study was to quantify the effects of spatial gradients in soil characteristics on the growth and development of mangrove wetlands. The JABOWA-FORET (Botkin et al. 1972, Shugart 1984) individual gap model was used as a basic design to develop a model to simulate mangrove forest development with links to soil nutrient dynamics. Nutrient cycling in open mangrove ecosystems is more complex than in terrestrial ecosystems, because it is controlled by both nutrient cycling within the mangrove, and net exchange of materials between the wetland and coastal waters. The model was first tested against field survey data on mangrove forests with a known hurricane-disturbance history along a defined nutrient gradient. The model was then used to project the general trajectory of forest structure development under specific initial conditions. Finally, the model explored the effects of edaphic conditions on mangrove structure by simulating mangrove forest dynamics along the spatial gradient of soil nutrient availability and salinity.

METHODS

Model description

The basic structure of the mangrove wetland model, MANGAL, includes a model that simulates demographic dynamics of mangroves (FORMAN) and another model that tracks nutrient resources in soil (NUMAN). The FORMAN model, which is a modification of the JABOWA and FORET models, was used to calculate rates of recruitment, growth and mortality for mangrove tree species in a 0.05 ha plot. The model used a gap size of 500 m^2, which was typical for lightning gap sizes among the study sites (Chapter 2). The NUMAN model (Chapter 4), which simulates soil organic matter dynamics in a mangrove wetland, was used to link soil fertility with tree growth. Fig. 5.1 is a conceptual model of the MANGAL model. The linkage of both the FORMAN and NUMAN models into an integrated MANGAL model represents the initial efforts to develop an ecosystem-based approach to simulating the properties of mangrove wetlands.

In general, the FORMAN model represents tree growth on an annual basis for individual trees in a forest gap. The species-specific optimal growth rate of a mangrove is decreased by taking into account the effects of resource availability (light and nutrients), toxic stress (soil salinity) and average climate as measured by the number of growing degree days. A set of parameters for each species is given in Table 5.1. The structure of the JABOWA and FORET models has been well documented (Shugart 1984, Botkin 1993), so only specific modifications from JABOWA and FORET that were used to develop the FORMAN model will be discussed in detail.

The optimal growth of trees: The FORET model assumes that the growth equation for a tree under optimal conditions is:

$$\frac{dD}{dt} = \frac{G \cdot D \cdot (1-D \cdot H) / (D_{max} \cdot H_{max})}{(274+3b_2 D-4b_3 D^2)} \qquad [1]$$

in which D is the DBH (diameter at breast height) of the tree (cm), H is tree height (cm), D_{max} and H_{max} are maximum values of diameters and heights for a given tree species. G, b_2 and b_3 are species-specific growth parameters. The optimal growth is constrained by life history traits. However, the realized growth is limited by shading, temperature, nutrient availability and soil salinity in the FORMAN model.

Light effect: The light that reaches a given tree is a function of total leaf area in the canopy above the tree. Leaf area was assumed proportional to leaf weight, which is in turn proportional to tree diameter:

$$LW = a \cdot D^b; \qquad [2]$$

$$LA = c \cdot LW; \qquad [3]$$

where LW and LA are leaf weight (g) and leaf area (m^2); *a* and *b* are species-specific constants (Cintrón and Schaeffer-Novelli 1984); *c* is the specific ratio of leaf area to leaf weight. The light extinction through the canopy is calculated as:

$$Q(h) = Q_0 \exp(-k \int_h^\infty LA(h')dh') \qquad [4]$$

where $Q(h)=Q_0$ is the available light at a height (h); Q_0 is incident light; LA(h') is the cumulative leaf area above height h. A typical attenuation constant (k) for the canopy of a mangrove forest is 0.5 (Clough 1992).

Botkin et al. (1972) used two expressions to calculate the reduction of growth by shading effect, r:

$$r_s(AL) = 1-\exp[-4.64 \cdot (AL-0.05)] \qquad [5]$$

$$r_i(AL) = 2.24 \cdot \{1-\exp[-1.136 \cdot (AL-0.08)]\} \qquad [6]$$

where r_s and r_i are the reduction of photosynthesis rates for shade-tolerant and shade-intolerant trees, respectively. AL is available light on the tree, which is equal to Q(h). Field observations indicate that *R. mangle* and *A. germinans* are more tolerant of shading than *L. racemosa* (Wadsworth 1959, Ball 1980, Roth 1992). Based on comparisons of potential growth and partition of biomass among these three species in two manipulated light levels, McKee (1995b) found that *L. racemosa* was more competitive at high levels of light. In FORMAN, $r_s(AL)$ was calculated using equation [5] for *R. mangle* and *A. germinans*, while $r=(r_s(AL)+r_i(AL))/2$ was used for *L. racemosa* (Fig. 5.2).

Temperature effect: Botkin et al. (1972) assumed that the effect of temperature on growth was a response to an annual accrued number of degree days above some threshold temperature. They calculated the number of growing degree-days as follows:

DEGD =

$$\frac{365}{2\pi}(T_{July}-T_{Jan})-\frac{365}{2}(T_{base}-\frac{T_{July}+T_{Jan}}{2})+\frac{365}{\pi}[\frac{(T_{base}-\frac{T_{July}+T_{Jan}}{2})^2}{(T_{July}-T_{Jan})}] \qquad [7]$$

where T_{July}, T_{Jan} and T_{base} are average temperature in January, July and base temperature, respectively, in which all temperatures are in degrees Fahrenheit. FORMAN followed the same equation except using 47 °F (mean temperature of the coldest month at the northern limit of the mangrove distribution) as the base temperature instead of 40 °F. Mangroves are tropical plants, which have an optimal tree growth in the lower tropical latitudes where peak biomass occurs (Twilley et al. 1992, Saenger and Snedaker 1993). The temperature multiplier T(DEGD) was modified for the FORMAN model. JABOWA and FORET models used a parabolic function to represent the degree day effect, which is not suitable for tropical

mangroves. Instead, equation [8] was used to describe the effect of climate (global temperatures) on mangrove growth (Fig. 5.2):

$$T(DEGD) = 1-(DEGD_{min}/DEGD)^2; \quad [8]$$

where $DEGD_{min}$ is the extreme low value of DEGD within the range of species distribution. *A. germinans* has the most northern distribution in the northern hemisphere (Sherrod and McMillan 1985). The growth multiplier approached 1.0 with an increase in growing degree days. There was no maximum degree day limitation in the FORMAN model.

Salinity stress: The abundance of salt is the single most important factor in the mangrove environment that regulates growth, height, survival and zonation of mangroves (Lugo and Snedaker 1974). Mangroves are facultative halophytes since they do not require salt water for growth but are able to tolerate high salinity (Tomlinson 1986). McMillan (1974) compared the response of three mangrove species to short term hypersaline exposure and found that *R. mangle* and *L. racemosa* has a narrower salt-tolerance than *A. germinans*. The relative tolerance of three mangrove species under greenhouse conditions was found to be similar among the three mangrove species within a salinity range of 0-45 g/kg (McKee 1995b). The interspecific differential response of mangroves to salinity occurred at salinities from 45- 60 g/kg, which inhibited the growth of *R. mangle* and *L. racemosa* significantly more than that of *Avicennia germinans*. The growth multiplier of salinity was sigmoid and calculated as follows (Rastetter 1990):

$$S(SALT)=1/\{1+\exp[d\cdot(U_i-U)]\} \quad [9]$$

where S(SALT) is the multiplier, U is the salinity, U_i is the value of U where the multiplier is 0.5, and d is a constant. Salinity has no effect on the growth of all three species of mangrove from 0 to about 35 g/kg (Fig. 5.2). At salinity >50 g/kg the level of tolerance to salinity occurs at the following rank: *A. germinans* > *L. racemosa* > *R. mangle*. The upper

tolerance of salinity for *R. mangle* is about 70 g/kg, compared to 85 g/kg for *L. racemosa* and 100 g/kg for *A. germinans*, which are similar to field observations by Odum et al. (1982).

Nutrient resource: The pool of available nutrients in mangrove soils is a product of several processes that proceed on different time scales including plant production (aboveground and belowground), decomposition of litter fall, mineralization of organic matter, input by rainfall, sedimentation by tide and runoff, and uptake by plants. The NUMAN model (Chapter 4) was developed to simulate the availabilities of nitrogen and P in mangrove soils by coupling the simultaneous effect of these processes. In brief, the NUMAN model was modified from the SEMIDEC (Morris and Bowden 1986) and CENTURY (Parton et al. 1987) models of soil organic matter for marshes and grasslands, respectively. NUMAN was calibrated with field measurements in the Shark River estuary and estimated rates of several processes including nitrogen mineralization, P accumulation from exogenous sources, and export of organic detritus from mangrove wetlands to coastal waters. The NUMAN model was modified and linked to the demographic FORMAN model to form the MANGAL model. The only modification of the NUMAN in the MANGAL model was that soil was treated as a single depth without considering vertical distribution of C, nitrogen and P. Soil depth in MANGAL was established relative to the vertical distribution of the root system, which was estimated at 150 cm in the present version. The change in soil elevation due to organic matter production and decomposition, and input of allochthonous inorganic material was calculated as an accretion rate. Leaf and twig litter, and fine root production were calculated based on forest basal area as simulated by FORMAN. Dead wood and large root production were calculated based on the biomass of individual dead trees that occurred during the simulation. Litter from the canopy was added to the

forest floor at the end of each year.

Nutrient availabilities expressed as a rate of nitrogen mineralization and concentration of total P from NUMAN were constraints on mangrove growth. The classification of tree species into three types of nutrient tolerance has been commonly applied in forest gap models (Weinstein 1982, Aber et al. 1982, Pastor and Post 1986). The following function is used to limit growth of plants in responses to nutrient availability (Weinstein et al. 1982):

$$S(NUT) = c_1 + c_2 \cdot RNA + c_3 \cdot RNA^2 \qquad [10]$$

where S(NUT) is a growth modification factor; c_1, c_2 and c_3 are coefficients; RNA is relative nutrient availability with a value from 0 to 1.0. Based on the differential responses of the three mangrove species to nutrient levels in a greenhouse study (McKee 1995b), the responses of three mangrove species to availability of nutrient resource were differentiated (Fig. 5.2).

RNA based on nitrogen was calculated as a ratio of net nitrogen mineralization to nitrogen required in plant uptake. If the rate of nitrogen mineralization was greater than uptake, RNA had a value of 1.0. However, if uptake exceeded the mineralization rate, RNA equalled the ratio of net mineralization to uptake. Total P concentrations in mangrove soil were used to calculate RNA because they represent the net effect of plant uptake and exogenous inputs. Plants can absorb P from soil by excreting phosphatase without the microbial oxidation of organic matter and associated nitrogen (McGill and Cole 1981). The soil P-availability index, based on extractions with dilute acid among my study sites, was related to total soil P (Chapter 2). In the present version of MANGAL, RNA based on total P (per unit area soil) was calculated using a Monod equation that describes the function of total soil P vs mangrove forest basal area (Chapter 3):

$$PR = \frac{(R_{ac} - R_{min})PR_{max}}{R_{ac} - R_{min} + \alpha} \quad [11]$$

where PR is production, PR_{max} is the maximum production, R_{ac} is the amount of resource acquired, R_{min} is nutrient availability at zero production and α is half-saturation constant with respect to R_{ac} (see Bridgham et al. 1995 for details). The fit of the Monod model with data from 10 mangrove forests was significant (r^2=0.80), and R_{min} was positive (15.2 g P/m^2) with a half-saturation constant of soil P of 29.3 gP/m^2 to a depth of 40 cm (Chapter 3). The ratio of PR/PR_{max} was used as an index of the relative availability of P. Tree growth was only constrained by the most limiting element in any one year. The smaller RNA value of either nitrogen or P was used as the nutrient multiplier for plant growth.

Realized growth: Equation [1] was multiplied by equations [8], [9], [10], and by either equation [5] or [6], to produce the growth equation used in the FORMAN model:

$$dD/dt = \frac{G \cdot D \cdot (1 - D \cdot H/D_{max} \cdot H_{max})}{(274 + 3b_2 D - 4b_3 D_2)} \cdot T(DEGD) \cdot r(AL) \cdot S(NUT) \cdot S(SALT). \quad [12]$$

Sapling establishment: The number of saplings added annually to a simulated plot (gap) was a function of the maximum number of saplings, the amount of light, and site condition (Botkin 1993):

$$E = \xi \cdot f(AL) \cdot S \cdot Q \quad [13]$$

where E is the number of saplings that enter a simulated plot in a year, ξ is a uniformly chosen random number (0 to 1.0), f(AL) is a function of available light, S is the species-specific annual maximum number of saplings that can be added to a plot, and Q is the site specific condition for recruitment of each species. In the current version of FORMAN, S

was set at 30 for each species, and the number of saplings added to a plot for each species was as follows for *R. mangle* and *A. germinans:*

$$E=\xi \cdot AL^{2} \cdot 30 \cdot Q. \quad [14]$$

For *L. racemosa* the equation was:

$$E=\xi \cdot AL^{2.5} \cdot 30 \cdot Q. \quad [15]$$

These functions assumed that mangrove saplings enter a plot at the maximum rate if the canopy is open. However, the sapling recruitment rate decreased rapidly as the canopy closed, as indicated by an increase in leaf area index. Saplings of *L. racemosa* were less shade-tolerant than *R. mangle* and *A. germinans* (Wadsworth 1959, Ball 1980, Roth 1992). Saplings entered the plot at a size (DBH) of 1.27 cm. Q depended on the condition of the site for recruitment.

Mortality: Two sources of mortality were included in the model: age-dependent mortality and mortality caused by suppressed growth. The probability of mortality for each tree was handled as in other gap models (Botkin et al. 1972, Shugart 1984) and increased with age. Trees whose rate of DBH growth was < 0.01 cm for two consecutive yrs were subjected to additional mortality (Solomon et al. 1986, Pastor and Post 1986).

The study forest

The study sites are located along the Shark River estuary on the west coastal plain of Everglades National Park (Fig. 2.1). Davis (1940) suggested that mangrove forests in the downstream region of the estuaries in southwestern Everglades are "probably the optimum growth of mangroves in the Americas". Coastal forested wetlands in the southwestern Everglades of south Florida extending from the Whitewater Bay region to Ten Thousand

Islands include one of the greatest mangrove areas in the Gulf of Mexico (Davis 1940, Smith et al. 1994). Mangroves have developed in this region for more than 3000 yrs (Scholl 1964a,b). Three mangrove species, *R. mangle* L., *A. germinans* (L.) Stearn and *L. racemosa* (L.) Gaertn., form a continuous band of forested wetlands that extend from the Gulf of Mexico to the inland limit of periodic salt water influence. Mangrove wetlands in this region recovered by natural succession after the disturbance of Hurricane Donna in 1960, with an instant mortality of mangroves reported at 50 to 70%, but the eventual tree mortality was higher (Craighead and Gilbert 1962).

Model simulations

The first step in this modeling exercise was to simulate the regeneration of three mangrove forests (S1, S3 and S4) after disturbance by Hurricane Donna along the Shark River estuary (Fig. 2.1). MANGAL was used for this comparison. Detailed descriptions of the forest structure and soil characteristics along the Shark River estuary were presented in Chapters 2, 3 and 4. To compare simulation results of mangrove forest development after 34 yrs of regeneration with field observations, the initial conditions of the stands were needed. Although tree mortality of mangroves was extreme high following Hurricane Donna, the presence of a few large trees presently in the study sites indicates that there was some survival following the disturbance (Chapter 3). Survivors were identified by DBH in 1995 and a reasonable mean growth rate of DBH for each species. Tree mean growth rates were estimated based on measurements of DBH between 1995 and 1996 along the Shark River estuary and in a mangrove forest recovering from Hurricane Andrew (1992) near the mouth of Broad River. The mean DBH growth rates in the last 34 yrs were estimated as 0.5, 0.4 and 0.2 cm/yr for *L. racemosa*, *A. germinans* and *R. mangle*. Therefore, trees presently

found at each site with DBH >34 times the mean DBH growth rate for the respective species are considered survivors of the 1960 disturbance. Initial DBH of survivors in 1960 was hindcasted as difference between DBH in 1995 minus 34 x mean DBH growth rate. For species that have a high sprout ability after the loss of a trunk, such as *L. racemosa* (Wadsworth 1959), multiple stems were treated as sprouts from the disturbance by Hurricane Donna in 1960. In the model, new sprouts were the same as a sapling. The model used this reconstructed data set as initial stand conditions and simulated 50 times. Because of the stochastic properties of the model, the model was run 50 times and output was averaged over 50 simulated plots.

Site-specific initial conditions included initial trees described above, soil fertility, salinity, and recruitment. The initial soil concentrations of organic matter, nitrogen, and P, along with pore water salinity, among the three sites were based on field measurements (Chapters 3, 4). Several site-specific rates of soil processes, such as inorganic matter accumulation, export, and P accumulation, were estimated with the NUMAN model as described in Chapter 4. Q (the site condition for sapling recruitment in a specific site) was user-defined based on parent tree density and model calibration. For *L. racemosa*, *R. mangle*, and *A. germinans.*, Q was 1: 1: 0.27 in S1; 1: 0.83: 0.27 in S3; 0.1: 0.83: 0.1 in S4, respectively.

The second model exercise was to project mangrove succession in the downstream site (S1) of the Shark River estuary. MANGAL used the measured data in the plots in 1994 as initial vegetation condition and run for 500 yrs. The sensitivity of model to recruitment was tested. One projection assumed the same sapling recruitment as run for the first 34 yrs as noted above, the other assumed the equal sapling recruitment for all three species.

In the model, the growth of each tree was constrained by four environmental

variables including light, temperature, nutrient availability and salinity, in which nutrient availability and salinity were related to soil characteristics and hydrologic regime. I assumed that soil fertility and salinity were relatively constant as a function of location in an environmental setting. Results of simulations using the FORMAN model compared the response of three mangrove species to the axes of soil nutrient resource and salinity stress. The spatial gradient in relative nutrient availability (RNA) in the model was basically the concentration of total P among the study sites (Chapter 4). These response surfaces can be used to investigate the potential landscape distribution of species and relative competitive success (Botkin 1993). In this model exercise, I assumed that the maximum number of saplings that entered all simulated plots annually was equal for all three mangroves, and there was no effect of site conditions on sapling recruitment (Q=1).

The program was written in ANSI C. Data structure of the linked lists was used as to connect each individual tree in the simulated plot. Linked lists are dynamic, the length of the list can increase or decrease as necessary when trees are added or deleted in the simulated plot, respectively.

RESULTS

Regeneration following disturbance

The first test of the MANGAL model was to compare field measurements obtained from 400 m^2 plots in three mangrove sites along the Shark River estuary with simulations of forest regeneration from 1960 to 1994 in response to the disturbance by Hurricane Donna (Chapter 3). The simulated results of total basal area were similar to observed values in each respective mangrove site (Fig. 5.3). The differences in basal area at the downstream

locations (S1 and S3) and intermediate location (S4) were due to soil nutrient availability and species composition. Concentrations of soil total P in S1 and S3 were significantly greater than in S4 (Chapter 3). The model also predicted that the percentage of total basal area by species was very close to the observed values in all three sites (Fig. 5.4). In the downstream sites, *L. racemosa* made the largest contribution to total basal area; however, *R. mangle* was dominate at the intermediate site.

One merit of using the individual-based approach to develop ecosystem models is the ability to simulate specific information at several hierarchical levels. For example, not only can the total metrics of a forest be described in the simulations, such as basal area, but also species-specific size class distributions can be analyzed. A comparison of size-class distribution in forest structure between simulation results and field observations can provide insights into the performance of MANGAL. The model captured the shapes of the *R. mangle* size-class distribution, indicating high densities in small size-classes (<8 cm DBH) in all three sites (Fig. 5.5). The model predicted a decline in density of size-classes <6-8 cm, which was a good fit with observed results in S1, but not in S3. A decline in density of these size classes was not observed in either field or simulated results in S4. This may be related to the higher light levels on the forest floor, which allows the establishment of saplings. The size-class distribution of *L. racemosa* was bell shaped, which was significantly different from the patten observed for *Rhizophora* (Fig. 5.5, 5.6). Although there were differences between simulated and field results among some size-classes, the model generally followed the pattern with low stem frequencies in larger and smaller size-classes. *L. racemosa* was a minor component in S4, saplings that entered the simulated plot were reduced, which was probably due to a lack of parent trees in this site and poor soil fertility. *L. racemosa* dominated in the medium to large size-classes in S1 and S3, which

was an initial response to forest regeneration after a disturbance, indicating this species has pioneer qualities in this region of intertidal zone. Densities of *A. germinans* in all sites were lowest compared to the other two species; however, this species had a higher frequency in the largest size cohort (DBH>20 cm), because they represented survivors of the hurricane disturbance (Fig. 5.7). The model was able to tract the growth of these survivors, which indicated that the reconstructed data of the simulations were reasonable scenarios. The model also predicted that there was a bell-shaped pattern of size class distribution, which was similar to the field data in S1.

Projection of mangrove succession

Significant changes in species dominance using basal area were observed when MANGAL was run for an additional 500 yrs to project patterns in mangrove succession at S1 (Fig. 5.8). In the downstream site of the Shark River estuary, higher soil fertility favored a quick recovery of *L. racemosa* after the forest canopy was removed by hurricane force winds. Simulations using either the same sapling recruitment as in the first 34 yrs (Fig. 5.8A) or those using the equal sapling recruitment for all three species (Fig. 5.8B) predicted that *L. racemosa* continued to dominate in total basal area for the next 30 to 40 yrs. However, long-term succession of mangroves was sensitive to recruitment for each species. The dominance of *L. racemosa* was gradually replaced by *R. mangle* if the recruitment of *A. germinans* was kept at low rates (Fig. 5.8A). However, if there was no site effect on maximum sapling recruitment for all three species, *A. germinans* was able to quickly overcome *L. racemosa* and total basal area of the plot increased significantly (Fig. 5.8B). The decline of *L. racemosa* was due to low recruitment of this species under sever shading.

Salinity and nutrient response surfaces

FORMAN was developed as a tool to investigate the dynamics of mangrove wetlands in relation to their soil characteristics. In these simulations, I was interested in examining the sensitivity of mangrove succession to spatial gradients in soil conditions. Several biological and physical factors that can have an important impact on mangrove structure, such as seedling predation and hurricanes, were not included in this analysis. However, FORMAN model is able to explore other environmental gradients by minor modifications of specific parameters. There was no limit to recruitment among the three species in these simulations.

Model simulations of forest development were adjusted by changing conditions of soil fertility and salinity, using a constant climatic condition (temperature) similar to south Florida. In this simulated landscape gradient, total basal area of mangroves increased with increased soil fertility, but decreased with increased soil salinity (Fig. 5.9). Extremely low nutrient availability severely limited mangrove development. Current mangrove wetlands in the lower Shark River estuary, approximately at 35 yrs, located in optimal soil conditions (low salinity and high fertility) achieved a high total basal area, which was close to the basal area of these forests after 100 yrs. After 200 and 300 yrs, total basal area had a higher variance compared to values in 35 and 100 yrs. This may be related to demographic stochasticity in the older forest.

The differential responses in basal area of three mangrove species were observed along temporal scales and environmental gradients. In 35 yrs, *L. racemosa* had the maximal basal area at salinities <50 g/kg and RNA >0.5, but this species was excluded in areas with low soil fertility and high salinity. Growth of *R. mangle* was slow and this species was a small component of total basal area compared with the other two species in fertile soil. *A. germinans* dominated in areas of salinity >60 g/kg (Fig. 5.10). If the model was allowed to

continue to run up to yr 100, niche differentials (associated with soil resource use and tolerance to salt) were significant along both nutrient resource and salinity gradients (Fig. 5.11). *L. racemosa* remained dominant in fertile and low salinity regions; *R. mangle* outcompeted the other two mangrove species and mainly occupied the regions of poor soil fertility. *A. germinans* flourished and achieved very high basal area in plots where both soil salinity and fertility were higher, whereas *L. racemosa* and *R. mangle* were excluded from these plots. The long-term simulations (200 to 300 yrs) indicated that *A. germinans* subsequently increased steadily in the plots with higher fertility and a wide range of salinities, whereas the basal area of *L. racemosa* declined (Fig. 5.12, 5.13). The dominance of *L. racemosa* was eventually replaced by *A. germinans*, however, *R. mangle* and *A. germinans* formed mixed associes in these plots.

DISCUSSION

Although gap phase dynamics as a natural phenomenon has been described for more than four decades (Watt 1947) and widely examined in temperate and tropical forests, the importance of gap dynamics in mangrove wetlands has only recently been discussed (Smith 1992, Smith et al, 1994). The concept of gap dynamics as a driving natural phenomenon of vegetation patterns has been applied in the development of forest dynamic models (Shugart 1984). The applications of individual-based models to describe dynamics of tropical forests were few compared with hundreds of individual-based models developed for temperate forest. This restriction has been connected with the lack of available data for diverse species in tropical forests, which limits the parameterization of these models (Botkin 1993, Liu and Ashton 1995). Data for tropical mangrove forests are also limited, but mangrove species

richness in the Neotropics is much lower than in upland tropical forests. The development of the MANGAL model represents a synthesis of available data for three Caribbean mangrove species as applied to individual gap models to explore the long-term dynamics of mangrove forest development.

MANGAL simulates mangrove forest development by integrating demographic processes and soil nutrient dynamics. Tests of the model against data measured from three 34 yr mangrove forests along the Shark River estuary provide strong support for the successional dynamics predicted by MANGAL. The model tracked well total basal area, and species-specific contributions to total basal area. The model also appeared to predict the frequency of species-specific size-class distributions. These comparisons between simulation results and field observations provide confidence that MANGAL can project mangrove forest dynamics.

MANGAL predicted that *L. racemosa* dominates in the early stages of forest development because of its fast growth potential in fertile soil conditions, along with its ability to sprout. *L. racemosa* sprouts more vigorously than *A. germinans* after the loss of the tree trunk, however *R. mangle* does not have this potential (Wadsworth 1959). Also *L. racemosa* had a high growth rate under high light and soil nutrient availability under greenhouse conditions (McKee 1995b). A high growth rate of *L. racemosa* was observed in the Everglades National Park after disturbance by Hurricane Andrew in 1992 (Smith 1995, Twilley et al. unpublished data). The model predicted that the high light conditions required for *L. racemosa* to regenerate restricts its development to early stages of gap dynamics. Once the canopy of a gap closes, *L. racemosa* regeneration is severely limited and it becomes a minor component of mangrove communities as the pioneer trees of this species die. Wadsworth (1959) observed that there were *A. germinans* and *R. mangle* seedlings but no

L. racemosa under a *L. racemosa* forest and implied that *L. racemosa* was relatively intolerant to shading. Differential shade-tolerance has been proposed as an important agent of interspecific competition during mangrove succession. Ball (1980) found that seedlings of *R. mangle* tend to persist for a longer period than those of *L. racemosa* under the forest canopy, based on historical aerial photographs, measurements of seedling and sapling densities, and frequency of live and dead trees in south Florida. She suggested that *L. racemosa* was being replaced by *R. mangle* because of their difference in shade-tolerance. Putz and Chan (1986) synthesized long-term observations from permanent plots in a Malaysian mangrove forest. They also demonstrated that shade-tolerant species, such as *Bruguiera gymnorrhiza*, steadily increased in abundance in the mangrove forest dominated by *Rhizophora apiculata*.

Several authors have drawn attention to the importance of gaps in the forest canopy on the establishment and growth of mangroves (Macnae 1968, Putz and Chan 1986, Smith 1987a,b). Smith et al. (1994) further proposed that gaps are an important seedling source for mangrove regeneration after formation of large disturbed areas such as hurricanes. They compared the survivorship of mangroves between areas of forests that had formed gaps and reference areas with canopy after Hurricane Andrew. They found that mangroves in the gap areas had lower mortality than those under the canopy.

Field observations indicated the low density of *A. germinans* saplings, suggesting a low recruitment of *A. germinans* in my study sites. One possible explanation is the differential predation on mangrove seedlings. In south Florida, Smith et al. (1989) demonstrated that grapsid crabs and snails had a potential to consume more than 80% of *A. germinans* propagules in a 4 d experiment. However, their experiment showed there was no consumption on *R. mangle*. Seed predation has been proposed as a key factor influencing

mangrove structure and zonation in Australia (Smith 1987a, Smith et al. 1989). Except seed predation, the establishment of mangrove seedlings has been proposed to be controlled by the light, water level, tidal frequency, salinity, temperature, presence of a seedling source, and herbivory (Rabinowitz 1978, Smith 1987a, Smith et al. 1989, Robertson et al. 1990, Jiménez and Sauter 1991, Clarke 1993, Clarke and Allaway 1993, Ellison and Farnsworth 1993, McKee 1995a). The JABOWA/FORET models assume isometric spatial interaction among plots with regard to seed dispersal. Seed dispersal and seedling growth are not explicitly simulated in these former gap models. Further modification of the MANGAL model is needed to include seedling dispersal and the site specific establishment of saplings in mangrove forests.

Without exogenous disturbances, such as hurricanes, the model predicted that *A. germinans* increased in dominance if saplings of the three species have the equal possibility to enter a plot. Hurricanes occur several times during the life span of a mangrove tree in south Florida. Direct comparisons of simulation results with field measurements are difficult because of the immature stage of mangrove forest development in this region. One exception is a black mangrove forest near Flamingo in south western Florida described by Craighead (1971). That forest was about 250 yrs and dominated by *A. germinans* tree with mean DBH of about 1 m. Unfortunately, this forest was destroyed by the Labor Day storm in 1935.

Soil nutrient resources in mangroves vary with location in the horizontal intertidal zone (Boto and Wellington 1984, McKee 1995a) and longitudinal axis of an estuary (Chapter 2). The resource ratio hypothesis of plant succession predicts that spatial heterogeneity of resources favor different plant species in different locations (Tilman 1982). However, physical and chemical stress factors in mangroves such as high salinity might also lead to changes in species composition due to species-specific tolerances to these stressors. The model simulations with varying soil nutrient availability and salinities illustrate how the

competitive balance among species is altered by the environment. A continuum of species response surfaces to gradients of nutrients and salinity can be used to investigate the potential landscape distribution of these three mangrove species. The results of these simulations project the dominant influence of autogenic processes such as plant competition without impacts of disturbance. They therefore represent the realized niche of each species for the selected dimensions of soil nutrient resource and salinity stress (Botkin 1993). Because the model's sensitivity to spatial gradients of soil nutrient and salinity was emphasized here, other allogenic processes, such as hurricane disturbance which is an important factor to set back Caribbean mangroves (Roth 1992, Smith et al. 1994, Doyle et al. 1995), are not included in current simulations. However, MANGAL can be modified to explore and investigate the responses of mangroves to natural and human disturbance.

Table 5.1. Species-specific parameters used in the MANGAL model

Parameters	*Avicennia germinans*	*Laguncularia racemosa*	*Rhizophora mangle*
G	162	243	267
D_{max} (cm)	140	80	100
H_{max} (cm)	3500	3000	4000
AGE_{max} (yr)	300	200	250
b_2	48.04	71.58	77.26
b_3	0.172	0.447	0.396
a	38.9033	38.9033	27.551
b	1.6205	1.6205	1.7914
$DEGD_{min}$	5782	7636	7636
U_i (g/kg)	72.0	65.0	58.0
d	-0.18	-0.20	-0.25
c_1	-0.5	-1.0	0
c_2	2.87963	4.42437	1.33469
c_3	-1.6554	-2.50	-0.72425
S	30	30	30

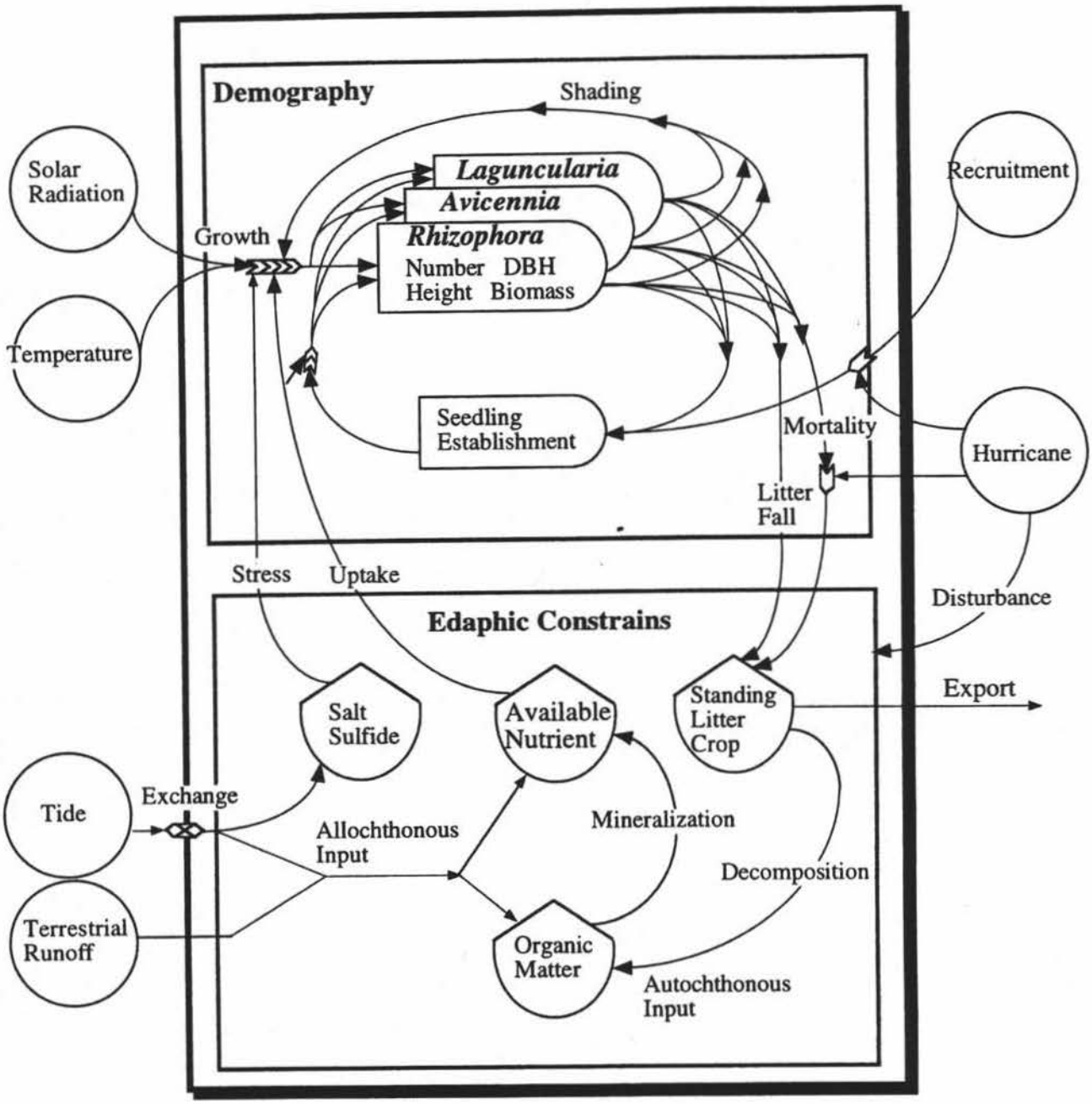


Figure 5.1. Conceptual model of mangrove forest development including edaphic constraints.

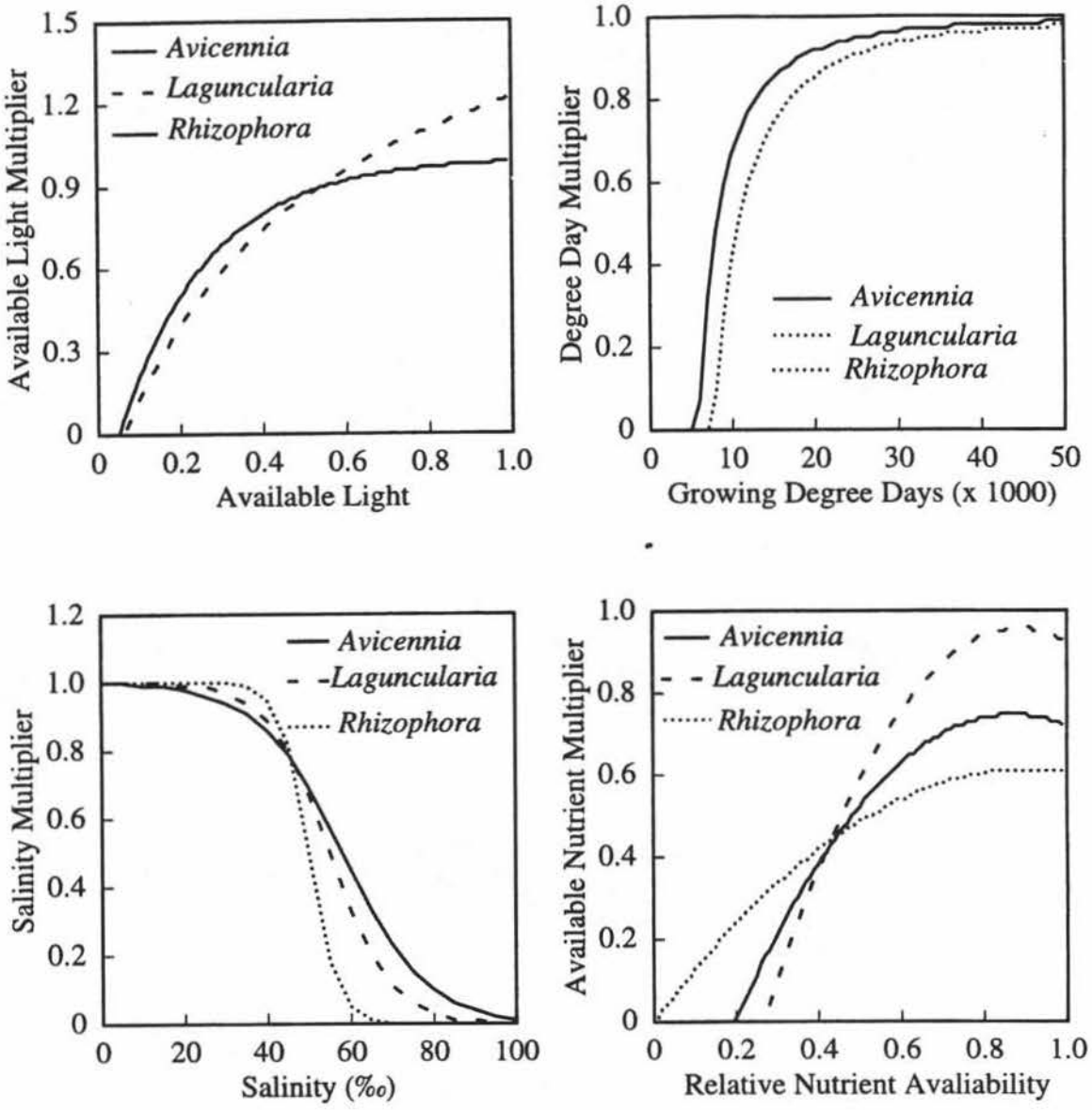


Figure 5.2. Growth multiplier curves for three mangrove species.

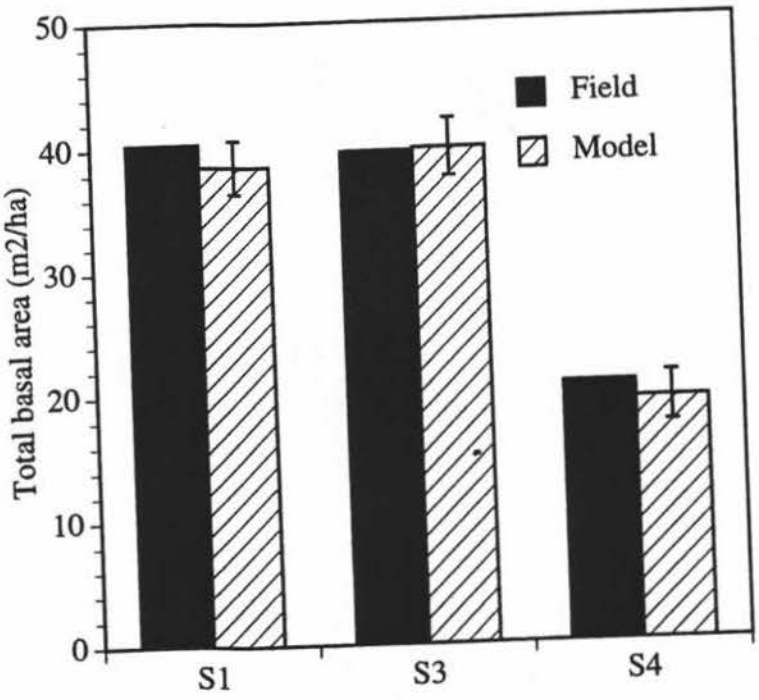


Figure 5.3. Comparison of simulated and measured total basal area of three mangrove forests along the Shark River estuary. Simulation results were expressed as average ± S.D. of 50 runs by MANGAL.

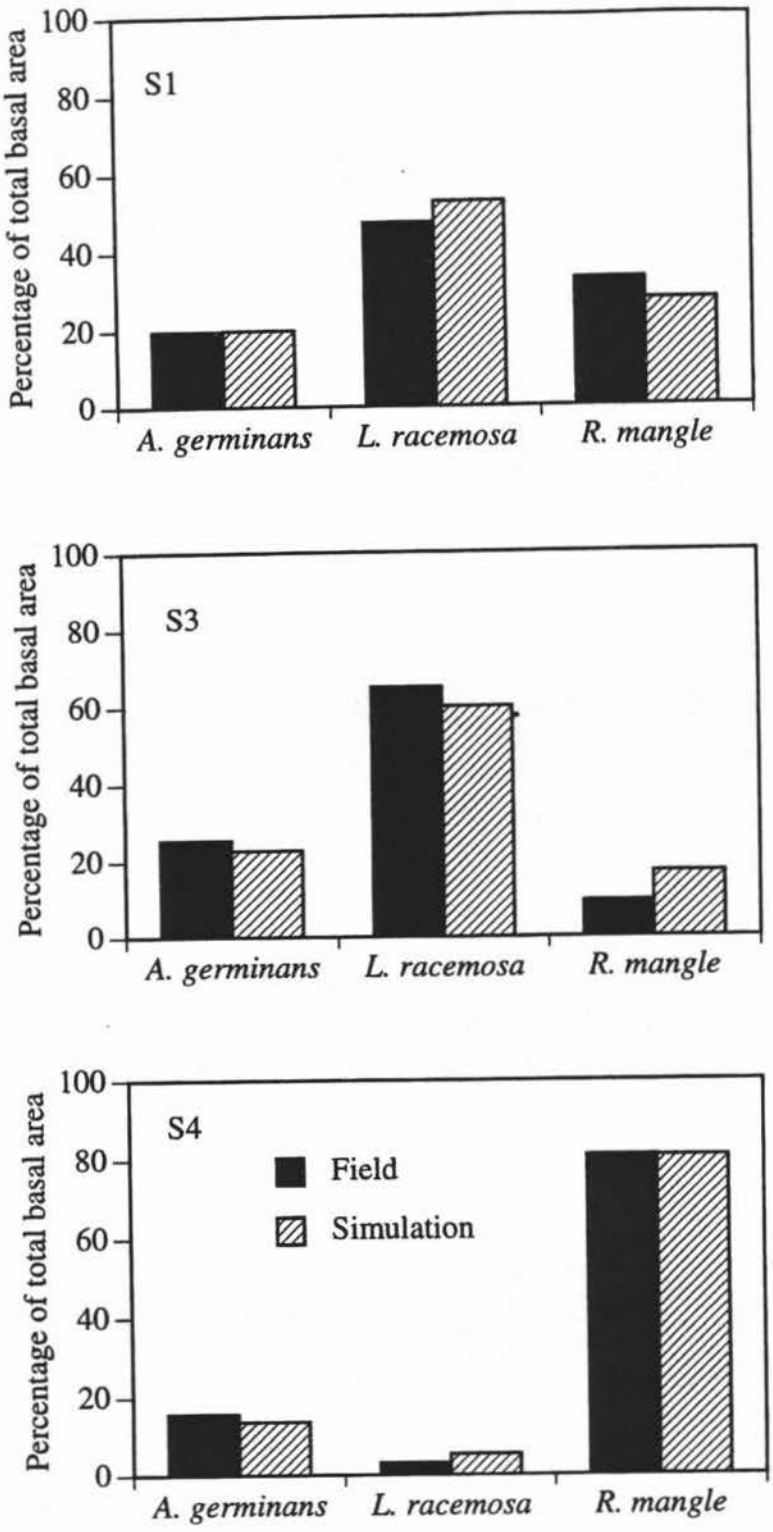


Figure 5.4. Comparison of relative dominance for three mangrove species using basal area between field surveys and simulations of the MANGAL model.

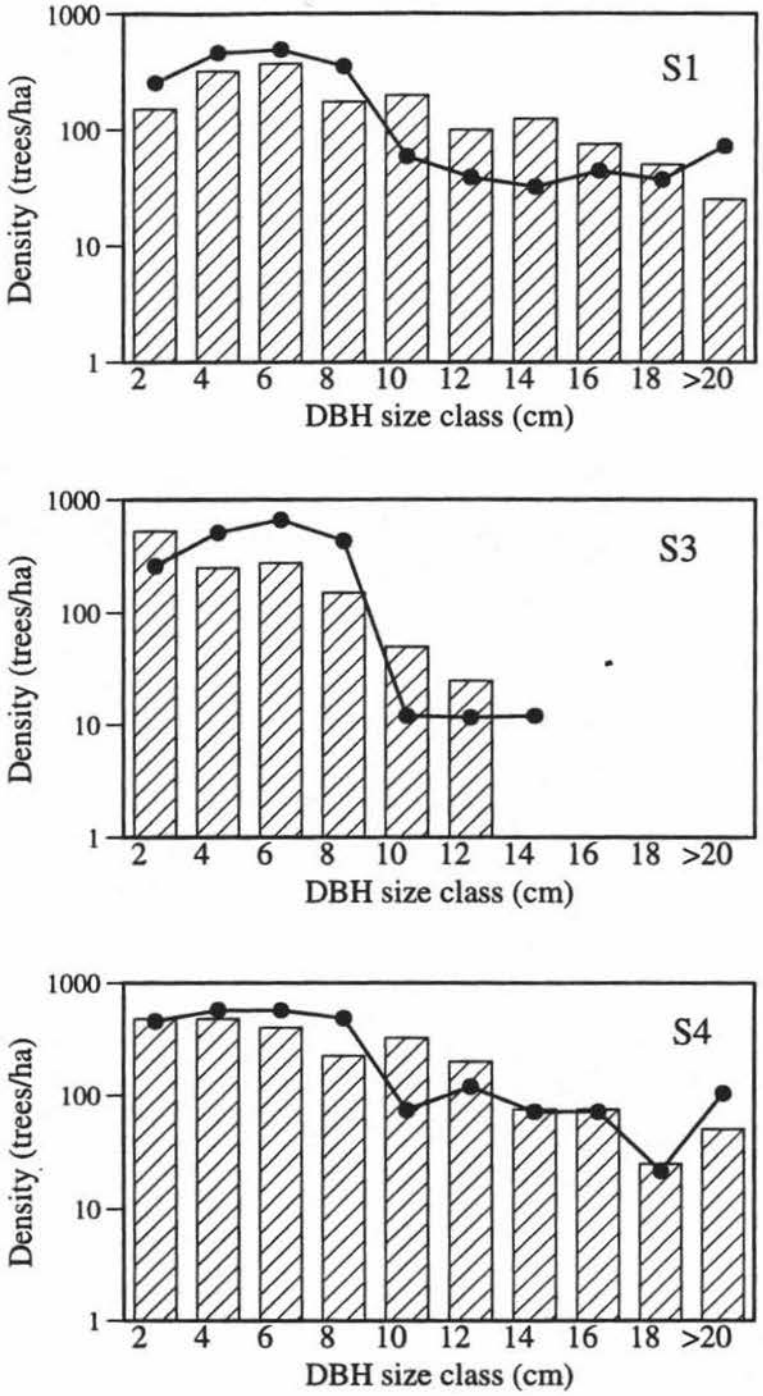


Figure 5.5. Size-class distribution of *Rhizophora mangle* for three mangrove sites. Solid line is the average of 50 simulations of the MANGAL model. Bar represents the field surveys.

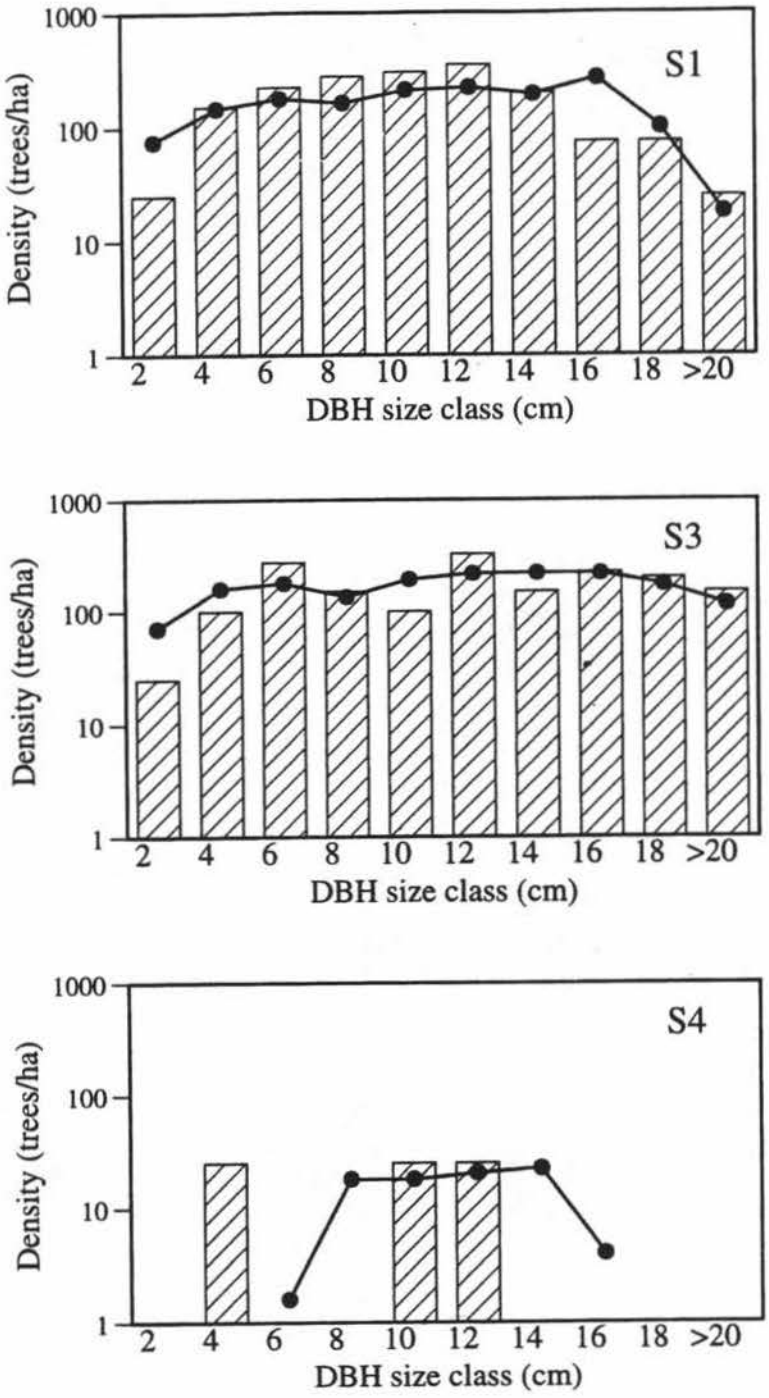


Figure 5.6. Size-class distribution of *Laguncularia racemosa* for three mangrove sites. Solid line is the average of 50 simulations of the MANGAL model. Bar represents the field surveys.

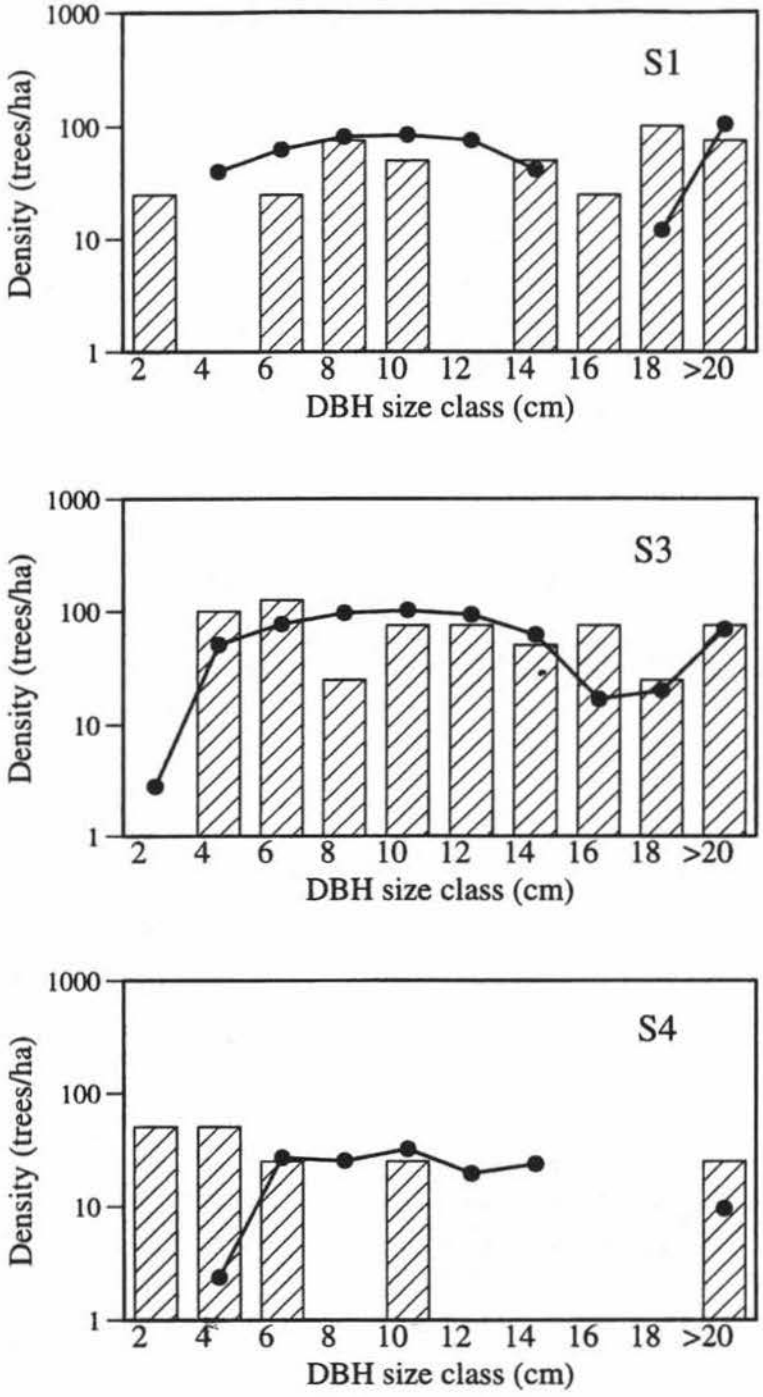


Figure 5.7. Size-class distribution of *Avicennia germinans* for three mangrove sites. Solid line is the average of 50 simulations of the MANGAL model. Bar represents the field surveys.

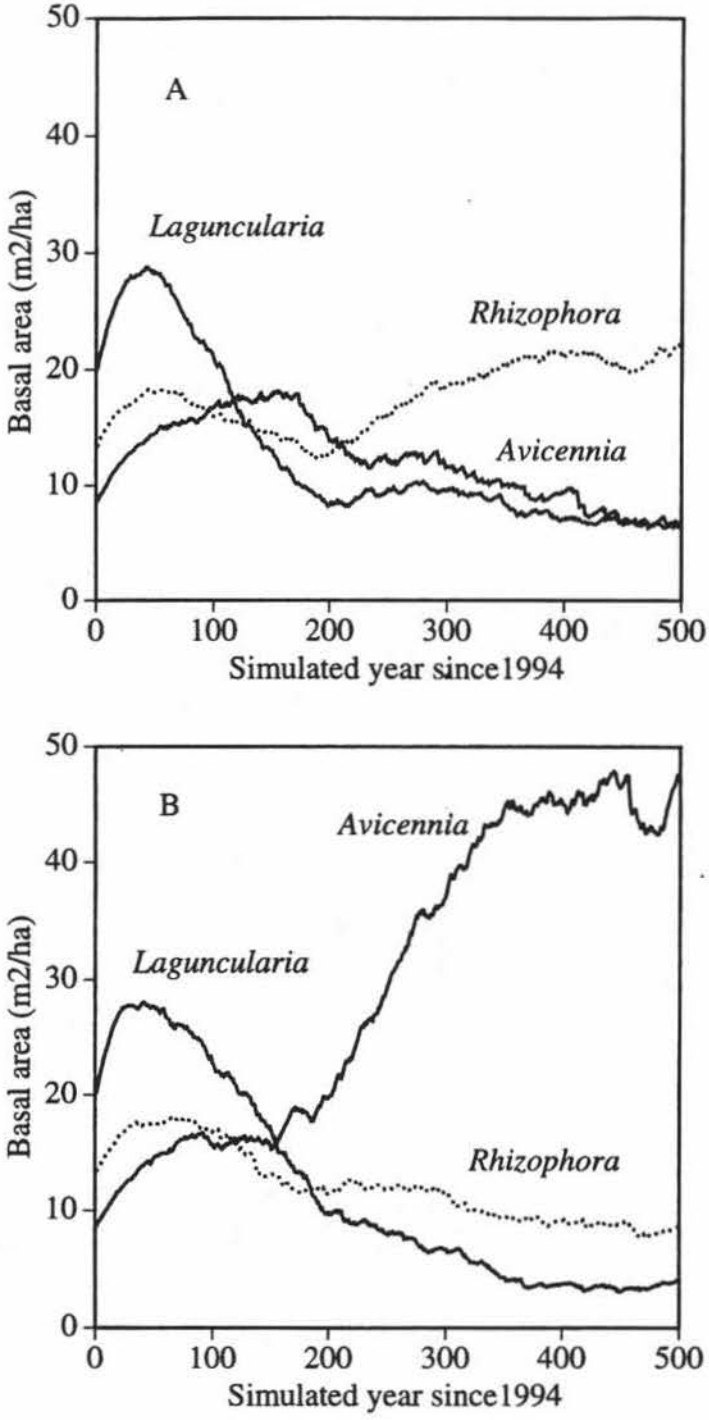


Figure 5. 8. Projected basal area of three mangrove species at the marine site (S1) of the Shark River estuary by the MANGAL model. A: represents low *Avicennia germinans* recruitment. B: represents the equal recruitment for three species.

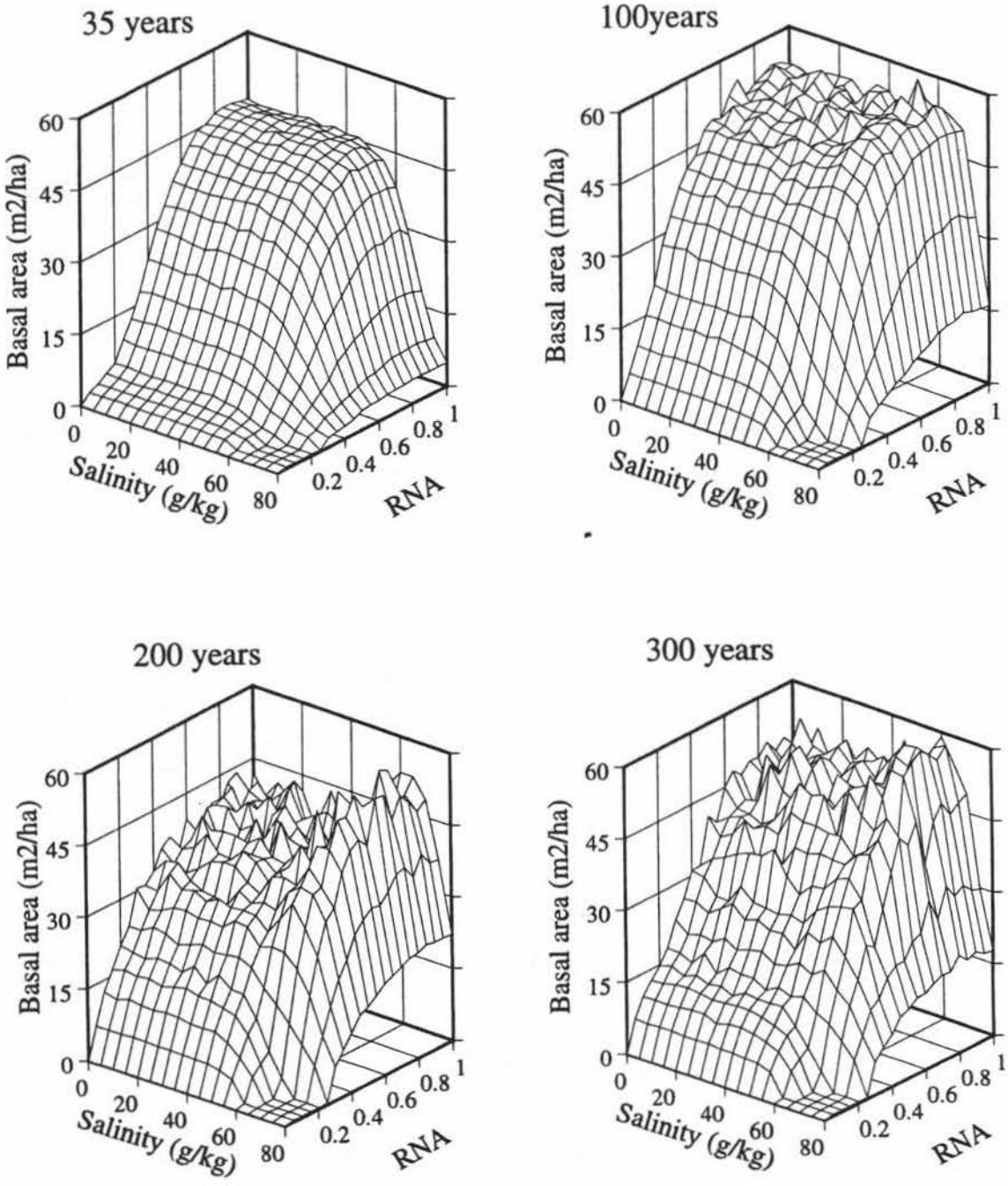


Figure 5.9. Simulated total basal area of mangrove forests along gradients of soil nutrient availability and salinity by FORMAN model.

Rhizophora mangle

Avicennia germinans

Laguncularia racemosa

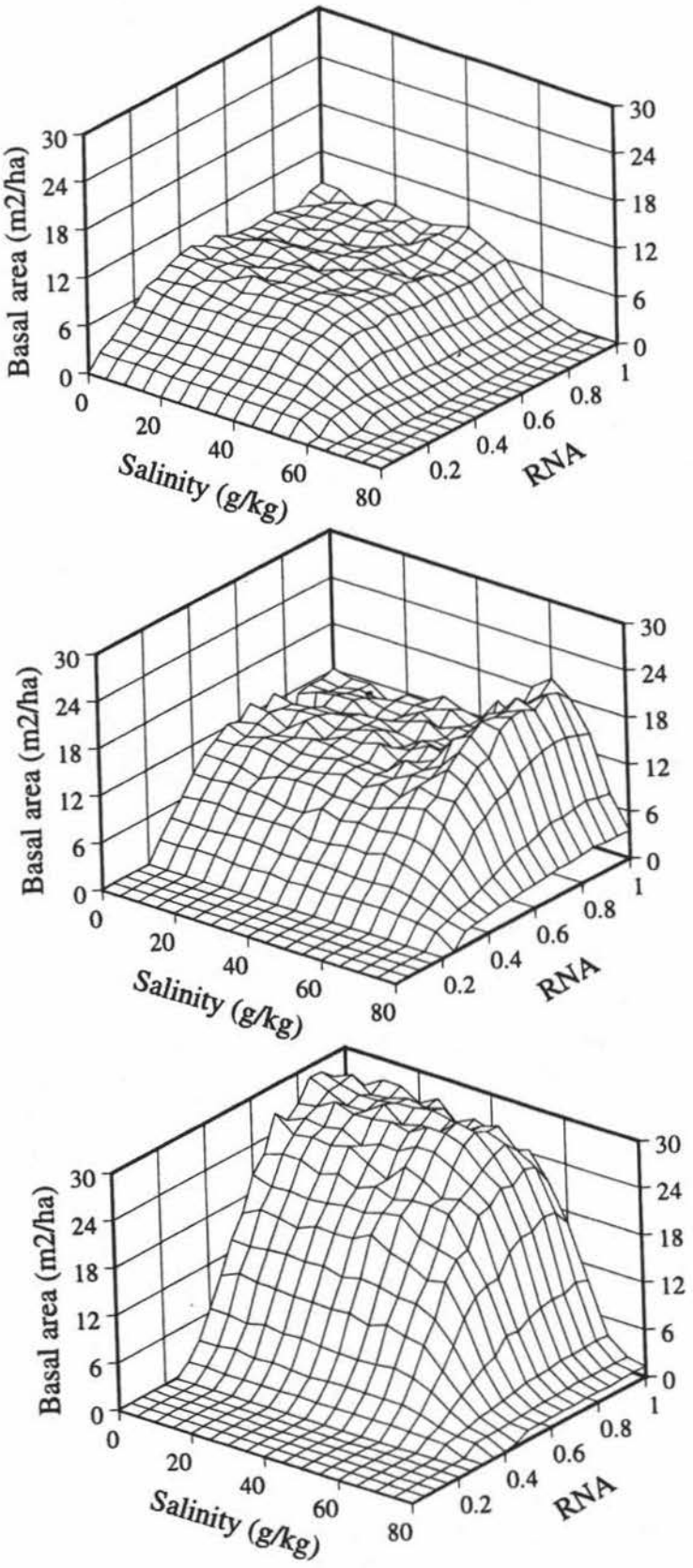


Figure 5.10. Simulated succession of mangrove forest gaps after 35 years of development along gradients of soil nutrient availability and salinity stress by the FORMAN model.

Rhizophora mangle

Avicennia germinans

Laguncularia racemosa

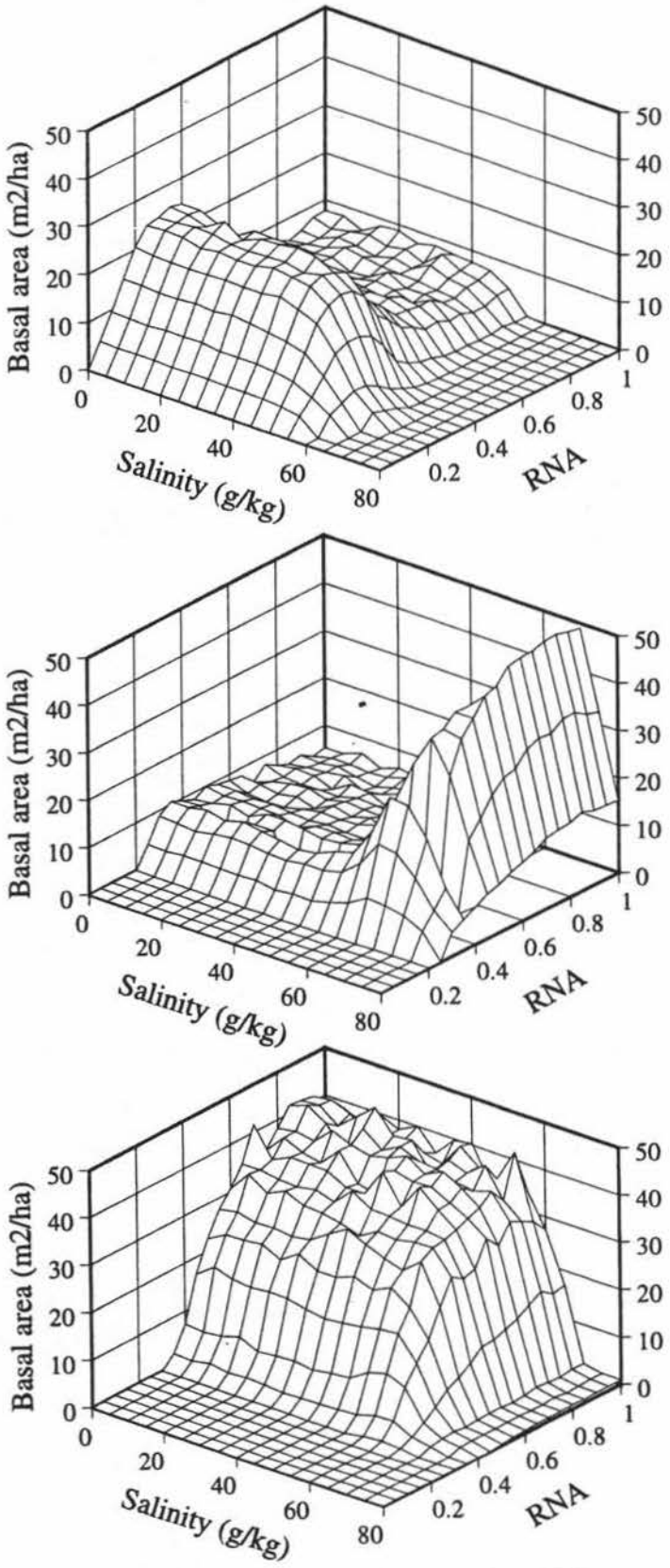


Figure 5.11. Simulated succession of mangrove forest gaps after 100 years of development along gradients of soil nutrient availability and salinity stress by the FORMAN model.

Rhizophora mangle

Avicennia germinans

Laguncularia racemosa

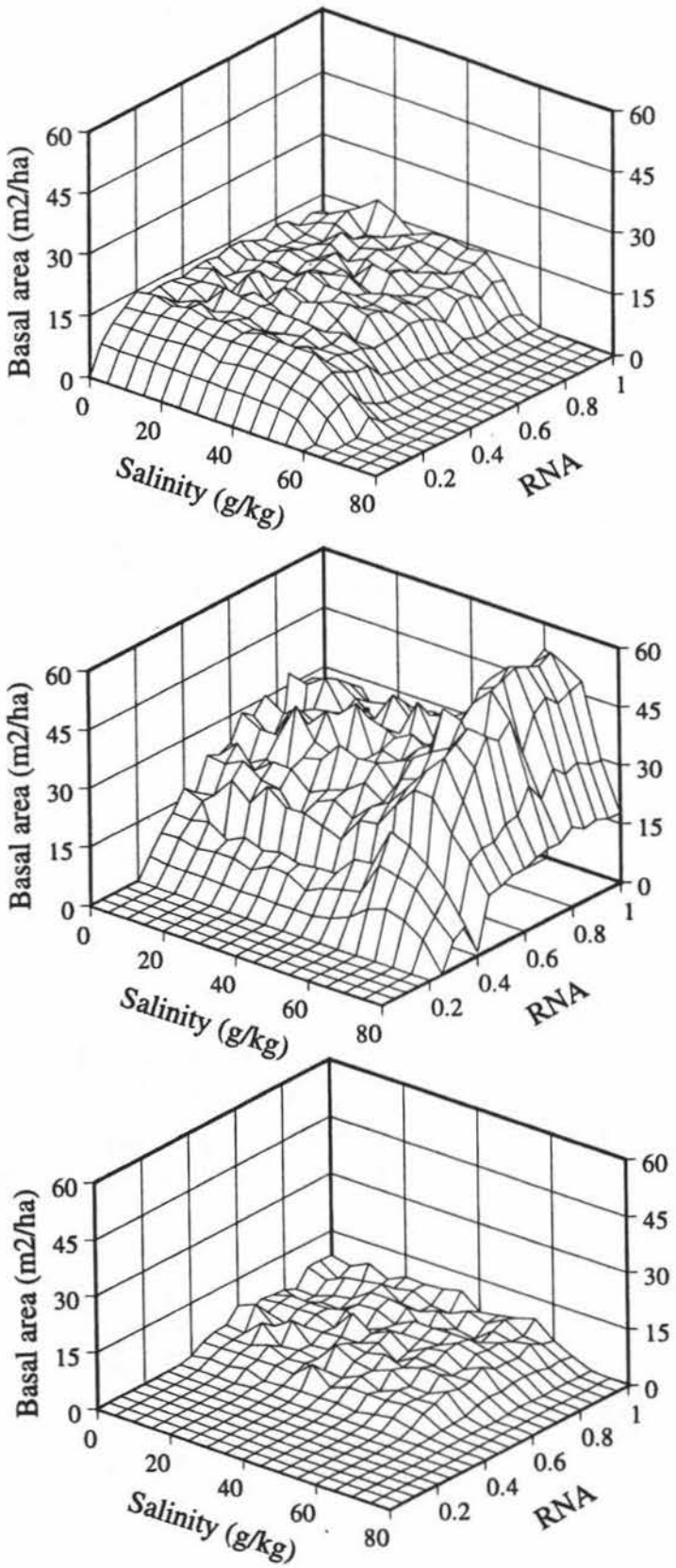


Figure 5.13. Simulated succession of mangrove forest gaps after 300 years of development along gradients of soil nutrient availability and salinity stress by the FORMAN model.

LITERATURE CITED

Abd. Aziz, S. A. and D. B. Nedwell. 1986. The nitrogen cycle of an east coast, U.K., saltmarsh: I. Nitrogen assimilation during primary production, detrital mineralization. Estuarine, Coastal and Shelf Science **22**: 559-575.

Aber, J. D. and J. M. Melillo 1982. FORTNITE: a computer model of organic matter and nitrogen dynamics in forest ecosystems. Research Bulletin. University of Wisconsin. Madison, Wisconsin.

Aber, J. D., J. M. Melillo, K. J. Nadelhoffer, J. Pastor and R. D. Boone. 1991. Factors controlling nitrogen cycling and nitrogen saturation in northern temperate forest ecosystems. Ecological application **1**: 303-315.

Alongi, D. M. 1996. The dynamics of benthic nutrient pools and fluxes in tropical mangrove forests. Journal of Marine Research **54**: 123-148.

Alongi, D. M., K. G. Boto and A. I. Robertson. 1992. Nitrogen and phosphorous cycles. Pages 252-292 *in* A. I. Robertson and D. M. Alongi, editors. Tropical mangrove ecosystems. American Geophysical Union, Washington, D.C..

Alongi, D. M., P. Christoffersen and F. Tirendi. 1993. The influence of forest type on microbial-nutrient relationships in tropical mangrove sediments. Journal of Experimental Marine Biology and Ecology **171**: 201-223.

Aspila, K. I., H. Agemian and A. S. Y. Chau. 1976. A semi-automated method for the determination of inorganic, organic and total phosphate in sediments. Analyst **101**: 187-197.

Ball, M. C. 1980. Patterns of secondary succession in a mangrove forest of southern Florida. Oecologia **44**: 226-235.

Benner, R., P. G. Hatcher and J. I. Hedges. 1990. Early diagenesis of mangrove leaves in a tropical estuary: bulk chemical characterization using solid-state ^{13}C NMR and elemental analyses. Geochimica et Cosmochimica Acta **54**: 2003-2013.

Benner, R., E. R. Peele and E. Hodson. 1986. Microbial utilization of dissolved organic matter from leaves of the red mangrove, *Rhizophora mangle*, in the fresh creek estuary, Bahamas. Estuarine, Coastal and Shelf Science **23**: 607-619.

Binkley, D. and P. Vitousek. 1989. Soil nutrient availability. Pages 75-96 *in* R. W. Pearcy, J. Ehleringer, H. A. Mooney and P. W. Rundel, editors. Plant physiological ecology - field methods and instrumentation. Chapman & Hall, London.

Blackburn, T. H. and K. Henricksen. 1983. Nitrogen cycling in different types of sediments from Danish waters. Limnology and Oceanography **28**: 477-493.

Blasco, F. 1984. Climatic factors and the biology of mangrove plants. Pages 18-35 *in* S. C. Snedaker and J. G. Snedaker, editors. The mangrove ecosystem: research methods. UNESCO, Paris, France.

Boon, P. I., D. J. W. Moriarty and P. G. Saffigna. 1986. Rates of ammonium turnover and the role of amino-acid deamination in seagrass (*Zostera capricorni*) beds of Moreton Bay, Australia. Marine Biology **91**: 259-268.

Botkin, D. B. 1993. Forest dynamics - An ecological model. Oxford University Press, Oxford.

Botkin, D. B., J. F. Janak and J. R. Wallis. 1972. Some ecological consequence of a computer model of forest growth. Journal of Ecology **60**: 849-872.

Boto, K. G. 1991. Nutrients and mangroves. Pages 129-145 *in* D. W. Connell and D. W. Hawker, editors. Pollution in tropical aquatic systems. CRC Press, Inc., Boca Raton, Florida.

Boto, K. G. and J. S. Bunt. 1981. Tidal export of particulate organic matter from a northern Australian mangrove system. Estuarine, Coastal and Shelf Science **13**: 247-255.

Boto, K. G., J. S. Bunt and J. T. Wellington. 1984. Variations in mangrove forest productivity in northern Australia and Papua New Guinea. Estuarine, Coastal and Shelf Science **19**: 321-330.

Boto, K. G., P. Saffingna and B. F. Clough. 1985. Role of nitrate in nitrogen nutrition of the mangrove *Avicennia marina*. Marine Ecology Progress Series **21**: 259-265.

Boto, K. G. and J. T. Wellington. 1983. Phosphorus and nitrogen nutritional status of a northern Australian mangrove forest. Marine Ecology Progress Series **11**: 63-69.

Boto, K. G. and J. T. Wellington. 1984. Soil characteristics and nutrient status in a northern Australian mangrove forest. Estuaries **7**: 61-69.

Boto, K. G. and J. T. Wellington. 1988. Seasonal variations in concentrations and fluxes of dissolved organic and inorganic materials in a tropical, tidally-dominated, mangrove waterway. Marine Ecology Progress Series **50**: 151-160.

Bowden, W. B. 1984. A nitrogen-15 isotope dilution study of ammonium production and consumption in a marsh sediment. Limnology and Oceanography **29**: 1004-1015.

Bridgham, S. D., J. Pastor, C. A. McClaugherty and C. J. Richardson. 1995. Nutrient-use efficiency: a litterfall index, a model, and a test along a nutrient-availability gradient in north Carolina peatlands. The American Naturalist **145**: 1-21.

Burke, I. 1989. Control of nitrogen mineralization in a sagebrush steppe landscape. Ecology **70**: 1115-1126.

Canham, C. D. and P. L. Marks. 1985. The response of woody plants to disturbance: Patterns of establishment and growth. Pages 197-217 *in* S. T. A. Pickett and P. S. White, editors. The ecology of natural disturbance and patch dynamics. Academic Press, Inc., New York.

Carlson, P. R. and L. A. Yarbro. 1988. Physical and biological control of mangrove pore water chemistry. Pages 112-132 *in* D. D. Hook, W. H. McKee Jr. and H. K. Smith et al., editors. The ecology and management of wetlands. Timber Press, Portland, Oregon.

Carlson, P. R., L. A. Yarbro, C. F. Zimmermann and J. R. Montgomery. 1983. Pore water chemistry of an overwash mangrove island. Florida Scientist **46**: 239-249.

Carter, M. R., L. A. Burns, T. R. Cavinder, K. R. Dugger, P. L. Fore, D. E. Hicks, H. L. Revells and T. W. Schmidt 1973. Ecosystem analysis of the big cypress swamp and estuaries. Environmental Protection Agency, Region IV, Atlanta, Georgia.

Chapman, V. J. 1976. Mangrove vegetation. J. Cramer, Vaduz, Germany.

Cintrón, G., A. E. Lugo, D. J. Pool and G. Morris. 1978. Mangroves of arid environments in Puerto Rico and adjacent islands. Biotropica **10**: 110-121.

Cintrón, G. and Y. Schaeffer-Novelli. 1984. Caracteristicas y desarrollo estructural de los manglares de Norte y Sur America. Programa Regional de Desarrollo Cientifico y Technologico **25**: 4-15.

Clarke, P. J. 1993. Dispersal of grey mangrove (*Avicennia marina*) propagules in southeastern Australia. Aquatic Botany **45**: 195-204.

Clarke, P. J. and W. G. Allaway. 1993. The regeneration niche of the grey mangrove (*Avicennia marina*): effects of salinity, light and sediment factors on establishment, growth and survival in the field. Oecologia **93**: 548-556.

Clough, B. F. 1992. Primary productivity and growth of mangrove forest. Pages 225-249 *in* A. I. Robertson and D. M. Alongi, editors. Tropical mangrove ecosystems. American Geophysical Union, Washington, DC.

Craft, C. B. and C. J. Richardson. 1993a. Peat accretion and phosphorus accumulation along a eutrophication gradient in the northern Everglades. Biogeochemistry **22**: 133-156.

Craft, C. B. and C. J. Richardson. 1993b. Peat accretion and N, P, and organic C accumulation in nutrient-enriched and unenriched Everglades peatlands. Ecological Applications **3**: 446-458.

Craighead, F. C. 1971. The trees of south Florida. University of Miami Press, Coral Gables, Florida.

Craighead, F. C. and V. C. Gilbert. 1962. The effects of Hurricane Donna on the vegetation of southern Florida. The Quarterly Journal of the Florida Academy of Sciences **25**: 1-28.

Crews, T., E, K. Kitayama, J. H. Fownes, R. H. Riley, D. A. Herbert, D. Mueller-Dombois and P. M. Vitousek. 1995. Changes in soil phosphorus fractions and ecosystem dynamics across a long chronosequence in Hawaii. Ecology **76**: 1407-1424.

Davis, J. H., Jr. 1940. The ecology and geologic role of mangroves in Florida. Pages 303-412. Carnegie Institute of Washington Publication Number 517. Washington, D. C.

Davis, S. M. 1991. Growth, decomposition, an nutrient retention of *Cladium jamaicens* Crantz and *Typha domingensis* Pers in Florida Everglades. Aquatic Botany **40**: 203-224.

Davis, S. M. 1994. Phosphorus inputs and vegetation sensitivity in the Everglades. Pages 357-378 *in* S. M. Davis and J. C. Ogden, editors. Everglades: The ecosystem and its restoration. St. Lucie Press, Delray Beach, Florida.

Day, J. W., W. H. Conner, F. Ley-Lou, R. H. Day and A. M. Navarro. 1987. The productivity and composition of mangrove forests, Laguna de Términos, Mexico. Aquatic Botany **27**: 267-284.

DeAngelis, D. L. and L. J. Gross. (Editors) 1992. Individual-based models and approaches in ecology: populations, communities and ecosystems. Chapman and Hall, New York.

DeBusk, W. F., K. R. Reddy, M. S. Koch and Y. Wang. 1994. Spatial distribution of soil nutrients in a northern Everglades marsh: Water Conservation Area 2A. Soil Science Society of America Journal **58**: 543-552.

DeKanel, J. and J. W. Morse. 1978. The chemistry of orthophosphate uptake from seawater on to calcite and aragonite. Geochimica Cosmochica Acta **42**: 1335-1340.

DeLaune, R. D., C. N. Reddy and W. H. J. Patrick. 1981. Accumulation of plant nutrients and heavy metals through sedimentation processes and accretion in a Louisiana salt marsh. Estuaries **4**: 328-334.

Denslow, J. S. 1985. Disturbance-mediated coexistence of species. Pages 307-324 *in* S. T. A. Pickett and P. S. White, editors. The ecology of natural disturbance and patch dynamics. Academic Press, Inc., New York.

Doyle, T. W. 1981. The role of disturbance in the gap dynamics of a montane rain forest succession model. Pages 56-73 *in* D. C. West, H. H. Shugart and D. B. Botkin, editors. Forest succession: Concept and application. Springer-Verlag, New York.

Doyle, T. W., T. J. Smith III and M. B. Robblee. 1995. Wind damage effects of hurricane Andrew on mangrove communities along the southwest coast of Florida, USA. Journal of Coastal Research **21**: 159-168.

Duever, M. J., J. F. Meeder, L. C. Meeder and J. M. McCollom. 1994. The climate of south Florida and its role in shaping the Everglades ecosystem. Pages 225-248 *in* S. M. Davis and J. C. Ogden, editors. Everglades - The ecosystem and its restoration. St. Lucie Press, Delray Beach, Florida.

Duke, N., C. 1992. Mangrove floristics and biogeography. Pages 63-100 *in* A. I. Robertson and D. M. Alongi, editors. Tropical mangrove ecosystems. American Geophysical Union, Washington, D.C.

Duke, N. C. and Z. S. Pinzón. 1992. Aging *Rhizophora* seedlings from leaf scar nodes: a technique for studying recruitment and growth in mangrove forests. Biotropica **24**: 173-186.

Egler, F. E. 1952. Southeast saline Everglades vegetation, Florida, and its management. Veg. Acta Geobot. **3**: 213-265.

Ellison, A. M. and E. J. Farnsworth. 1993. Seedling survivorship, growth, and response to disturbance in Belizean mangle. American Journal of Botany **80**: 1137-1145.

Feller, I. C. 1995. Effects of nutrient enrichment on growth and herbivory of dwarf red mangrove (*Rhizophora mangle*). Ecological Monographs **54**: 477-505.

Flores-Verdugo, F. J., J. W. Day Jr. and R. Briseño-Dueñas. 1987. Structure, litter fall, decomposition and detritus dynamics of mangroves in a Mexican Coastal Lagoon with an ephemeral inlet. Marine Ecology Progress Series **35**: 83-90.

Fourqurean, J. W., R. D. Jones and J. C. Zieman. 1993. Processes influencing waters column nutrient characteristics and phosphorus limitation of phytoplankton biomass in Florida Bay, FL, USA: inferences from spatial distribution. Estuarine, Coastal and Shelf Science **36**: 295-314.

Fourqurean, J. W., J. C. Zieman and G. Powell V. N. 1992. Phosphorus limitation of primary production in Florida Bay: Evidence from C:N:P ratios of the dominant seagrass Thalassia *testudinum*. Limnology and Oceanography **37**: 162-171.

Frank, D. A., R. S. Inouye, N. Huntly, G. W. Minshall and J. E. Anderson. 1994. The biogeochemistry of a north-temperate grassland with native ungulates: Nitrogen dynamics in Yellowstone National Park. Biogeochemistry **26**: 163-188.

Gale, P. M., K. R. Reddy and D. A. Graetz. 1994. Phosphorus retention by wetland soils used for treated wastewater disposal. Journal of Environmental Quality **23**: 370-377.

Gill, A. M. and P. B. Tomlinson. 1971. Studies on the growth of red mangrove (*Rhizophora mangle* L.) 3. phenology of the shoot. Biotropica **3**: 109-124.

Golley, F. B. 1975. Mineral cycling in a tropical moist forest ecosystem. University of Georgia Press, Athens, Georgia.

Golley, F., H. T. Odum and R. Wilson. 1962. A synoptic study of the structure and metabolism of a red mangrove forest in southern Puerto Rico in May. Ecology **43**: 9-18.

Gong, W. K. and J. E. Ong. 1990. Plant biomass and nutrient flux in a managed mangrove forest in Malaysia. Estuarine, Coastal and Shelf Science **31**: 519-530.

Hart, S. C. and A. J. Gunther. 1989. In situ estimates of annual net nitrogen mineralization and nitrification in a subarctic watershed. Oecologia **80**: 284-288.

Heald, E. J. 1969. The production of organic detritus in a south Florida estuary. Dissertation. University of Miami, Coral Gables, Florida.

Heald, E. J., M. A. Roessler and G. L. Beardsley. 1979. Litter production in a southwest Florida black mangrove community. *in* C. B. Rathburn, editors. Proceedings of the Florida Anti-Mosquito Association **50**:24-32.

Hesse, P. 1962. Phosphorus fixation in mangrove swamp muds. Nature **193**: 295-296.

Hesse, P. R. 1963. Phosphorus relationships in a mangrove swamp mud with particular reference to aluminum toxicity. Plant and Soil **19**: 205-218.

Hieltjes, A. H. M. and L. Lijklema. 1980. Fractionation of inorganic phosphates in calcareous sediments. Journal of Environmental Quality **9**: 405-407.

Huston, M., D. DeAngelis and W. Post. 1988. New computer models unify ecological theory. BioScience **38**: 682-691.

Jiménez, J. 1990. The structure and function of dry weather mangroves on the Pacific coast of Central America, with emphasis on *Avicennia bicolor* forests. Estuaries **13**: 182-192.

Jiménez, J. A., A. E. Lugo and G. Cintrón. 1985. Tree mortality in mangrove forests. Biotropica **17**: 177-185.

Jiménez, J. A. and K. Sauter. 1991. Structure and dynamics of mangrove forests along a flooding gradient. Estuaries **14**: 49-56.

Joye, S. B. and J. T. Hollibaugh. 1995. Influence of sulfide inhibition of nitrification on nitrogen regeneration in sediments. Science **270**: 623-625.

King, G. M., M. J. Klug, R. G. Wiegert and A. G. Chalmers. 1982. Relation of soil water movement and sulfide concentration to *Spartina alterniflora* production in a Georgia salt marsh. Science **218**: 61-63.

Koch, M. S. and K. R. Reddy. 1992. Distribution of soil and plant nutrients along a trophic gradient in the Florida Everglades. Soil Science Society of America Journal **56**: 1492-1499.

Komiyama, A., H. Moriya and K. Ogino. 1989. A quantitative analysis of root system of mangrove tree species in Iriomote Island, southern Japan. Galaxea **8**: 89-96.

Lacerda, L. D., V. Ittekkot and S. R. Patchineelam. 1995. Biogeochemistry of mangrove soil organic matter: a comparison between *Rhizophora* and *Avicennia* soils in south-eastern Brazil. Estuarine, Coastal and Shelf Science **40**: 713-720.

Lajtha, K. and W. H. Schlesinger. 1988. The biogeochemistry of phosphorus cycling and phosphorus availability along a desert soil chronosequence. Ecology **69**: 24-39.

Light, S. S. and J. W. Dineen. 1994. Water control in the Everglades: a historical perspective. Pages 47-84 *in* S. M. Davis and J. C. Ogden, editors. Everglades - The ecosystem and its restoration. St. Lucie Press, Delray Beach, Florida.

Liu, J. and P. S. Ashton. 1995. Individual-based simulation models for forest succession and management. Forest Ecology and Management **73**: 157-175.

Loope, L., M. Duever, A. Herndon, J. Snyder and D. Jansen. 1994. Hurricane impacts on uplands and freshwater swamp forest. BioScience **44**: 238-246.

Lugo, A. E. 1980. Mangrove ecosystem: Successional or steady state? Biotropica (Tropical Succession): 65-72.

Lugo, A. E., S. Brown and M. M. Brinson. 1988. Forested wetlands in freshwater and salt-water environments. Limnology and Oceanography **33**: 894-909.

Lugo, A. E., M. Sell and S. C. Snedaker. 1976. Mangrove ecosystem analysis. Pages 113-145 *in* B. C. Pattern, editors. System analysis and simulation in ecology. Academic Press, Inc., New York.

Lugo, A. E. and S. C. Snedaker. 1974. The ecology of mangroves. Annual Review of Ecology and Systematics **5**: 39-64.

Lugo, A. E. and S. C. Snedaker. 1975. Properties of a mangrove forest in southern Florida. Pages 170-212 *in* G. E. Walsh, S. C. Snedaker, and H. T. Teas, editors. Proceedings of the International Symposium on the Biology and Management of Mangroves, Institute of Food and Agricultural Sciences, University of Florida, Gainesville, Florida.

Lugo, A. E., R. R. Twilley and C. Patterson-Zucca. 1980. The role of black mangrove forests in the productivity of coastal ecosystems in south Florida. Report to EPA Corvallis Environment Research Laboratory, Corvallis, Oregon.

Lynch, J. C. 1989. Sedimentation and nutrient accumulation in mangrove ecosystem of the Gulf of Mexico. M.S. Thesis, University of Southwestern Louisiana. Lafayette, Louisiana.

Lynch, J. C., J. R. Meriwether, B. A. McKee, F. Vera-Herrera and R. R. Twilley. 1989. Recent accretion in mangrove ecosystem based on ^{137}Cs and ^{210}Pb. Estuaries **12**: 284-299.

Macnae, W. 1968. A general account of the fauna and flora of mangrove swamps and forests in the Indo-West-Pacific region. Advances Marine Biology **6**: 73-270.

McGill, W. B. and C. V. Cole. 1981. Comparative aspects of cycling of organic C, N, S, and P through soil organic matter. Geoderma **26**: 287-309.

McIvor, C. C., J. A. Ley and R. D. Bjork. 1994. Changes in freshwater inflow from the Everglades to Florida Bay including effects on biota and biotic processes: a review. Pages 117-148 *in* S. M. Davis and J. C. Ogden, editors. Everglades - The ecosystem and its restoration. St. Lucie Press, Delray Beach, Florida.

McKee, K. L. 1993. Soil physicochemical patterns and mangrove species distribution - reciprocal effects? Journal of Ecology **81**: 477-487.

McKee, K. L. 1995a. Seedling recruitment patterns in a Belizean mangrove forest: effects of establishment ability and physico-chemical factors. Oecologia **101**: 448-460.

McKee, K. L. 1995b. Interspecific variation in growth, biomass partition, and defensive characteristics of neotropical mangrove seedlings: response to light and nutrient availability. American Journal of Botany **82**: 299-307.

McKee, K. L., I. A. Mendelssohn and M. W. Hester. 1988. Reexamination of pore water sulfide concentration and redox potential near the aerial roots of *Rhizophora mangle* and *Avicennia germinans*. American Journal of Botany **75**: 1352-1359.

McMillan, C. 1974. Salt tolerance of mangroves and submerged aquatic plants. Pages 379-390 *in* R. J. Reimold and W. H. Queen, editors. Ecology of halophytes. Academic Press Inc, New York.

Miller, P. C. 1972. Bioclimate, leaf temperature, and primary production in red mangrove canopies in south Florida. Ecology **53**: 22-45.

Mitsch, W. J. and J. G. Gosselink. 1993. Wetlands. Van Nostrand Reinhold, New York.

Mitsch, W. J., M. Straskraba and S. E. JØrgensen. 1988. Summary and state of the art of wetland modelling. Pages 217-222 *in* W. J. Mitsch, M. Straskraba and S. E. JØrgensen, editors. Wetland Modelling. Elsevier, Amsterdam.

Mladenoff, D. J. 1987. Dynamics of nitrogen mineralization and nitrification in hemlock and hardwood treefall gaps. Ecology **68**: 1171-1180.

Morris, J. T. and W. B. Bowden. 1986. A mechanistic, numerical model of sedimentation, mineralization, and decomposition for marsh sediments. Soil Science Society of America Journal **50**: 96-105.

Nadelhoffer, K. J., A. E. Giblin, G. R. Shaver and J. A. Laundre. 1991. Effects of temperature and substrate quality on element mineralization in six arctic soils. Ecology **72**: 242-253.

Nickerson, H. H. and F. R. Thibodeau. 1985. Association between pore water sulfide concentrations and the distribution of mangroves. Biogeochemistry **1**: 183-192.

Odum, W. E. and E. J. Heald. 1972. Trophic analyses of an estuarine mangrove community. Bulletin Marine Science **22**: 671-738.

Odum, W. E., C. C. McIvor and T. J. Smith III. 1982. The ecology of the mangroves of south Florida: a community profile. U.S. Fish and Wildlife Service. FWS/OBS-81-24, Washington, D.C.

Odum, W. E., T. J. Smith III, J. K. Hoover, and C. C. McIvor. 1984 The ecology of tidal freshwater marshes of the tidal freshwater marshes of the United States east coast: A community Profile. U.S. Fish and Wildlife Service, FWS/OBS-83/17, Washington, D.C.

Olsen, S. R. and L. E. Sommers. 1982. Phosphorus. Pages 403-430 *in* A. L. Page, R. H. Miller and D. R. Keeney, editors. Methods of soil analysis. Part 2. Chemical and microbiological properties. American Society of Agronomy and Soil Science Society of America, Madison, Wisconsin.

Onuf, C. P., J. M. Teal and I. Valiela. 1977. Interactions of nutrients, plant growth and herbivory in a mangrove ecosystem. Ecology **58**: 514-526.

Osborne, K. and T. J. Smith, III. 1990. Differential predation on mangrove propagules in open and closed canopy forest habitats. Vegetatio **89**: 1-6.

Pacala, S. W., C. D. Canham, J. Saponara, J. A. Silander Jr., R. K. Kobe and E. Ribbens. 1996. Forest models defined by field measurements: estimation, error analysis and dynamics. Ecological Monographs **66**: 1-43.

Parkinson, R. W., R. D. DeLaune and J. R. White. 1994. Holocene sea-level rise and the fate of mangrove forests within the wider Caribbean region. Journal of Coastal Research **10**: 1077-1086.

Parsons, T. R., Y. Maita and C. M. Lalli. 1984. A manual of chemical and biological methods for seawater analysis. New York, Pergamon Press.

Parton, W. J., D. S. Schimel, C. V. Cole and D. S. Ojima. 1987. Analysis of factors controlling soil organic matter levels in Great Plains grasslands. Soil Science Society of America Journal **51**: 1173-1179.

Parton, W. J., J. W. B. Stewart and C. V. Cole. 1988. Dynamics of C, N, P and S in grassland soils: A model. Biogeochemistry **5**: 109-131.

Pastor, J., J. D. Aber, C. A. McClaugherty and J. M. Melillo. 1984. Aboveground production and N and P cycling along a nitrogen mineralization gradient on blackhawk island, Wisconsin. Ecology **65**: 256-268.

Pastor, J. and W. M. Post. 1986. Influence of climatic; soil moisture, and succession on forest carbon and nitrogen cycles. Biogeochemistry **2**: 3-27.

Pastor, J., M. A. Stillwell and D. Tilman. 1987. Nitrogen mineralization and nitrification in four Minnesota old fields. Oecologia **71**: 481-485.

Pearlstine, L., H. McKellar and W. Kitchens. 1985. Modeling the impacts of river diversion on bottomland forest communities in the Santee River Floodplain, South Carolina. Ecological Modelling **29**: 283-302.

Phipps, R. L. 1979. Simulation of wetlands forest dynamics. Ecological Modelling **7**: 257-288.

Pickett, S. T. A. and P. S. White. 1985a. Natural disturbance and patch dynamics: An introduction. Pages 3-13 *in* S. T. A. Pickett and P. S. White, editors. The ecology of natural disturbance and patch dynamics. Academic Press, Inc., New York.

Pickett, S. T. A. and P. S. White, (editors). 1985b. The ecology of natural disturbance and patch dynamics. Academic Press, Inc., New York.

Polglase, P. J., N. B. Comerford and E. J. Jokela. 1992. Mineralization of nitrogen and phosphorus from soil organic matter in southern pine plantation. Soil Science Society of America Journal **56**: 921-927.

Pool, D. J., A. E. Lugo, and S. C. Snedaker. 1975. Litter production in mangrove forests of southern Florida and Puerto Rico. Pages 213-237 *in* G. E. Walsh, S. C. Snedaker, and H. T. Teas, editors. Proceedings of the International Symposium on Biology and Management of Mangroves, University of Florida, Gainesville, Florida.

Pool, D. J., S. C. Snedaker and A. E. Lugo. 1977. Structure of mangrove forests in Florida, Puerto Rico, Mexico, and Costa Rica. Biotropica **9**: 195-212.

Powell, A. B., D. E. Hoss, W. F. Hettler, D. Peters and S. Wagner. 1989. Abundance and distribution of ichthyoplankton in Florida Bay and adjacent waters. Bulletin of Marine Science **44**: 35-48.

Provost, M. W. 1973. Mean high water mark and use of tidelands in Florida. Florida Scientist **36**: 50-66.

Putz, F. E. and H. T. Chan. 1986. Tree growth, dynamics, and productivity in a mature mangrove forest in Malaysia. Forest Ecology and Management **17**: 211-230.

Rabinowitz, D. 1978. Early growth of mangrove seedlings in Panama, and an hypothesis concerning the relationship of dispersal and zonation. Journal of Biogeography **5**: 113-133.

Rastetter, E. B. 1990. A spatially explicit model of vegetation-habitat interactions on barrier islands. Pages 353-378 *in* M. G. Turner and R. H. Gardner, editors. Quantitative methods in landscape ecology. Springer-Verlag, New York.

Reddy, K. R., R. D. DeLaune, W. F. DeBusk and M. S. Koch. 1993. Long-term nutrient accumulation rates in the Everglades. Soil Science Society of America Journal **57**: 1147-1155.

Rey, J. R., J. Shaffer, T. Kain, R. Stahl and R. Crossman. 1992. Sulfide variation in the pore and surface waters of artificial salt-marsh ditches and a natural tidal creek. Estuaries **15**: 257-269.

Rivera-Monroy, V. H., J. W. Day, R. R. Twilley, F. Vera-Herrera and C. Coronado-Molina. 1995a. Flux of nitrogen and sediment in a fringe mangrove forest in Terminos Lagoon, Mexico. Estuarine, Coastal and Shelf Science **40**: 139-160.

Rivera-Monroy, V. H. and R. R. Twilley. 1996. The relative role of denitrification and immobilization on the fate of inorganic nitrogen in mangrove sediments of Terminos Lagoon, Mexico. Limnology and Oceanography **41**: 284-296.

Rivera-Monroy, V. H., R. R. Twilley, R. G. Boustany, J. W. Day, F. Vera-Herrera and M. C. Ramirez. 1995b. Direct denitrification in mangrove sediments in Términos Lagoon Mexico. Marine Ecology Progress Series **126**: 97-109.

Robertson, A. I. and P. A. Daniel. 1989. Decomposition and the annual flux of detritus from fallen timber in tropical mangrove forests. Limnology and Oceanography **34**: 640-646.

Robertson, A. I., R. L. Giddins and T. J. Smith III. 1990. Seed predation by insects in tropical mangrove forests: extent and affects on seed viability and growth of seedlings. Oecologia **83**: 213-219.

Robertson, A. I. and M. J. Phillips. 1995. Mangroves as filters of shrimp pond effluent: predictions and biogeochemical research needs. Hydrobiologia **295**: 311-321.

Robertson, G. P., M. A. Huston, F. C. Evans and J. M. Tiedje. 1988. Spatial variability in a successional plant community: patterns of nitrogen availability. Ecology **69**: 1517-1524.

Roman, C. T., N. G. Aumen, J. C. Trexler, R. J. Fennema, W. F. Loftus and M. A. Soukup. 1994. Hurricane Andrew's impact on freshwater resources. BioScience **44**: 247-255.

Rosenfeld, J. K. 1979a. Interstitial water and sediment chemistry of two cores from Florida Bay. Journal of Sedimentary Petrology **49**: 989-994.

Rosenfeld, J. K. 1979b. Ammonium adsorption in nearshore anoxic sediments. Limnology and Oceanography **24**: 356-364.

Roth, L. 1992. Hurricane and mangrove regeneration: Effects of Hurricane Joan, October 1988, on the vegetation of Lsla del Venado, Bluefieds, Nicaragua. Biotropica **24**: 375-384.

Saenger, P. and S. C. Snedaker. 1993. Pantropical trends in mangrove above-ground biomass and annual litterfall. Oecologia **96**: 293-299.

SAS. 1989. SAS user's guide: Statistics. SAS Institute, Cary, North Carolina.

Schimel, D., M. A. Stillwell and R. G. Woodmansee.. 1985. Biogeochemistry of C, N, and P in a soil catena of the shortgrass steppe. Ecology **66**: 276-282.

Scholl, D. W. 1964a. Recent sedimentary record in mangrove swamps and rise in sea level over the southwestern coast of Florida, Part I. Marine Geology **1**: 344-366.

Scholl, D. W. 1964b. Recent sedimentary record in mangrove swamps and rise in sea level over the southwestern coast of Florida, Part II. Marine Geology **2**: 343-364.

Sell, M. G. 1977. Modelling the response of mangrove ecosystems to herbicide spraying, hurricane, nutrient enrichment and economic development. Ph.D. Dissertation, University of Florida, Gainesville, Florida.

Sherrod, C. L. and C. McMillan. 1985. The distribution history and ecology of mangrove vegetation along the northern Gulf of Mexico coastal region. Contributions in Marine Science **28**: 129-140.

Shugart, H. H. 1984. A theory of forest dynamics: The ecological implications of forest succession models. Springer-Verlag, New York.

Shugart, H. H., M. S. Hopkins, I. P. Burgess and A. T. Mortlock. 1980. The development of a succession model for subtropical rain forest and its application to assess the effects of timber harvest at Wiangaree State Forest, New South Wales. Journal of Environmental Management **11**: 243-265.

Shugart, H. H., T. M. Smith and W. M. Post. 1992. The potential for application of individual-based simulation models for assessing the effects of global change. Annual Review of Ecology and Systematics **23**: 15-38.

Silver, W. L. 1994. Is nutrient availability related to plant nutrient use in humid tropical forests? Oecologia **98**: 336-343.

Smith, T. J., III, 1987a. Seed predation in relation to tree dominance and distribution in mangrove forests. Ecology **68**: 266-273.

Smith, T. J., III, 1987b. Effects of seed predators and light level on the distribution of *Avicennia marina* (Forsk.) Vierh. in tropical, tidal forests. Estuarine, Coastal and Shelf Science **25**: 43-51.

Smith, T. J., III, 1988. Differential distribution between subspecies of the mangrove *Ceriops tagal*: competitive interactions along a salinity gradient. Aquatic Botany **32**: 79-89.

Smith, T. J., III, 1992. Forest structure. Pages 101-136 *in* A. I. Robertson and D. M. Alongi, editors. Tropical mangrove ecosystems. American Geophysical Union, Washington, D. C.

Smith, T. J., III, 1995. Interspecific differences in mangrove growth and regeneration following catastrophic disturbance. Supplement to the Bulletin of the Ecological Society of America **76**: 248.

Smith, T. J., III, K. G. Boto, S. D. Frusher and R. L. Giddins. 1991. Keystone species and mangrove forest dynamics: the influence of burrowing by crabs on soil nutrient status and forest productivity. Estuarine, Coastal and Shelf Science **33**: 419-432.

Smith, T. J., III, H. T. Chan, C. C. McIvor and M. B. Robblee. 1989. Comparisons of seed predation in tropical, tidal forests from three continents. Ecology **70**: 146-151.

Smith, T. J., III, M. B. Robblee, H. R. Wanless and T. W. Doyle. 1994. Mangroves, hurricanes, and lightning strikes. BioScience **44**: 256-262.

Snedaker, S. C. 1982. Mangrove species zonation: Why? Pages 111-125 *in* D. N. Sen and R. S. Rajopurohit, editors. Tasks for vegetation science Vol. 2. Dr. W. Junk Publishers, The Hague, Netherlands.

Snedaker, S. C. and M. S. Brown 1981. Water quality and mangrove ecosystem dynamics. Environmental Research Laboratory, Gulf Breeze, Florida. EPA-600/4-81-022.

Snedaker, S. C., J. F. Meeder, M. S. Ross and R. G. Ford. 1994. Discussion of Ellison, J. C. and Stoddart, D. R., 1991. Mangrove ecosystem collapse during predicted sea-level rise: holocene analogues and implications. Journal of Coastal Research 7:151-165. Journal of Coastal Research **10**: 497-498.

Solomon, A. M. 1986. Transient response of forests to CO_2-induced climate change: simulation experiments in eastern North America. Oecologia **68**: 567-579.

South Florida Water Management District 1992. Surface water improvement and management plan for the Everglades. Supporting information document. South Florida Water Management District. West Palm Beach, Florida.

Stanford, R. L. 1976. Nutrient cycling in a south Florida mangrove ecosystem. M.S. Thesis. University of Florida, Gainesville, Florida.

Strickland, J. D. H. and T. R. Parsons. 1972. A practical handbooks of sea-water analysis. Fisheries of Research Board of Canada **167**: 1-310.

Steyer, G. D. 1988. Litter dynamics and nitrogen retranslocation in three types of mangrove forests in Rookery Bay, Florida. M.S. Thesis. University of Southwestern Louisiana. Lafayette, Louisiana.

Thibodeau, F. R. and N. H. Nickerson. 1986. Differential oxidation of mangrove substrate by *Avicennia germinans* and *Rhizophora mangle*. American Journal of Botany **73**: 512-516.

Thom, B. G. 1982. Mangrove ecology - a geomorphological perspective. Pages 3-17 *in* B. F. Clough, editors. Mangrove ecosystems in Australia. Australian National University Press, Canberra.

Thom, B. G. 1984. Coastal landforms and geomorphic processes. Pages 3-17 *in* S. C. Snedaker and J. G. Snedaker, editors. The mangrove ecosystem: research methods. UNESCO, Paris, France.

Thomas, T. M. 1974. A detailed analysis of climatological and hydrological records of south Florida with reference to man's influence upon ecosystem evolution. Pages 82-122 *in* P. J. Gleason, editors. Environments of south Florida, Present and Past, Memoir 2. Miami Geological Society, Miami.

Thomlinson, P. B. 1986. The botany of mangroves. Cambridge University Press, Cambridge, United Kingdom.

Tilman, D. 1982. Resource competition and community structure. Princeton University Press, Princeton, New Jersey.

Tilmant, J. T., R. W. Curry, R. Jones, A. Szmant, J. C. Zieman, M. Flora, M. B. Robblee, D. Smith, R. W. Snow and H. Wanless. 1994. Hurricane Andrew's effects on marine resources. BioScience **44**: 230-237.

Turner, M. G. 1989. Landscape ecology: the effect of pattern on process. Annual Review of Ecology and Systematics **20**: 171-197.

Twilley, R. R. 1985. The exchange of organic carbon in basin mangrove forests in a southwest Florida estuary. Estuarine, Coastal and Shelf Science **20**: 543-557.

Twilley, R. R. 1995. Properties of mangrove ecosystems related to the energy signature of coastal environments. Pages 43-62 *in* C. Hall, editors. Maximum power. University of Colorado Press, Boulder, Colorado.

Twilley, R. R., R. H. Chen and T. Hargis. 1992. Carbon sinks in mangroves and their implications to carbon budget of tropical coastal ecosystem. Water, Air, and Soil Pollution **64**: 265-288.

Twilley, R. R., A. E. Lugo and C. Patterson-Zucca. 1986. Production, standing crop, and decomposition of litter in basin mangrove forests in southwest Florida. Ecology **67**: 670-683.

U. S. Environmental Protection Agency 1979. Methods for the analysis of water and wastes. USEPA Environmental Monitoring Support Lab., Cincinnati, Ohio.

Van der Valk, A. G. and P. M. Attiwill. 1984. Decomposition of leaf and root litter of Avicennia Marina at Westernport Bay, Victoria, Australia. Aquatic Botany **18**: 205-221.

Vitousek, P. M. and J. S. Denslow. 1986. Nitrogen and phosphorus availability in treefall gaps of a lowland tropical rainforest. Journal of Ecology **74**: 1167-1178.

Wadsworth, F. H. 1959. Growth and regeneration of white mangrove in Puerto Rico. Caribbean Forester **20**: 59-69.

Walbridge, M. R. 1991. Phosphorus availability in acid organic soils of the lower north Carolina coastal plain. Ecology **72**: 2083-2100.

Walbridge, M. R. and P. M. Vitousek. 1987. Phosphorus mineralization potentials in acid organic soils: processes affecting $^{32}PO_4^{3-}$ isotope dilution measurements. Soil Biology and Biochemistry **19**: 709-717.

Wang, J. D., J. van de Kreeke, N. Krishnan and D. Smith. 1994. Wind and tide response in Florida Bay. Bulletin of Marine Science **54**: 579-601.

Wanless, H. R., R. W. Parkinson and L. P. Tedesco. 1994. Sea level control on stability of Everglades wetlands. Pages 199-223 *in* S. M. Davis and J. C. Ogden, editors. Everglades: The ecosystem and its restoration. St. Lucie Press, Delray Beach, Florida.

Warner, J. H. 1990. Successional patterns in a mangrove forest in southwestern Florida. M.S. Thesis, University of Southwestern Louisiana, Lafayette, Louisiana.

Watt, A. S. 1947. Pattern and process in the plant community. Journal of Ecology **35**: 1-22.

Wedin, D. A. and J. Pastor. 1993. Nitrogen mineralization dynamics in grass monocultures. Oecologia **96**: 186-192.

Wedin, D. A. and D. Tilman. 1990. Species effects on nitrogen cycling: a test with perennial grasses. Oecologia **84**:

Weinstein, D. A., H. H. Shugart and D. C. West 1982. The long-term nutrient retention properties of forest ecosystems: A simulation investigation. Oak Ridge National Laboratory, Oak Ridge, Tennessee.

Wolaver, T. G. and J. D. Spurrier. 1988. The exchange of phosphorus between a euhaline vegetated marsh and the adjacent tidal creek. Estuarine, Coastal and Shelf Science **26**: 203-214.

Woodroffe, C. D. 1983. Development of mangrove forests from a geological perspective. Pages 1-17 *in* H. J. Teas, editors. Task for vegetation science Vol. 8. Dr W. Junk Publishers, The Hague, Netherlands.

Woodroffe, C. D. 1992. Mangrove sediments and geomorphology. Pages 7-41 *in* A. I. Robertson and D. M. Alongi, editors. Coastal and estuarine studies. American Geophysical Union, Washington, D. C.

Woodroffe, C. D. and J. Grindrod. 1991. Mangrove biogeography: the role of Quaternary environmental and sea-level change. Journal of Biogeography **18**: 479-492.

Zhang, Q. and J. Zak. 1995. Effects of gap size on litter decomposition and microbial activity in a subtropical forest. Ecology **76**: 2196-2204.

Zwolsman, J., J. G. 1994. Seasonal variability and biogeochemistry of phosphorus in the Scheldt estuary, south-west Netherlands. Estuarine, Coastal and Shell Science **39**: 227-248.

Chen, Ronghua, B.S., Xiamen University, 1983; M.S., Xiamen University, 1986;
Doctor of Philosophy, University of Southwestern Louisiana, Summer 1996
Major: Environmental and Evolutionary Biology
Title of Dissertation: Ecological analysis and simulation models of landscape patterns in mangrove forest development and soil characteristics along the Shark River estuary, Florida
Dissertation director: Dr. Robert R. Twilley
Pages in dissertation: 168; Words in abstract: 348

ABSTRACT: Landscape patterns of mangrove forest development following large-scale disturbances in relation to soil nutrient resources and toxic stresses were examined along the Shark River estuary, Florida. Patterns of forest structure were based on 34 years of growth since Hurricane Donna destroyed most of mangrove forests in 1960. Basal area, biomass increment and stature of forests at the downstream marine sites were higher than those at the upstream and intermediate sites. Pore water salinities in the mangrove soils were below hypersalinity and sulfide concentrations were generally lower than other reported values in mangrove soils. Total soil phosphorus, available phosphorus and nitrogen mineralization rates increased from the landward to seaward zones along the estuary. Soil properties in the downstream marine region included high availability of nutrient resources and low concentrations of stressors supporting a region of optimum growth of mangroves. However, phosphorus input from the Gulf of Mexico leads to a gradient of soil phosphorus resources along the estuary, which may determine the landscape development of mangrove wetlands in this land-margin ecosystem.

Simulation models were developed to investigate landscape patterns of mangrove forest development. A soil organic matter model (NUMAN) demonstrated that the landscape gradients of sediment characteristics are contributed by plant production, litter decomposition and export, and allochthonous input of inorganic materials. A forest dynamic model (FORMAN) used an individual-based approach to simulate mangrove forest development. The

FORMAN and NUMAN models were integrated into as single model (MANGAL) that accurately simulated the recovery of mangrove forests along the gradient of soil nutrient availability. Simulated basal areas by species fit well with data from field surveys. MANGAL adequately tracked patterns of species-specific size-class distribution along the estuarine gradient. Simulated basal areas of mangrove species along gradients of soil nutrient resources and salinities illustrated a change in competitive balance among species that was time dependent. *Laguncularia racemosa* dominated in fertile soils with low salinity stress at early stages of recovery, but its abundance decreased while *Avicennia germinans* increased in dominance. The dominance of *Rhizophora mangle* was limited to regions with low nutrient availability and low salinity.

BIOGRAPHICAL SKETCH

Ronghua Chen was born in Fujian, People's Republic of China on October 27, 1962. He received a Bachelor of Science degree in Botany in July, 1983 and a Master of Science degree in Plant Ecology in May, 1986 respectively from Xiamen University, P. R. China. He worked as a lecturer from 1986 to 1991 in the Department of Biology at Xiamen university. In August 1991, he entered the doctoral program in Environmental and Evolutionary Biology and was awarded the degree of Doctor of Philosophy by The University of Southwestern Louisiana in 1996.